Dissertation
zum Erwerb des Doctor of Philosophy (Ph.D.) an
der Medizinischen Fakultät der
Ludwig-Maximilians-Universität zu München

Dendritic cell progenitor trafficking and identification and functional analyses of dendritic cells with distinct developmental origin

vorgelegt von:

Johanna Marie Salvermoser

aus:

Pfaffenhofen an der Ilm

Jahr: 2020

_____

First supervisor: *Prof. Dr. Barbara Schraml*

Second supervisor: *Prof. Dr. Anne Krug*

Third supervisor: *Prof. Dr. Christian Schulz*

Fourth supervisor: *PD. Dr. rer. nat. Caspar Ohnmacht*

Dean: **Prof. Dr. med. dent. Reinhard Hickel**

Datum der Verteidigung:
09.03.2020

ABSTRACT

Conventional dendritic cells (cDCs), are the major antigen-presenting cell type that bridges the innate and adaptive immune system. DCs are constantly replenished from myeloid bone marrow progenitors which latest stage, pre-cDC, leave the BM, seeds the peripheral tissues and further differentiates into two functionally and developmentally distinct subsets, cDC1 and cDC2. This study aimed to investigate DC development by assessing the trafficking of pre-cDCs and by analyzing the effect of a specific depletion of DC progenitors. The signals that regulate the recruitment of pre-cDCs to different peripheral organs are poorly understood. Therefore, this study aimed to identify pre-cDCs in different peripheral organs and to find differences in expression pattern of trafficking receptors. In this study 39 trafficking receptors have been identified to be expressed on pre-cDCs of the analysed tissues and showed differences in the expression patterns between peripheral organs. These receptors are interesting candidates to further study differences in the recruitment of pre-cDCs to different peripheral tissues This can provide possibilities to influence the recruitment of pre-cDCs in certain diseases, where the replenishment of cDCs is accelerated. To generate a DC deficient model, DNGR-1/ CLEC9A expressing cells and its progeny were depleted by crossing *Clec9a-Cre* mice to Rosa-lox-STOP-lox- diphtheria toxin (DTA) mice. Despite cDC progenitors being diminished in these mice, as expected, cells that phenotypically resemble cDC2 arise independent of conventional DC progenitors. As these cells show somatic rearrangements of the Ig-heavy gene locus, typical for lymphoid cells, they were termed lymphoid DC2. A lymphoid origin of DCs has been shown *in vitro* as well as in adoptive transfer studies, however, the reason for this dual origin and under which physiological settings lymphoid derived DC2 develop and replenish myeloid-derived cDCs is unknown. To test the hypothesis that lymphoid DCs represent a subset of cells with distinct functions that replace myeloid-derived DCs in certain types of diseases, functional analyses were performed. Indeed, less lymphoid DC2 showed TNFα expression after LPS stimulation compared to DC2 from control mice. Furthermore, less lymphoid DC2 showed migration towards CCR7 ligands suggesting a migration defect. Additionally, increased cell death of lymphoid DC2 compared to DC2 from control mice was found *in vitro.* Increased cell death, on the one hand, provides evidence that lymphoid DC2 behave different from bona fide cDC2, on the other hand it impedes the interpretation of quantitative functional analyses, such as migration assays. Taken together, depletion of myeloid DC progenitors in *Clec9a*^{Cre}*Rosa*^{DTA} mice provides an artificially induced situation in which DC2 like cells can develop in the absence of myeloid DC progenitor. Furthermore, preliminary findings indicate that lymphoid DC2 show functional differences to bona fide cDC2 which argues for the requirement of a redundant developmental pathway to create a situation adapted repertoire of cells.

TABLE OF CONTENTS

ABSTRACT **3**

TABLE OF FIGURES AND TABLES **7**

ABBREVIATIONS **9**

1. INTRODUCTION **10**

1.1 DENDRITIC CELLS ARE IMPORTANT ACTIVATORS OF IMMUNE RESPONSES 10

1.2 LOCALIZATION AND MIGRATION OF DCS 11

1.2.1 DC localization in peripheral organs *11*

1.2.2 DC localization in lymphoid organs *12*

1.2.3 Dendritic cell migration *15*

1.3 HISTORY OF DENDRITIC CELL ONTOGENY 16

1.3.1 The lymphoid origin of dendritic cells *17*

1.3.2 The myeloid origin of conventional dendritic cells *18*

1.3.3 Subset commitment of dendritic cell progenitors *19*

1.4 MOUSE MODELS ARE USED TO DISTINGUISH DCS FROM OTHER MONONUCLEAR PHAGOCYTES AND TO IDENTIFY THEIR FUNCTIONS 20

2. AIM OF THE THESIS **23**

3. MATERIALS AND METHODS **24**

3.1 ANIMAL HUSBANDRY 24

3.2 GENOTYPING BY PCR 24

3.3 CELL ISOLATION FROM DIFFERENT TISSUES 25

3.3.1 Bone marrow *25*

3.3.2 Spleen, thymus and lymph nodes *25*

3.3.3 Lung and kidney *25*

3.3.4 Small intestine and colon *26*

3.3.5 Skin *26*

3.4 FLOW CYTOMETRY 26

3.5 CELL ENRICHMENT 27

3.5.1 Positive enrichment *27*

3.5.2 Lin depletion *27*

3.6 CYTOSPINS AND HEMACOLOR STAINING 28

3.7 MULTIPLEX QUANTITATIVE PCR USING FLUIDIGM 28

3.8 *IN VITRO* DENDRITIC CELL MIGRATION THROUGH TRANSWELLS 28

3.9 EAR EXPLANT ASSAY 29

3.10 CELL CULTURE 29

3.10.1 Flt3L cultures *29*
3.10.2 GM-CSF cultures *29*
3.11 ELISAs and Cytokine bead assay 30
3.12 Diphtheria toxin (DT) mediated Cell ablation in Clec9A$^{cre/DTR}$Rosa^{DTR} mice 30
3.13 *In vitro* cytokine production 30
3.14 Polymerase chain reaction for DJ-rearrangements of the heavy chain locus 30
3.15 Microscopic analysis of *in vitro* chemotactic migration of dendritic cells 31
3.16 Immunofluorescence staining of lymph nodes 31
3.17 Statistical Analyses 32
3.18 Table of Antibodies 32

4. RESULTS 35

4.1 Identification of potential regulators for trafficking of dendritic cell progenitors in steady-state 35
4.1.1 Analyses on pre-cDC subset distribution in the tissues reveals no direct correlation with dendritic cell subsets *35*
4.1.2 Multiplex qPCR screen for migration-related receptors reveals 39 trafficking receptors to be expressed on pre-cDCs in peripheral tissues *37*
4.1.3 In vitro migration of pre-cDCs in transwell assay as a basic tool for the verification of relevance for trafficking receptors in pre-cDC migration *41*
4.2 *Clec9a*-mediated ablation of conventional dendritic cells suggests a lymphoid path to generating dendritic cells *in vivo* 41
4.2.2 Myeloproliferation in Clec9a$^{cre/cre}$Rosa^{DTA} mice *41*
4.2.3 Incomplete depletion of cDC2 in Clec9a$^{cre/cre}$Rosa^{DTA} mice *45*
4.2.4 Loss of dendritic cell progenitors in Clec9a^{cre}Rosa^{DTA} mice *47*
4.2.5 Loss of dendritic cells and their progenitors upon DT treatment of Clec9a$^{cre/cre}$Rosa^{DTR} mice *48*
4.2.6 Progenitors of dendritic cells in Clec9a$^{cre/cre}$Rosa^{DTA} mice are inefficient in producing dendritic cells in vitro *50*
4.2.7 DC2 from Clec9a$^{cre/cre}$Rosa^{DTA} mice phenotypically resemble bona fide dendritic cells *53*
4.2.8 DC2 from Clec9a$^{cre/cre}$Rosa^{DTA} mice produce cytokines in response to CpG and LPS in comparable frequencies to cDC2 from control mice *55*
4.2.9 DC2 from Clec9a$^{cre/cre}$Rosa^{DTA} mice have somatic rearrange-ments in the IgH locus suggesting a lymphoid origin *56*
4.2.10 Clec9a$^{cre/cre}$Rosa^{DTA} mice show a trend to increased Common Lymphoid Progenitors (CLP) *57*
4.3 Clec9A$^{cre/cre}$Rosa^{DTA} mice show a potential reduction in DC2 migration compared to bona fide DC2 58

4.3.2 Reduced migratory DC2 in the skin draining but not mesenteric lymph nodes from Clec9a$^{cre/cre}$Rosa^{DTA} mice compared to bona fide cDC2 ..... *58*

4.3.3 Reduced numbers of DC2 after migration from the skin of from Clec9a^{cre}Rosa^{DTA} mice but also in the isolation from the skin *63*

4.3.4 Splenic Lymphoid DC2 migrate less towards CCR7 ligands in vitro in steady-state but not upon activation *66*

4.3.5 lymphoid DC2 show increased necrosis in culture and increased Apoptosis after transmigration in the presence of CCR7 ligands *70*

4.3.6 The localization of the lymphoid DC2 in the inguinal LN appears disturbed in immunofluorescence sections *72*

5. DISCUSSION 75

5.1 PRE-CDC SUBSET DISTRIBUTION DOES NOT ALWAYS CORRELATE TO DC SUBSET DISTRIBUTION IN TISSUES 75

5.2 DIFFERENTIAL RECRUITMENT OF PRE-CDCS TO DIFFERENT PERIPHERAL TISSUES 76

5.3 DC DEPLETION IN *CLEC9A$^{CRE/CRE}$ROSA^{DTA}* MICE LEADS TO REPLENISHMENT OF DC2 BY PHENOTYPICALLY SIMILAR CELLS OF LYMPHOID ORIGIN 78

5.4 POTENTIAL PROGENITORS OF DC2 IN *CLEC9A$^{CRE/CRE}$ROSA^{DTA}* MICE 81

5.4.1 DC progenitors *81*

5.4.2 Monocytes and other myeloid progenitors *82*

5.4.3 Plasmacytoid dendritic cells *82*

5.4.4 Common lymphoid progenitors *83*

5.5 THE PHYSIOLOGICAL RELEVANCE OF FUNCTIONAL DIFFERENCES BETWEEN DENDRITIC CELLS WITH DIFFERENT ORIGIN 84

5.5.1 Cytokine production *84*

5.5.2 Migration *85*

5.5.3 Cell death *87*

5.5.4 localization *87*

REFERENCES 89

APPENDIX 100

PUBLICATIONS ARISING FROM THIS WORK: 100

ACKNOWLEDGEMENTS 101

AFFIDAVIT 102

TABLE OF FIGURES AND TABLES

FIGURE 1: SCHEME FOR DC MIGRATION FROM THE SKIN TO THE DRAINING LN. 12
FIGURE 2: ORGANIZATION OF LYMPHOCYTES IN THE LYMPH NODE. 14
FIGURE 3: DC MIGRATION RELEVANT CHEMOKINES AND RECEPTORS 15
FIGURE 4: CCL19 AND CCL21 MEDIATED CCR7 SIGNALLING. 16
FIGURE 5: MYELOID DEVELOPMENT OF CDCS, PDCS, AND MONOCYTE-DERIVED CELLS. 19
FIGURE 6: REPRESENTATIVE GATING STRATEGY OF DCS AND THEIR PRECURSORS. 36
FIGURE 7: DC AND PRE-CDC SUBSET DISTRIBUTION ACROSS LYMPHOID AND NON-LYMPHOID ORGANS. 37
FIGURE 8: SORT PURITY OF BONE MARROW DC PROGENITORS. 39
FIGURE 9: CANDIDATE RECEPTORS FOR PRE-CDC MIGRATION. 40
FIGURE 10: CCL2 INDUCED MIGRATION OF BONE MARROW PRE-CDCS. 41
FIGURE 11: CLEC9A$^{CRE/CRE}$ROSA^{DTA} MICE SHOW SPLENOMEGALY. 41
FIGURE 12: CLEC9A$^{CRE/CRE}$ROSA^{DTA} MICE EXHIBIT NEUTROPHILIA AND MONOCYTOSIS. 42
FIGURE 13: CLEC9A$^{CRE/CRE}$ROSA^{DTA} MICE HAVE INCREASED SERUM LEVELS OF FLT3L. 43
FIGURE 14: CLEC9A$^{CRE/CRE}$ROSA^{DTA} MICE COMPARABLE LEVELS OF GROWTH FACTORS AND CHEMOKINES IN THE SERUM. 44
FIGURE 15: CD8+ T-CELLS ARE DIMINISHED IN THE SPLEEN OF CLEC9A$^{CRE/CRE}$ROSA^{DTA} MICE. 45
FIGURE 16: DEPLETION OF CDC1 BUT NOT CDC2 IN CLEC9A$^{CRE/CRE}$ROSA^{DTA} MICE. 46
FIGURE 17: EQUAL QUANTIFICATION OF PDCS AND RPMS IN THE SPLEENS OF CLEC9A$^{CRE/CRE}$ROSA^{DTA} AND CONTROL MICE. 47
FIGURE 18: LOSS OF DC PRECURSORS IN CLEC9A$^{CRE/CRE}$ROSA^{DTA} MICE. 48
FIGURE 19: NO MANIFESTATION OF NEUTROPHILIA AND MONOCYTOSIS IN CLEC9A$^{CRE/CRE}$ROSA^{DTR} MICE 24 HOURS AFTER DT INJECTION. 49
FIGURE 20: EFFICIENT DEPLETION OF DCS IN CLEC9A$^{CRE/CRE}$ROSA^{DTR} MICE. 49
FIGURE 21: LOSS OF PRE-CDCS IN CLEC9A$^{CRE/CRE}$ROSA^{DTR} MICE. A. 50
FIGURE 22: LOWER EXPRESSION OF CD135 ON CELLS RESEMBLING PRE-CDCS IN THE SPLEEN OF CLEC9A$^{CRE/CRE}$ROSA^{DTA} MICE. 51
FIGURE 23: REMAINING PRE-CDCS FROM CLEC9A$^{CRE/CRE}$ROSA^{DTA} MICE DO NOT GENERATE CDC *IN VITRO*. 51
FIGURE 24: BONE MARROW PROGENITORS FROM CLEC9A$^{CRE/CRE}$ROSA^{DTA} MICE DO NOT GENERATE CDC IN FLT3L CULTURES IN VITRO. 52
FIGURE 25: BONE MARROW PROGENITORS FROM CLEC9A$^{CRE/CRE}$ROSA^{DTA} MICE DO NOT GENERATE CDC IN GM-CSF CULTURES IN VITRO. 53
FIGURE 26: PHENOTYPIC COMPARISON OF DC2 FROM OF CLEC9A$^{CRE/CRE}$ROSA^{DTA} AND CONTROL MICE. 55
FIGURE 27: CYTOKINE PRODUCTION OF DC2 FROM OF CLEC9A$^{CRE/CRE}$ROSA^{DTA} AND CONTROL MICE AFTER STIMULATION. 56
FIGURE 28: DC2 FROM CLEC9A$^{CRE/CRE}$ROSA^{DTA} MICE SHOW D-J REARRANGEMENTS. 57
FIGURE 29: QUANTIFICATION OF COMMON LYMPHOID PROGENITORS (CLPS) IN THE BM OF CLEC9A$^{CRE/CRE}$ROSA^{DTA} AND CONTROL MICE. 58

FIGURE 30: COMPARABLE CELLULARITY BUT INCREASE OF A CD64^{+}CD11B^{+} POPULATION IN DIFFERENT LNS IN CLEC9A^{CRE}ROSA^{DTA} MICE. 59

FIGURE 31: REPRESENTATIVE GATING OF RESIDENT AND MIGRATORY DC SUBSETS AS WELL AS LC IN DIFFERENT OF CLEC9A$^{CRE/CRE}$ROSA^{DTA} AND CONTROL MICE. 60

FIGURE 32: QUANTIFICATION OF MIGRATORY DC2 IN THE INGUINAL (A) AND AURICULAR (B) AND MESENTERIC (C) LN OF CLEC9A$^{CRE/CRE}$ROSA^{DTA} AND CONTROL MICE IN BOTH FREQUENCY AND COUNTS. 62

FIGURE 33: EQUAL CCR7 EXPRESSION ON MIGRATORY AND RESIDENT DC2 IN THE INGUINAL LN OF CLEC9A$^{CRE/CRE}$ROSA^{DTA} AND CONTROL MICE. 63

FIGURE 34: REDUCED MIGRATION OF LYMPHOID DC2 BUT NOT LC OUT OF EAR FROM HETEROZYGOUS CLEC9A$^{+/CRE}$ROSA^{DTA} AND HOMOZYGOUS CLEC9A$^{CRE/CRE}$ROSA^{DTA} MICE. 64

FIGURE 35: REPRESENTATIVE GATING OF DC SUBSETS IN THE DERMIS AS WELL AS LC IN THE EPIDERMIS OF THE EAR. 65

FIGURE 36: QUANTIFICATION OF LANGERHANS CELLS AND DC2 IN THE SKIN OF HETEROZYGOUS CLEC9A$^{+/CRE}$ROSA^{DTA} (A) AND HOMOZYGOUS CLEC9A$^{CRE/CRE}$ROSA^{DTA} (B) MICE. 66

FIGURE 37: REDUCED MIGRATION OF SPLENIC LYMPHOID DC2 TO CCR7 LIGANDS. 67

FIGURE 38: COMPARABLE IN VITRO CHEMOTACTIC MIGRATION OF DC2 FROM CLEC9A$^{CRE/CRE}$ROSA^{DTA} AND CONTROL MICE IN 3D ENVIRONMENTS. 68

FIGURE 39: COMPARABLE REGULATION OF ACTIVATION MARKERS ON SPLENIC DC2 FROM CLEC9A$^{CRE/CRE}$ROSA^{DTA} AND CONTROL MICE AFTER CULTURE FOR 18H. 69

FIGURE 40: COMPARABLE MIGRATION OF SPLENIC LYMPHOID DC2 TO CCR7 LIGANDS AFTER ACTIVATION WITH LPS. 70

FIGURE 41: SPLENIC LYMPHOID DC2 SHOW INCREASED APOPTOSIS AFTER TRANSWELL MIGRATION TOWARDS CCR7 LIGANDS AND INCREASED NECROSIS IN LYMPHOID DC2 AFTER CULTURE. 71

FIGURE 42: IMMUNOFLUORESCENCE IMAGES OF INGUINAL LN SECTIONS FROM CONTROL AND CLEC9A$^{CRE/CRE}$ROSA^{DTA} MICE. 74

FIGURE 43: SCHEME FOR LYMPHOID PROGENITORS FILLING THE CDC2 NICHE WHEN MYELOID DC PRECURSORS ARE LOST IN CLEC9A^{CRE}ROSA^{DTA} MICE. 80

TABLE 1: PCR PRIMERS 24

TABLE 2: PCR PROGRAMS 25

TABLE 3 LIST OF TARGET MIGRATION RELATED RECEPTORS 38

TABLE 4 PRE-CDC SORTS FROM SELECTED LYMPHOID AND NON-LYMPHOID ORGANS 39

ABBREVIATIONS

ABBREVIATION	FULL NAME
aLN	Auricular lymph node
APC	Antigen presenting cell
BATF3	Basic leucine zipper transcriptional factor ATF like-3
BM	Bone marrow
CCL	Chemokine ligand
CCR	Chemokine Receptor
CD	Cluster of differentiation
CDC	Conventional dendritic cell
CDP	Common dendritic cell precursor
CLEC9A	C-type lectin domain family 9 member A
CLP	Common lymphoid progenitor
CMP	Common myeloid progenitor
DC	Dendritic cell
DNA	Deoxyribonucleic acid
DNGR-1	Dendritic cell natural killer lectin group receptor-1
DP	Double positive
DT	Diphtheria toxin
DTA	Diphtheria toxin (catalytically active) subunit A
DTR	Diphtheria toxin receptor
FLT3L	Fms-like tyrosine kinase 3 ligand
GAG	Glycosaminoglycans
GFP	Green fluorescent protein
HSC	Hematopoietic stem cell
iLN	Inguinal lymph node
IL	Interleukin
IRF4	Interferon regulatory factor 4
IRF8	Interferon regulatory factor 8
LC	Langerhans cell
LMPP	Lymphoid primed multipotent progenitor
LN	Lymph node
MDP	Macrophage dendritic cell progenitor
MHCII	Major histocompatibility complex II
migDC	Migratory dendritic cells
MLN	Mesenteric lymph node
MNP	Mononuclear phagocytes
pDC	Plasmacytoide dendritic cell
resDC	Resident dendritic cells
SP	Single positive
TBM	Total bone marrow
YFP	Yellow fluorescent protein

1. INTRODUCTION

1.1 DENDRITIC CELLS ARE IMPORTANT ACTIVATORS OF IMMUNE RESPONSES

Dendritic cells (DCs) have first been described based on their morphology as stellate cells that adhere to glass surfaces by Steinman et al 1973 and were further described to express high levels of major histocompatibility complex II (MHCII). DCs are the most potent antigen presenting cells (APC) and activators of T-cell responses (Banchereau & Steinman, 1998; Nussenzweig et al., 1981; Steinman & Cohn, 1973; Steinman & Witmer, 1978; Steinman, Kaplan, Witmer, & Cohn, 1979), making them important regulators of immune responses that bridge innate and adaptive immune responses. DCs are short-lived cells that reside in the peripheral organs and patrol their surroundings for pathogen and damage associated antigens (Gallo & Gallucci, 2013; Kamath, Henri, Battye, Tough, & Shortman, 2002). Upon antigen encounter, DCs become activated and transport the antigen to the draining lymph nodes (LN) to initiate T-cell responses (Merad, Sathe, Helft, Miller, & Mortha, 2013). Additionally, DCs contribute to tolerance against self-antigens or food antigens (Merad et al., 2013). Such tolerance is induced by DCs through taking up and transporting peripheral self- or oral antigens, to the thymus or peripheral lymphoid organs and participating in deletion of reactive T-cells or induction of T regulatory cells (Iberg, Jones, & Hawiger, 2017; Merad et al., 2013).

The DC population consists of plasmacytoid DCs (pDCs) and conventional DCs (cDCs), which are important for the immune responses against viruses and extra-/intracellular pathogens, respectively (Schraml & Reis e Sousa, 2015; Vu Manh, Bertho, Hosmalin, Schwartz-Cornil, & Dalod, 2015). These DC populations have been found conserved in mice and men (Schlitzer & Ginhoux, 2014). CDCs are typically identified based on the expression of the surface markers CD11c and MHCII can further be subdivided into two functionally and transcriptionally distinct subsets, so-called cDC1 and cDC2 (Guilliams et al., 2014). cDC1 and cDC2 based on the expression of surface markers CD8, CD24, XCR-1, DEC205 and CD11b, CD4, CD172a, respectively (Guilliams et al., 2014). The different subsets of DCs cannot only be distinguished from each other by the expression of surface markers but also differ in their immunological functions (Mildner & Jung, 2014). The main function of pDCs is their defence against viruses by producing large amounts of Type I interferons (Cella et al., 1999; Perussia, Fanning, & Trinchieri, 1985; Siegal et al., 1999). cDC1 recognize intracellular pathogens, activate $CD8^+$ T-cells via cross-presentation of antigens on MHCI molecules and initiate Th1 responses. cDC2 recognize extracellular pathogens and initiate Th2 and Th17 responses (Dudziak, Kamphorst, Heidkamp, Buchholz, & Nussenzweig, 2007; Guilliams et al., 2014; Hildner et al., 2008; Pooley, Heath, & Shortman, 2001). In addition to the ability of DCs to activate T-cell responses upon inflammation, DCs are also important for the tolerance against self-antigen

and regulate innate immune responses for example by producing cytokines like IL-12 and IL-23 (Arora et al., 2014; Banchereau & Steinman, 1998; Kinnebrew et al., 2012; Reis e Sousa et al., 1997; Whitney et al., 2014). As in most lymphoid organs, the distribution DC subsets shows that cDC2 are the predominant population in LNs and spleen, whereas cDC1 are more abundant than cDC2 in the thymus (Pakalniškytė & Schraml, 2017).

1.2 LOCALIZATION AND MIGRATION OF DCS

DCs have been found in many lymphoid and non-lymphoid organs, such as the lymph nodes, spleen, small intestine, kidneys, lungs, skin, heart, and brain (D'Agostino, Gottfried-Blackmore, Anandasabapathy, & Bulloch, 2012). Although the expression of surface markers on DCs can vary between the peripheral tissues, the key antigen-presenting function remains the same (Malissen, Tamoutounour, & Henri, 2014; Persson et al., 2013). In the non-lymphoid organs, DCs patrol their environment for pathogens that have entered the tissue for example through the skin, gut, or lung. From here the DCs transport the antigen via lymphatic vessels to the draining lymph nodes to initiate T-cell responses (**Figure 1**). The migration and the localization of DCs within lymphoid organs are mediated by the chemokine receptor 7 (CCR7) which gets upregulated in DCs upon activation (Braun et al., 2011; Calabro et al., 2016; Förster et al., 1999; Yanagihara, Komura, Nagafune, Watarai, & Yamaguchi, 1998). This transport is especially important in inflammatory situations to initiate immune responses against pathogen-derived antigens, but migration of DCs also occurs in steady-state conditions which is important to induce tolerance against peripheral self-antigens (Merad et al., 2013). For the proper function of DCs, the localization in the tissues and migration play important roles (Eisenbarth, 2019).

1.2.1 DC LOCALIZATION IN PERIPHERAL ORGANS

The localization within the tissue has an important impact on DC function both in non-lymphoid and lymphoid organs. DCs are localized so that they can easily reach incoming antigens to further transport and present it (Eisenbarth, 2019). In peripheral non lymphoid organs, such as the small intestine and the lung, DCs localize subepithelial and extend their dendrites through the epithelial layer, which allows them to probe foreign antigens (Hoffmann et al., 2016; Rescigno, Rotta, Valzasina, & Ricciardi-Castagnoli, 2001; Sung et al., 2006). The small intestine contains three cDC subset of which the most abundant is the $CD11b^{+}CD103^{+}$ cDC2 subset followed by the $CD11b^{-}CD103^{+}$ cDC1 and the least frequent is the $CD11b^{+}CD103^{-}$ cDC2 (Persson et al., 2013). In the kidney, $CD11b^{+}$ DC2 are the predominant over cDC1 but additionally to these two subsets, also CD64 expressing pre-cDC derived cells exists that are much more frequent than cDC1 and cDC2 (Pakalniškytė & Schraml, 2017). In the skin, two distinct cell types of APCs exist. Langerhans cells (LCs), install the first layer of defence by

residing in the epidermis (Deckers, Hammad, & Hoste, 2018; **Figure 1**). Although LCs have overlapping functions with cDCs in terms of migration and antigen presentation, LCs, other than cDCs, are of embryonic origin and are maintained in the skin by self-renewal (Deckers et al., 2018). CDCs of the skin reside in the dermis and patrol there for foreign antigens (**Figure 1**) (Henri, Guilliams, et al., 2010a). The DCs in the skin can be divided into several different subsets which suggests adaptation to specific functions in this tissue (Henri, Poulin, et al., 2010b). The most frequent DC subset in the skin is the $CD207^{-}CD11b^{+}$ DCs, followed by $CD207^{-}CD11b^{-}$ DCs and the least frequent subsets are the $CD207^{+}$ CD103- and the $CD207^{+}CD103^{+}$ DCs (Henri, Poulin, et al., 2010b).

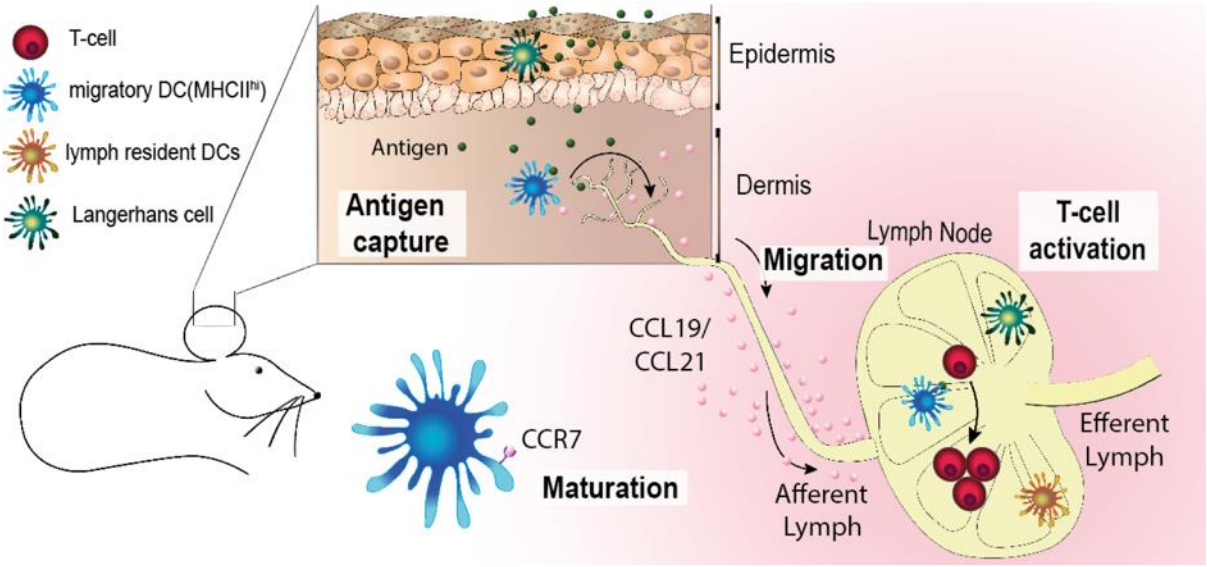

Figure 1: Scheme for DC migration from the skin to the draining LN. Migratory cDCs (blue) in the skin localize to the dermis, whereas LCs (green) can be found in the epidermis. Both cell types patrol for antigens and upon activation upregulate the chemokine receptor CCR7, which recognizes CCL19 as well as CCL21. Thereupon, DCs and LCs migrate along a CCL19/21 gradient towards the lymph vessel and in the lymph vessel to the draining LN. In the draining LN, DCs that immigrated from the peripheral organ can be distinguished from LN resident DCs (orange). The activated migratory DCs from the LN present the antigen to T-cells (red) in the LN to induce proliferation.

1.2.2 DC LOCALIZATION IN LYMPHOID ORGANS

The lymph nodes are the place where DCs migrate to after they have taken up antigen in the periphery (Alvarez, Vollmann, & Andrian, 2008). Therefore, LNs contain the DCs that have migrated from the drained organ, which are then called migratory dendritic cells. In addition to the migratory DCs, also tissue-resident DCs can be found in the LNs (Hashimoto, Miller, & Merad, 2011). The exact location, to which DC localize in the lymphoid organs is especially important because the B and T-cells localize to very confined regions within the LNs so the DCs can only function to activate their target cells when they colocalize (Eisenbarth, 2019). An alteration in the localization of DC subsets can, therefore, have a major influence on their

function to prime T and B-cell responses (Yi & Cyster, 2013). In steady-state, resident and migratory DCs can be distinguished based on the levels of the surface molecules CD11c and MHCII as $CD11c^{hi}$ $MHCII^{+}$ resident DC and $CD11c^{+}MHCII^{hi}$ migratory DCs (Hashimoto et al., 2011), however, in inflammation this discrimination often fails due to upregulation of these markers and can only be achieved for cDC1 by using different markers, such as CD103 for migratory DC1 and CD8α for resident cDC1 (Eisenbarth, 2019; Merad et al., 2013; Waithman et al., 2013). Resident and migratory DCs are functionally distinct and this division of labour is also represented in their spatio-temporal localization. The localization of B-cells, T-cells, and DCs in the LN is depicted in **Figure 2**. Migratory DCs enter the LN parenchyma through the subcapsular sinus in a CCR7 independent manner and from here migDC2 are furthermore directed to either the interfollicular zone at the T-cell-B-cell border dependent on EBI2, whereas migratory cDC1 are directed to the deep T-cell zone (Braun et al., 2011; Gerner, Kastenmüller, Ifrim, Kabat, & Germain, 2012; Gerner, Torabi-Parizi, & Germain, 2015; Schumann et al., 2010). These differences in localization of migratory DC2 goes in hand with their function as inducers of different T-cell responses as it coincides with the localization of T-cells subsets. Migratory cDC2 can therefore induce Th2 T-cells and TfH cells as some $CD4^{+}$ T-cells also localize at the T-cell B-cell border in close proximity to B-cells whereas migratory cDC1 induce Th1 cells and $CD8^{+}$ T-cells, which localize to the deep T-cell zone (Dudziak et al., 2007; Gerner et al., 2015; Pooley et al., 2001; Qi, Egen, Huang, & Germain, 2006; Randolph, Inaba, Robbiani, Steinman, & Muller, 1999; Reuter et al., 2015; Y. Suzuki et al., 2004b). In contrast to migratory DCs, resident DCs receive their antigen either from draining the lymph or via antigen-hand over from other cells, such as migratory DCs. Following that they can also induce T-cell responses (Allan et al., 2006; Ersland, Wüthrich, & Klein, 2010; Gurevich et al., 2017). The difference between resident and migratory DCs, therefore, lays in the access to and origin of the antigen. The localization of resident DCs only marginally varies from the localization of migratory DCs to get access to the antigen. The resident DC2 are located close to the lymphatic sinuses and like migratory DC2 also in the interfollicular zone but closer to the medullary side where they capture particulate antigens from the lymph (Gerner et al., 2015). Resident DC1 are located in the deep T-cells zone and presumably form a network with migratory DC1 (Gerner et al., 2015; Kissenpfennig et al., 2005; Kitano et al., 2016).

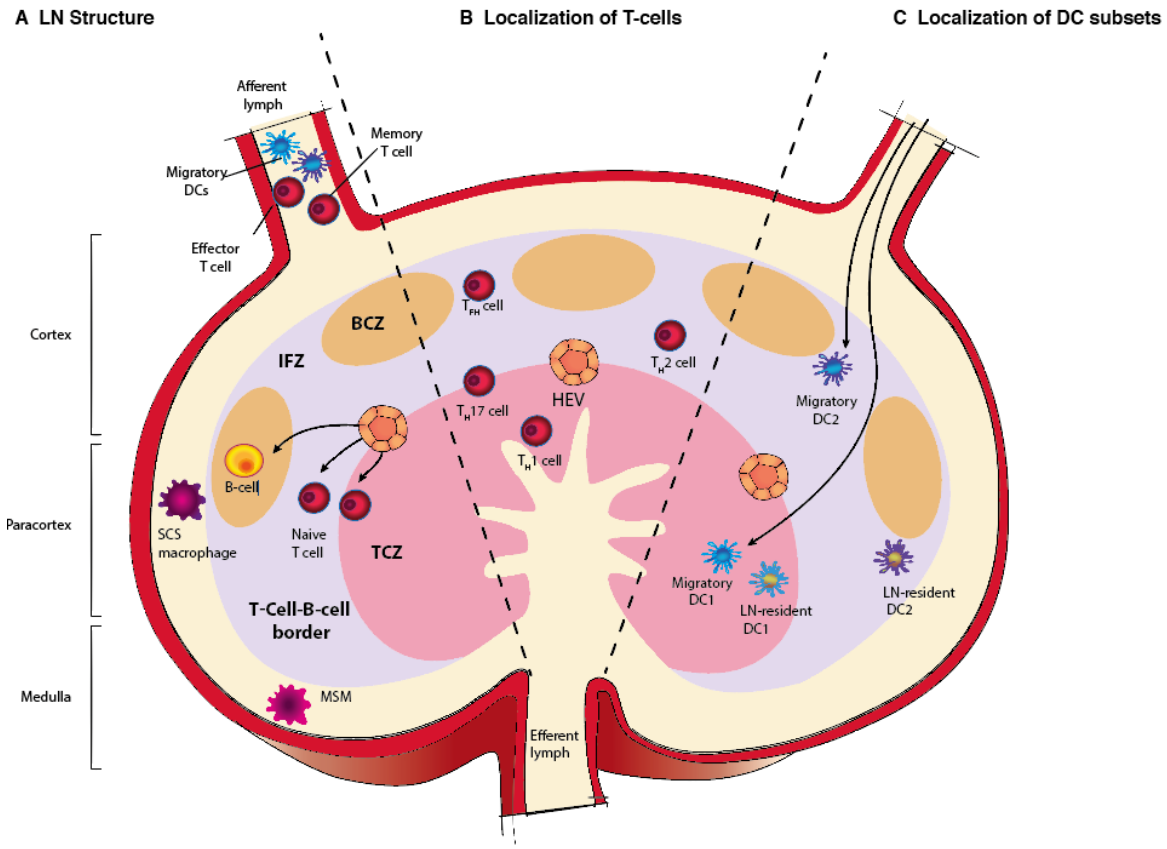

Figure 2: Organization of lymphocytes in the lymph node. A. Schematic overview of the general LN structure. Orange zones indicate B-cells zones (BCS), red structure represents T-cells zone (TCZ). Interfollicular zones (IFZ) are the connection between the BCZs. Between the TCZ and the T-cell-B-cell border high endothelial venules (HEV) are displayed. Furthermore, subcapsular sinus (SCS) macrophages and medullary sinus macrophages are shown in the SCS and medullary sinus, respectively. **B.** Localization of different T-cell subpopulations in the different zones of the LN. **C.** Location of cDC1 (violet border) and cDC2 (cyan border) among migratory DCs (filled with blue) and resident DCs (filled with yellow), respectively. Modified from (Eisenbarth, 2019).

The spleen is the largest secondary lymphoid organ, which drains the circulatory systems as it filters blood to recycle red blood cells and clear blood-borne antigens (Eisenbarth, 2019). It is essential to support rapid B- and T-cell responses against circulating antigens (Mebius & Kraal, 2005). For these purposes, the spleen is divided into the blood filtering regions, the so-called red pulp and the lymphoid compartments that contain the immune cells which are called white pulp (Mebius & Kraal, 2005). The sub-organization of the white pulp resembles the LN structure and, therefore, is divided into T- and B-cell compartments (Mebius & Kraal, 2005). In the spleen, most DC2 localize to the bridging channels close to the T-cell zone and only some can be found in the marginal zone or red pulp of the spleen (Dudziak et al., 2007). cDC1, in contrast, can be found within the T-cell zones but also in the marginal zone (De Smedt et al., 1996; Idoyaga, Suda, Suda, Park, & Steinman, 2009; Kraal, Twisk, Tan, & Scheper, 1986). After the encounter of a microbial stimulus, the DCs in the spleen have been shown to redistribute to the T-cell zones, which is important to get in contact with and activate T-cells (Idoyaga et al., 2009; Reis e Sousa et al., 1997).

1.2.3 DENDRITIC CELL MIGRATION

DC migration is facilitated by several chemokines, such as CCL19 and CCL21, CCL17, CCL22, CXCL12, CCL8 (Rapp et al., 2019; Ricart, Yang, Hunter, Chen, & Hammer, 2011; Sokol, Camire, Jones, & Luster, 2018; Stutte et al., 2010) and their respective chemokine receptors CCR7, CCR4, CCR8, CXCR4 and CXCR7. The interaction of the relevant chemokines and receptors is shown in **Figure 3** (Ohl et al., 2004).

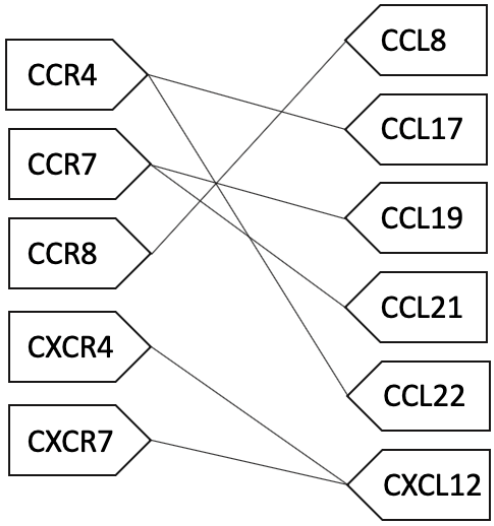

Figure 3: DC migration relevant chemokines and receptors. Chemokine receptors and the corresponding chemokines are linked with a line. Adapted from 2(Bachelerie et al., 2014)

The CCL19/CCL21-CCR7 axis provides the most important directional cue for the trafficking of DCs to and within the LN (Ohl et al., 2004). Gradients of the CCR7 binding chemokines CCL19 and CCL21 are built up by expression in the tissues (Förster, Davalos-Misslitz, & Rot, 2008; Hauser et al., 2016; Link et al., 2007; Worbs, Mempel, Bölter, Andrian, & Förster, 2007). Although CCL19 and CCL21 bind to the same receptor, they act in different ways depending on their expression pattern and structure (Hjortø et al., 2016). CCL19 and CCL21 share only 25% sequence identity and are expressed by different cell types (Ott et al., 2006). Whereas both chemokines are expressed by stromal cells in the T-cell zones of the LN, CCL19 is also expressed by DCs and can act in an autocrine fashion (Carlsen, Haraldsen, Brandtzaeg, & Bækkevold, 2005; Katou et al., 2003; Luther, Tang, Hyman, Farr, & Cyster, 2000; Ngo, Tang, & Cyster, 1998). CCL21 has an additional C-terminal tail, which facilitates enhanced affinity to glucosaminoglycans (GAGs) (Hromas et al., 1997; Love et al., 2012). Through cleavage of the C-terminal tail of CCL21 by DC-derived proteases or plasmin the soluble form of CCL21 is generated that forms a chemotactic gradient (Lorenz et al., 2016; Schumann et al., 2010). The chemotactic gradient is further maintained by the GAG affinity of CCL21, which enables it to bind to the extracellular matrix and cell surfaces (Schumann et al., 2010). The immobilized CCL21 gradient provides a strong stimulus for haptokinetic movement of the DCs in the tissue towards the lymph vessel (Weber et al., 2013). The N-termini of CCL19 and CCL21 facilitate

the binding to CCR7 but provoke distinct receptor signalling as depicted in **Figure 4**. Binding of both CCL19 and CCL21 leads to receptor phosphorylation of the G-protein coupled receptor CCR7 by GRK6, β-arrestin 2 recruitment, and downstream signalling but binding of CCL21 induces a stronger intracellular calcium release and stronger ERK signalling (Hauser et al., 2016; Hjortø et al., 2016; Ricart et al., 2011) whereas CCL19 serves as a more potent chemotactic cue that initiates better recruitment of β-arrestin 2 and initializes CCR7 internalization more effectively, which leads to desensitization of the receptor (Bardi, Lipp, Baggiolini, & Loetscher, 2001; Byers et al., 2008; Hjortø et al., 2016; Kohout et al., 2004; Otero, Groettrup, & Legler, 2006; Zidar, Violin, Whalen, & Lefkowitz, 2009). DC migration, therefore, is a very complex process that is regulated by different chemokines that have different effects on the migration.

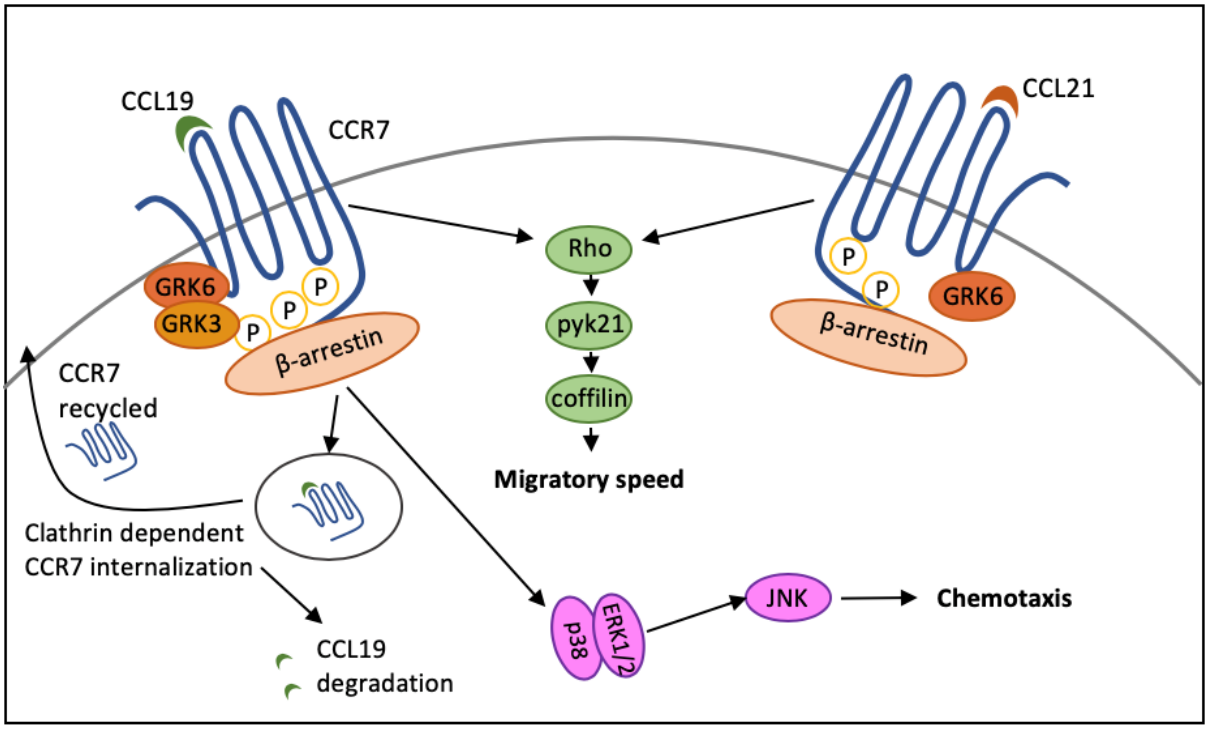

Figure 4: CCL19 and CCL21 mediated CCR7 signalling. CCL19 and CCL21 both bind theCCR7 but initiate divergent intracellular responses. Both facilitate migration via CCR7, Rho, pyk21, and cofilin, but CCR19 is stronger in inducing chemotaxis and CCR7 internalization. Adapted from (Noor & Wilson, 2012)**.**

1.3 HISTORY OF DENDRITIC CELL ONTOGENY

Historically, DCs are a population of cells belonging to the mononuclear phagocyte (MNP) network, together with monocytes and macrophages (Guilliams et al., 2014). A reason for this classification was that monocytes were considered the precursor of DCs as, indeed, monocytes give rise to DCs especially in culture conditions with GM-CSF and IL-4 (Romani et al., 1994; Sallusto & Lanzavecchia, 1994). With the advances in technology since that time, however, the cells of the MNP network can be distinguished in populations with different functions and origins for example by making use of expression patterns of surface molecules

and flow cytometric analyses (Guilliams et al., 2014). There are however still limitations of distinction of populations within the MNP network resulting from the fact that cells can adapt their surface marker expression to the microenvironment of the organ they are residing in and in the course of activation in inflammatory conditions. As an example, DCs in the kidney express the surface marker CD64, which is generally thought to mark cells of monocyte origin, which complicates the assignment to a developmental origin (Langlet et al., 2012; Schraml et al., 2013). In addition, monocytes further differentiate into cells resembling either DCs or macrophages during infection (Cheong et al., 2010) and these monocyte-derived DCs (moDCs) show great overlap of surface receptors and express for example the typical DC surface markers CD11c and MHCII but differ in their function (Guilliams et al., 2014). It becomes obvious, that origin plays an important role in the classification of specific cell lineages order to fully understand their turn over in different conditions and especially because origin can have an impact on the function of the cells. For DCs, the origin still is a highly debated field because, *in vitro*, multiple progenitors were shown to give rise to DC (Manz, Traver, Miyamoto, Weissman, & Akashi, 2001b). Why the development of DCs can be so diverse and under which physiological conditions this redundancy is required is not fully understood yet.

1.3.1 THE LYMPHOID ORIGIN OF DENDRITIC CELLS

Lymphoid and myeloid progenitors are thought to branch after the multipotent progenitor (MPP) stage. Lymphoid-primed multipotent progenitors (LMPPs) further differentiate into common lymphoid progenitors (CLPs), which give rise to the lymphoid lineage, including B and T-cells. Common myeloid progenitors (CMPs) exclusively generate granulocytes, monocytes and dendritic cells (Nimmo, May, & Enver, 2015). One indicator to distinguish cells of lymphoid origin is D-J rearrangements in the heavy chain locus of the B-cell receptor (Borghesi et al., 2004). These rearrangements occur as an early event in the commitment of progenitors to the lymphoid lineage and depend on the expression of Rag1 (Borghesi et al., 2004; Schlissel, Corcoran, & Baltimore, 1991; Welner et al., 2009). Many studies have shown that lymphoid progenitors, such as the CLPs, LMPPs and pro-B cells can give rise to cDCs under certain conditions like, in *in vitro* systems and after adoptive transfer into irradiated mice (Björck & Kincade, 1998; Izon et al., 2001; Manz, Traver, Miyamoto, Weissman, & Akashi, 2001b; Naik et al., 2013; Traver et al., 2000; Welner et al., 2008). Interestingly, the DCs obtained from lymphoid origin and the DCs that were obtained from myeloid origin show no functional difference in mixed leukocyte reactions as well as IL-12 production after different stimuli (Manz, Traver, Miyamoto, Weissman, & Akashi, 2001b; Wu et al., 2001). However, it has been reported that TLR9 stimulation increases the potential of lymphoid progenitors to give rise to DCs (Welner et al., 2008; 2009) implying that lymphoid progenitors are more prone

to give rise to DCs under inflammatory conditions. In steady state, however, it is generally thought that cDCs derive from myeloid progenitors as they are not labelled in *IL7R-creRFP* reporter mice that label lymphoid progenitors based on the expression of the IL7 receptor (Schlenner et al., 2010). Furthermore, CMPs are more potent at producing cDC outcome compared to CLPs (Manz, Traver, Miyamoto, Weissman, & Akashi, 2001b; Traver et al., 2000). In the thymus, but not in the spleen, DC1 have been shown to have signs of lymphoid past and therefore are considered to be lymphoid derived in this specific tissue (Corcoran et al., 2003). Nevertheless, it remains unknown if lymphoid DC poiesis happens in other organs under specific physiological conditions and why the DC potential exists in progenitors of different hematopoietic lineages despite functional redundancy.

1.3.2 THE MYELOID ORIGIN OF CONVENTIONAL DENDRITIC CELLS

In steady-state, cDCs are considered to belong to the myeloid lineage (Corcoran, Manz, Traver). The development of cDCs starts in the BM: Downstream of hematopoietic stem cells (HSC) and multipotent progenitors (MPP), common myeloid progenitors (CMPs) differentiate that further give rise to granulocyte-monocyte progenitors that develop into macrophage dendritic cell progenitors (MDPs) (Auffray et al., 2009). MDPs can give rise to both monocytes and common dendritic cell progenitors (CDPs) and the development starting from the MDPs is depicted in **Figure 5** (Liu et al., 2009; Naik et al., 2007; Onai et al., 2007). CDPs give rise to cells resembling pDCs and pre-cDCs (Auffray et al., 2009; Fogg et al., 2006; Naik et al., 2007; Onai et al., 2007; Rodrigues et al., 2018). The development until the pre-cDC stage takes place in the bone marrow (BM). From there pre-cDCs migrate into the blood and home to peripheral tissues where they fully differentiate into the different subsets of cDCs (Liu et al., 2009). The factors that regulate the BM egress of pre-cDCs and their homing to different peripheral tissues are not fully understood. But it has been shown that CXCR4 expression on pre-cDCs facilitates the retention to the BM (H. Nakano, Lyons-Cohen, Whitehead, Nakano, & Cook, 2017). Furthermore, CCR2 and CX3CR1 expression in pre-cDCs are known to be relevant for the migration to the lung, in steady-state, whereas only CCR2 is relevant for the migration of pre-cDCs to the inflamed lung (H. Nakano et al., 2017).

DC development depends on different growth factors, such as Flt3L but also GMCSF (Banchereau & Steinman, 1998; Durai et al., 2018; Inaba et al., 1992; Maraskovsky et al., 1996; Pulendran et al., 1997; Saunders et al., 1996). These cytokines are also commonly used to differentiate DCs from BM precursors *in vitro* however, while Flt3L cultures yield mainly pDCs and cDCs, GMCSF cultures also give rise to a mixture of cell types including monocyte-derived macrophages, monocyte-derived dendritic cells but also CDP derived DCs (Helft et al., 2017; Karsunky, Merad, Cozzio, Weissman, & Manz, 2003). For studying the function of

DCs, culture systems are a useful tool to generate large amounts of DCs however it has to be considered which progenitor is expanded by which growth factor and that this could have an effect on the functionality of the cells.

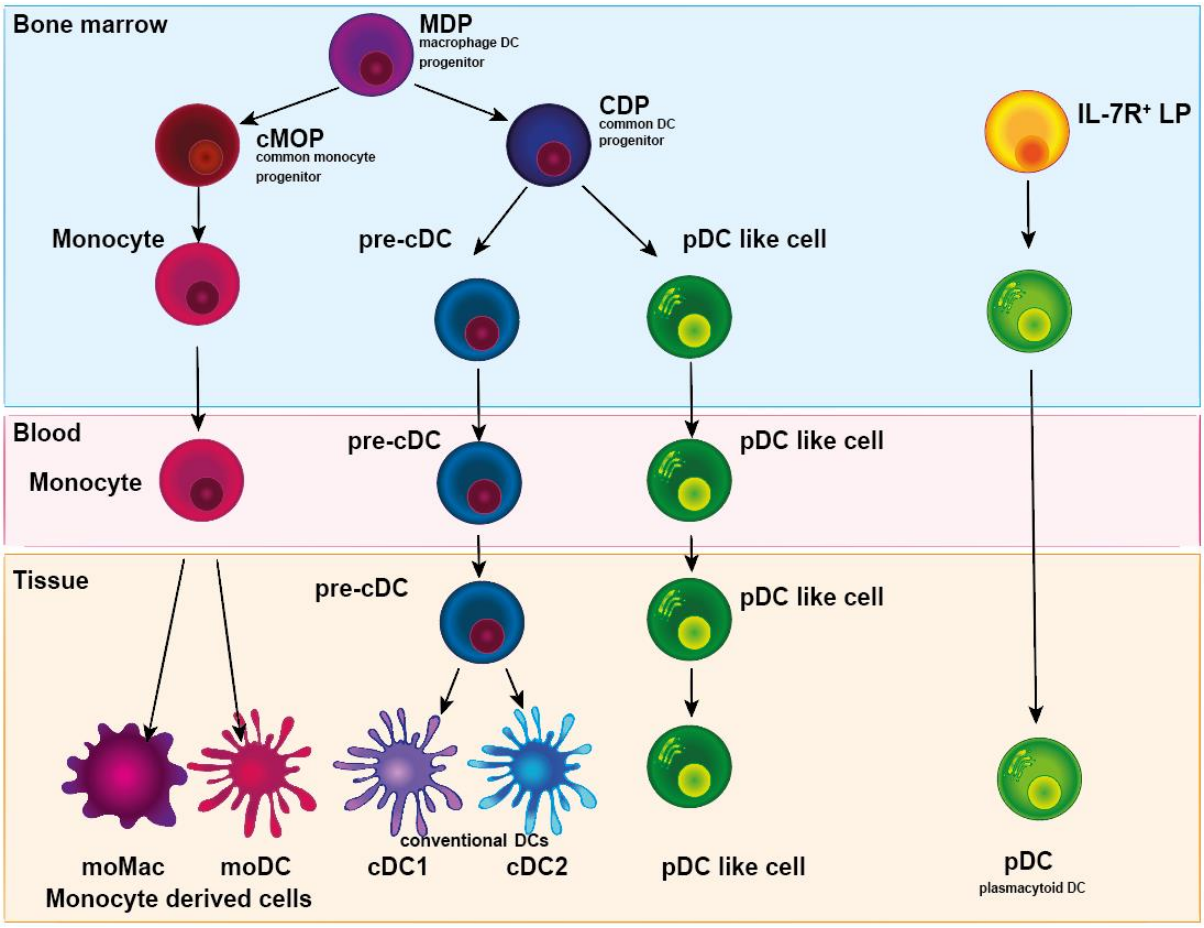

Figure 5: Myeloid development of cDCs, pDCs, and monocyte-derived cells. Downstream of hematopoietic stem cells macrophage and dendritic cell progenitors (MDPs) develop within the myeloid lineage. MDPs have the potential to generate either the monocytes via common monocyte progenitors (cMOPs) or conventional dendritic cells via the common dendritic cell progenitor CDP and the immediate DC precursor pre-cDC. pDCs were originally thought to derive from CDPs however recent evidence shows that IFN-producing pDCs derive from IL7R^{+} lymphoid progenitors (LPs) and suggests to call CDP derived pDCs pDC like cells (Rodrigues et al., 2018). The background color indicates the location of the cell type in the body.

1.3.3 Subset commitment of dendritic cell progenitors

The two cDCs subsets cDC1 and cDC2 that are typically distinguished are developmentally and functionally distinct (Guilliams et al., 2014). It is however not clear whether the differentiation into the two main DC subsets shows plasticity or flexibility of one common progenitor or if they derive from distinct progenitors that have split from upstream progenitors. Pre-cDC differentiation into cDC1 or cDC2 takes place in the different peripheral organs and the differentiation is known to depend on different transcription factors for the different subsets. Transcription factors that are important for the development of cDC1 are IRF8, Batf3 and NFIL3 (Hildner et al., 2008; Kashiwada, Pham, Pewe, Harty, & Rothman, 2011; Schiavoni et

al., 2002) whereas cDC2 development depends on RelB, Pu1, RBPJ and IRF4 (Caton, Smith-Raska, & Reizis, 2007; Chopin et al., 2018; Guerriero, Langmuir, Spain, & Scott, 2000; Lewis et al., 2011; Satpathy et al., 2013; Schlitzer et al., 2013; S. Suzuki et al., 2004a; Wu et al., 1998). In different peripheral organs, different subset ratios of cDCs can be identified and also site-specific DC subsets exist for example in the lamina propria and in the kidney (Bogunovic et al., 2009; C. L. Scott, Tfp, Beckham, Douce, & Mowat, 2014). Therefore, one hypothesis is that signals within the organ of destination, the tissue microenvironment, dictate the differentiation into cDC1 or cDC2 or the tissue-specific subsets. Recent publications however have identified pre-committed pre-cDC populations already in the BM suggesting a subset imprinting at the CDP stage that initiates a transcriptomic program to either cDC1 or cDC2 regardless of the tissue microenvironment (Breton et al., 2016; Grajales-Reyes et al., 2015; J. Lee et al., 2015; Schlitzer et al., 2015; See et al., 2017). This suggests that the pre-cDCs pre-committed before they migrate to the different organs as well. This raises the question if there is differential recruitment to peripheral organs among the pre-committed pre-cDCs that explains the variation in DCs subsets and its ratio. A recent publication in this context suggests that the migration of different pre-cDC subsets is indeed differentially regulated by showing that the migration to melanoma tumours of pre-cDC1 but not pre-cDC2 depends on the expression of CXCR-3 (S. J. Cook et al., 2018).

1.4 Mouse models are used to distinguish DCs from other mononuclear phagocytes and to identify their functions

The phenotype of DCs partially overlaps with other cells of the MNP network. The distinction of DCs is especially difficult upon infection when monocyte differentiate into monocyte-derived DCs (Cheong et al., 2010). Therefore, it is necessary to develop models that help to identify DCs in the best case DCs of a certain developmental lineage. To further not only identify the cells based on their origin but also identify the specific function of the cells specific DC depletion models have been established. With these, one can ideally knock out all CDP derived DCs or one specific subset and compare the functionality of immune responses in the absence of these cells, to understand their specific immunogenic role.

The most abundantly used model to mark and manipulate cDCs are the *Itgax-DTR/GFP* mouse model (Hochweller, Striegler, Hämmerling, & Garbi, 2008; Jung et al., 2002) in which the CD11c promoter drives the expression of a diphtheria toxin receptor and a green fluorescent protein (GFP). Here, CD11c expressing cells are fluorescently labelled and can conditionally be depleted with the administration of diphtheria toxin (DT). This model is however not specific to DCs as depletion broadly affects cells of the MNP network, such as macrophages, Langerhans cells as well as plasmablasts, T-cells, and non-immune cells,

which leads to inconclusive results when analysing DC function (Bar-On et al., 2010; Bennett & Clausen, 2007; Jung et al., 2002; Probst et al., 2005; Tittel et al., 2012; van Blijswijk, Schraml, & Reis e Sousa, 2013). Other mouse models that are used to label cDCs or deplete them are the *Zbtb46-GFP* or *-DTR* model, respectively (Meredith et al., 2012; Satpathy et al., 2012). *Zbtb46* expression is more restricted to cDCs and not expressed by other immune cells except some activated monocytes, but the depletion of DCs with a single dose of DT is lethal in these mice, presumably due to *Zbtb46* expression in endothelial cells, which can only be circumvented by BM transplantation (Finger Stadler, Patel, Pacholczyk, Cutler, & Arce, 2017; Meredith et al., 2012; Rombouts et al., 2017). To deplete cDC1 specifically, different models are available, such as *CD205-DTR* (Fukaya et al., 2012), Batf3$^{-/-}$(Hildner et al., 2008), IRF8$^{-/-}$ (Aliberti et al., 2003; Schiavoni et al., 2002) and *XCR-1-DTRvenus* (Yamazaki et al., 2013). Specific depletion of the cDC2 has been reported in RelB$^{-/-}$ mice (Wu et al., 1998) and *Clec4a4-DTR* mice but here, analyses have been restricted to the lamina propria (Durai & Murphy, 2016; Muzaki et al., 2016).

Dendritic cell natural killer lectin group receptor-1 (DNGR-1), which is encoded by the gene *Clec9a,* was originally found to be expressed in cDC1 and to a lower extent also on pDCs but furthermore also expression on DC restricted precursors has been observed (Caminschi, Lahoud, & Shortman, 2009; Poulin et al., 2012; Sancho et al., 2009; Schraml et al., 2013). A lineage-tracing mouse model for cDCs was, therefore, established by crossing *Clec9a*^{cre} mice to Rosa26-stop^{flox}-enhanced yellow fluorescent protein (YFP). These mice faithfully trace cells that derive from CDPs. Additionally, pDCs are labelled due to their low-level DNGR-1 expression with fluorescence. The *Clec9a*^{cre}*Rosa*^{YFP} mouse model does, however, not label cells of other hematopoietic lineages and is therefore highly specific (Schraml et al., 2013). By crossing *Clec9a*^{cre} mice to a ROSA26-LSL-DTR strain, conditional depletion of cDC1, as well as cDC2, is possible that is highly specific (van Blijswijk et al., 2014).

What has to be considered when working conditional DC depletion models that rely on DTR expression and DT injection is that they have the disadvantage of showing reduced LN cellularity and DC frequency in mice expressing DTR without DT injection and therefore have to be used carefully (van Blijswijk et al., 2014). Furthermore, long-term DTR dependent DC depletion models cannot be used in chronic experiments due to the fact that mice develop antibodies against the DT, which lowers the depletion efficiency drastically (Rombouts et al., 2017).

What needs to be considered dealing with DC depletion models is that the depletion has effects on the homeostasis of other cells in the body as well, which can lead to secondary effects when analysing functional differences. Mice that have a depletion of all cDCs or even

only cDC1 have been reported to show increased spleen size as well as monocytosis and neutrophilia, which goes in hand with increased Flt3L levels (Birnberg et al., 2008; Finger Stadler et al., 2017; Hochweller et al., 2008; Jiao et al., 2014; Meredith et al., 2012; Rombouts et al., 2017; Sichien et al., 2016; Tittel et al., 2012; van Blijswijk et al., 2014). Therefore, DC depletion models are a useful means to study the function of DCs in general or of one subset specifically, however careful choice of the model in terms of specificity or inducibility as well as proper controls to avoid misinterpretation of results that derived from secondary effects are necessary. Furthermore, the development of more specific models will help to evolve a better understanding of the role of DCs in different immune responses.

2. AIM OF THE THESIS

This study aimed to address the development of dendritic cells. For this purpose, the trafficking of DC progenitors was taken into focus. The signals that regulate the egress of pre-cDCs from the BM and their entry into peripheral tissues were to be identified. Furthermore, the existence of pre-commitment in pre-cDCs has led to the hypothesis that pre-committed subsets are differentially recruited to different tissues. Therefore, this study aimed to determine regulators for the BM egress of pre-cDCs and pre-committed pre-cDC subsets and their homing to peripheral tissues. This will improve the understanding of pre-cDC recruitment in steady-state and further enable a comparison of pre-cDC recruitment in inflammatory settings during emergency haematopoiesis. Differences in the recruitment of pre-cDCs in inflammation can be clinically relevant because knowledge about recruitment provides a tool to improve immune responses.

In order to further study the function of DCs, *Clec9a*^{cre} mice were crossed to *Rosa26-lox-STOP-lox-DTA* mice to gain a depletion model that specifically lacks DCs. Thereby it can be studied how immune responses differ in the absence of DCs. This thesis aimed to characterize the mouse model in terms of DC depletion but further found that a population of cells resembling cDC2 developed independent of DC progenitors in these mice. This has led to the hypothesis that different DC progenitors are differentially triggered in certain conditions of inflammation to generate a situation-adapted repertoire of cDCs and directed the study to further gain knowledge on the origin of these cells as well as on functional differences that elucidate their specific role in immunity.

3. MATERIALS AND METHODS

3.1 ANIMAL HUSBANDRY

C57BL/6J, OTII/Thy1.1, Clec9a-Cre, Rosa26-lox-STOP-lox-DTA, and Rosa26-lox-STOP-lox-DTR mice were bred at ENVIGO, the core facility animal models in the Biomedical Center or at the Cancer Research UK in specific-pathogen-free conditions. All experiments were performed in accordance with national and institutional guidelines for animal care and were approved by the Regierung of Oberbayern or the Francis Crick Institute Animal Ethics Committee and the UK Home Office.

3.2 GENOTYPING BY PCR

To determine the genotype of transgenic lines (*Clec9a-Cre, Rosa26-lox-STOP-lox-DTA, and Rosa26-lox-STOP-lox-DTR)*, mice were genotyped using polymerase chain reaction (PCR). Ear samples were taken from the mice and digested for 3h at 56°C and shaking at 300rpm in 200µl quick lysis buffer (10mM TRIS, 150mM NaCl, 5mM EDTA, 0.05% tergitol NP40, pH 8.0) containing proteinase K (0.2mg/ml, Sigma). After the digestion, the samples were heat-inactivated for 10min at 90°C and 350rpm. The solution was centrifuged at 12700rpm for 5min and 1ul of the supernatant was directly used as DNA input to the PCRs. The genotyping PCR for the *Rosa26-lox-STOP-lox-DTA* locus was performed according to the protocol Gt (Rosa)26Sor$^{tm1(EYFP)Cos}$ provided from the Jackson Laboratory for the *Rosa26-lox-STOP-lox-EYFP locus.* The genotyping PCR for the *Rosa26-lox-STOP-lox-DTR* locus was performed according to the protocol Gt (ROSA)26Sor^{tm1sor} STD provided from the Jackson laboratory. The genotyping PCR was performed using 0.5µM common and 0.25µM of each wild type and mutant primers **Table 1** and run with the protocol shown in **Table 2**.

Table 1: PCR primers

PCR primers	Sequence 5'-3'
Clec9a-Cre-BS49 Common	AAA AGT TCC ACT TTC TGG ATG ATG A
Clec9a-Cre-BS47 Wild type	GGC TCT CTC CCC AGC ATC CAC A
Clec9a-Cre-A65 Mutant	TCA CTT ACT CCT CCA TGC TGA CG
RosaDTA Common	AAA GTC GCT CTG AGT TGT TAT
RosaDTA Wild type	GGA GCG GGA GAA ATG GAT ATG
RosaDTA Mutant	AAG ACC GCG AAG AGT TTG TC
RosaDTR Common Forward	AAA GTC GCT CTG AGT TGT TAT
RosaDTR Wild type Reverse	GGA GCG GGA GAA ATG GAT ATG
RosaDTR Mutant Reverse	AAT AGG AAC TTC GTC GAG C

Table 2: PCR programs

Cre and DTA				DTR		
Temperature	time	step		Temperature	time	step
95 °C	3 min	1		94 °C	5 min	1
95 °C	30 s	2		94 °C	30 s	2
60 °C	30 s	3		61 °C	1 min	3
72 °C	40 s	4 to 2 35 cycles		72 °C	1 min	4 to 2 35 cycles
72 °C	10 min	5		72 °C	10 min	5
4 °C	end	6		4 °C	end	6

3.3 CELL ISOLATION FROM DIFFERENT TISSUES

3.3.1 BONE MARROW

Femurs, tibias, and ilia (optional) were isolated from mice and cleaned from muscle and connective tissue. For sterile cultures the bones were quickly washed in 70% ethanol and washed again with sterile FACS-Buffer (DPBS, Sigma; 1% fetal bovine serum, Sigma; 2.5mM EDTA, Invitrogen; 0.02% sodium azide, Sigma, 10% w/v stock; for culturing of cells, FACS buffer without sodium azide was used). Bones were cut open from both sides and flushed with FACS buffer into a 70µm cell strainer (Falcon). Red blood cells were lysed by incubation of the cell pellet in 2ml red blood cell lysis buffer (Sigma) followed by washing with FACS buffer and repeated filtering of the suspension (70µm).

3.3.2 SPLEEN, THYMUS AND LYMPH NODES

Spleen, thymus, and LNs were cut in small pieces and digested in 1ml RPMI (Gibco) containing 200U/ml collagenaseIV (Worthington) and 0.2 mg/ml DNaseI (Roche) for 30min at 37°C shaking at 120rpm. The cell suspension was strained through a 70µm cell strainer and washed with FACS buffer. For cell isolation from spleen, erythrocytes were lysed as described for BM cells.

3.3.3 LUNG AND KIDNEY

Kidneys and lung were isolated from mice after perfusion of the heart with PBS in the left or right chamber, respectively. Organs were cut in small pieces and digested in 2ml RPMI (Gibco) containing 200U/ml collagenaseIV (Worthington) and 0.2 mg/ml DNaseI (Roche) for 1h at 37°C shaking at 120rpm. The cell suspension was strained through a 70µm cell strainer and washed with FACS buffer. The cell pellet was resuspended in 4ml of a 70% percoll solution overlaid by 4ml of a 37% percoll solution and again overlaid by 1ml of a 30% percoll solution

in a 15ml falcon tube. By centrifugation of the cells in this gradient at 2000rpm for 30min at room temperature without brakes leukocytes were enriched at the 70%-37% interphase. Percoll solutions were diluted from 100% percoll (GE Healthcare mixed 9:10 with 10x PBS) with PBS (37%) or HBSS (70% and 30%). After the centrifugation, the cells were collected at the 70%-37% interphase.

3.3.4 SMALL INTESTINE AND COLON

After removing the gut from the mouse, the fat, connective tissue and payer's patches were removed. The colon or small intestine were cut open longitudinally and the feces as well as the mucosa were removed in ice-cold PBS. 1cm long pieces were incubated for 20min in complete medium (RPMI (Gibco), 1% L-Glutamine (Sigma), 1% penicillin-streptomycin (Sigma), 1% sodium pyruvate (Sigma), 1% non-essential amino acids (Sigma), 50µM β-mercaptoethanol (Gibco)) additionally supplemented with 25mM HEPES (Gibco), 3% FCS, 5mM EDTA and 0.145mg/ml dithiothreitol (DTT, Roche) shaking at 180rpm. The pieces were then strained through a fine-meshed kitchen strainer and washed 3 times with 10ml serum-free medium containing 25mM HEPES and 2mM EDTA by repeated shaking on a vortex for 30sec and straining. Tissue pieces were then cut in small pieces and digested in 10ml serum free medium containing 200U/ml collagenaseIV (Worthington) and 0.2 mg/ml DNaseI (Roche) for 1h at 37°C shaking at 180rpm. After the digestion, the cell suspension was strained though a 70µm cell strainer and washed with ice-cold FACS buffer. Leukocytes were enriched using a percoll gradient as described above.

3.3.5 SKIN

For isolation of leukocytes from the skin, ears were cut from the mice, cartilage was removed, ears were weighed and split into dorsal and ventral halves. Each half was incubated floating on 1ml PBS containing 2U/ml dispaseII (Gibco) in a 24 well plate (Falcon) for 1-1.5h at 37°C. After the digestion, the ears were flattened on a petri dish with the epidermal side to the plate and the dermis was carefully separated from the epidermis using forceps. Dermis and epidermis were then separately cut in small pieces and digested in 2ml RPMI containing 200U/ml collagenaseIV (Worthington) and 0.2 mg/ml DNaseI (Roche) for 1h at 37°C while shaking at 120rpm. After the digestion, the cell suspension was strained through a 70µm cell strainer and washed with ice-cold FACS buffer. Leukocytes were enriched using a percoll gradient as described above.

3.4 FLOW CYTOMETRY

For cell surface staining, the single-cell suspensions were incubated with Fc-Block (purified CD16/32 Antibody in FACS buffer at 1:300 dilution) for 10min at 4°C. After this blocking step

a 2x antibody cocktail was added to the cell suspension, carefully mixed and incubated for 20 min at 4°C. The cell suspension was washed twice and resuspended in FACS buffer for analysis. For CCR7 staining, the cells were stained at 37°C for 45min. To exclude dead cells for the analysis, either DAPI was added at 0.25µg/ml final just before the acquisition or the cells were stained with a Fixable Viability Dye eFluor™ 780 (Thermo Fisher Scientific) or Zombie UV dye (Biolegend) according to the manufacturer's instructions. For the staining of apoptotic cells, surface stained cells were washed one additional time and resuspended in complete Medium with 10%FCS. 10min prior to acquisition 10µl annexin staining buffer was added to the sample (complete Medium with 0.5µg/ml annexin and 0.1M $CaCl_2$).

For intracellular cytokine staining, after extracellular surface staining, cells were fixed with 2% paraformaldehyde for 15 min at room temperature and subsequently washed in 0.05% saponin in PBS. The antibody mix against cytokines was prepared in 0.5% saponin and cells were stained with this for 20min. Cells were washed once with 0.05% saponin, once with FACS buffer and resuspended in FACS buffer for analysis. For intranuclear staining of IRF4 and IRF8, the FOXp3 transcription factor staining set (eBioscience-00-5523-00) was used according to the manufacturer's instruction and for intranuclear staining of Zbtb46 the transcription factor buffer from BDBioscience-562574 was used. Multiparameter analysis was performed at a BD Fortessa analyser (BD Biosciences) and analysed with FlowJo software (Tree Star Inc.). Cell sorting was performed at a BD Aria III Fusion or BD Aria III.

3.5 CELL ENRICHMENT

3.5.1 POSITIVE ENRICHMENT

$CD11c^+$ cells were enriched from splenic cell suspensions by magnetic separation using magnetic beads and LS columns from Miltenyi Biotec. $CD135^+$ cells were enriched using anti-biotin microbeads and LS-columns (Miltenyi Biotech) after staining the cells from different tissues with biotinylated anti-CD135 antibody.

3.5.2 LIN DEPLETION

For isolation of DC progenitors, BM cells were isolated as described above and stained with FITC conjugated antibodies against CD4, CD8, CD16/32, CD11b, B220, MHCII, Ter119, NK1.1. Lineage positive cells were then depleted by magnetic separation using anti-FITC microbeads on LD-columns (Miltenyi Biotech). Lineage depleted cells were sorted as follows: pre-cDC (Lin^-, $CD11c^+$, $CD172a^{int}$), MDP (Lin^-, $CD11c^-$, $CD115^+$, $CD135^+$, $CD117^{hi}$), CDP (Lin^-, $CD11c^-$, $CD115^+$, $CD135^+$, $CD117^{lo\text{-}int}$). For the isolation of $CD4^+$ T-cells, splenocytes and cells isolated from LNs by simply straining them through a 70µm cell strainer (Falcon) were enriched by Lineage depletion using FITC conjugated CD8, CD16/32, B220, MHCII, CD11c,

CD11b, NK1.1, and anti-FITC magnetic beads. Lineage positive cells were then depleted by magnetic separation using anti-FITC microbeads on LD-columns (Miltenyi Biotech).

3.6 CYTOSPINS AND HEMACOLOR STAINING

$CD11c^+$ cells were isolated from splenic single-cell suspensions using magnetic enrichment (Miltenyi Biotech), and sorted for live, single cells, $F4/80^{lo}$, $CD64^-$, $CD11c^+$ $MHCII^+$ $CD11b^+$, $CD172a^+$. 20 000 cells were spun on a microscope slide in a Shandon Cytospin 2 for 3min at 8000rpm and stained with Hemacolor® rapid staining kit (Merck).

3.7 MULTIPLEX QUANTITATIVE PCR USING FLUIDIGM

RNA was extracted from sort purified populations using the Qiagen micro Pus RNeasy kit, according to the manufacturer's instructions. RNA was transcribed into cDNA using the SuperscriptIII (Invitrogen) kit and random primers (Company). Primer mixes (Delta Gene Assays) for 96 targets were purchased from Fluidigm. The cDNA was pre-amplified using a mix of all delta gene assays according to the manufacturer's instruction (Fluidigm PN 100-5875 C1). The gene expression analysis on the pre-amplified samples was performed in a 96.96 IFC from Fluidigm that measures the expression of up to 96 targets in up to 96 samples in a Biomark HD according to the manufacturer's instructions (Fluidigm PN 100-9792 B1). Q-PCR results were calculated using the delta-delta Ct method and GAPDH was used as a housekeeping gene. Targets that did not show expression in all analysed pre-cDC populations were excluded from the analysis and potential targets were imported in a heatmap showing relative expression in all samples scaled per target.

3.8 *IN VITRO* DENDRITIC CELL MIGRATION THROUGH TRANSWELLS

DC migration assays in Transwells were performed adapted to previously published assays for BMDCs (Stutte et al., 2010; Williams, Morris, Rush, & Ketheesan, 2014). The *in vitro* migration assay was performed using 24-well Transwell® inlets (Corning®, CLS3421-48EA) with polycarbonate filters with 5µm pore size. The transwells were preincubated with the chemokine in 600ul complete medium in the lower well at 37°C, 5% CO_2 in a humidified incubator 1h before seeding the upper well. As chemokines CCL2 (indicated concentrations, R&D Systems), CCL19 (100ng/ml, PeproTech), CCL21 (100ng/ml, PeproTech) or CXCL12 (200ng/ml, R&D Systems) were used. Complete medium without chemokine served as the negative control. 10^5 total BM cells or CD11c enriched splenocytes as described above were seeded in 100µl complete medium to the inlet of the transwell and incubated at 37°C, 5% CO_2 in a humidified incubator for 2h. Optionally CD11c enriched splenocytes were stimulated with LPS (200ng/ml, Enzo) for 18h prior to seeding them in the transwell. After the incubation, the

inlets were removed and the cells that have migrated to the lower well were harvested, stained and quantified using flow cytometric analyses and CountBright™ Absolute Counting Beads (Thermo Fisher Scientific). For the calculation, the absolute count of a population that was harvested from the lower well was divided by the input count of the respective population giving the percentage of migrated cells for the indicated population.

3.9 EAR EXPLANT ASSAY

The ears were removed from the mouse, cartilage was removed, and the ears were weighed. Then the ears were soaked in 70% ethanol and air-dried under sterile conditions for 10min. After drying the ears were separated into dorsal and ventral halved and incubated in a 24 well plate with the dermal side sown on 1ml complete medium with 10% FCS for 2h at 37°C 5% CO_2 and then transferred to a 24 well plate with 1ml complete medium with 10% FCS with or without CCL19 (100ng/ml, PeproTech). The ears were incubated for 24h at 37°C and 5% CO_2 (Henri et al., 2001). After the incubation, the ears were removed from the Medium and the cells that have migrated to the medium were harvested, stained for flow cytometric analyses and counted using CountBright™ Absolute Counting Beads (Thermo Fisher Scientific).

3.10 CELL CULTURE

3.10.1 FLT3L CULTURES

Cells were seeded together with CD45.1 filler BM in 48 well plates and incubated at 37°C, 5% CO_2 for 7 days in RPMI (Biochrome), 10% fetal calf serum, 1% penicillin/ streptomycin, 1% non-essential amino acids, 1% sodium pyruvate, 1% L-Glutamine, 50µM β-mercaptoethanol and stimulated with 50ng/ml Flt3L from the cell culture supernatant of CHO-Flt3L-Flag cell line.

Total bone marrow cells or sorted cells were seeded (optional together with CD45.1 filler BM) in 48 well plates and incubated at 37°C, 5% CO_2 for 7 days in RPMI (Biochrome), 10% fetal calf serum, 1% penicillin/ streptomycin, 1% non-essential amino acids, 1% sodium pyruvate, 1% L-Glutamine, 50µM β-mercaptoethanol and stimulated with 50ng/ml from the cell culture supernatant of CHO-Flt3L-Flag cell line.

3.10.2 GM-CSF CULTURES

For GM-CSF only cultures a concentration of 10ng/ml GM-CSF (PeproTech) was used. 1.5 x 10^5 cells were seeded in one well of a 48 well plate in a total volume of 300µl. On day 2 half of the medium was removed and exchanged with fresh medium containing 20ng/ml GM-CSF. On day3 the complete medium was exchanged with medium containing 10ng/ml GM-CSF. On day 6 cells were harvested by pipetting and washing with PBS (Helft et al., 2015).

3.11 ELISAS AND CYTOKINE BEAD ASSAY

For Fms-like tyrosine kinase 3 ligand (Flt3L) ELISA the duoSet mFlt3L (DY427) from R&D Systems was used according to the manufacturer's recommendations. Briefly, flat bottom 96 microwell plates (Microlon®, HighBinding, Greiner Bio-One) were coated with 0.4µg/ml capture antibody in 0.2M sodium phosphate buffer overnight, washed with PBS 0.05% Tween20, blocked with PBS 10%FCS, incubated in 0.2µg/ml detection antibody and streptavidin HRP (1:200). Peroxidase substrate reaction was performed with ABTS buffer and substrate system (Sigma-Aldrich, 11204530001, 11204521001). The absorbance at 450nm was measured at the Microplate reader (Tecan Spark 10M). The concentration was calculated using a standard curve. G-CSF ELISA was performed with the Quantikine® ELISA kit from R&D Systems following the manufacturer's instructions

3.12 DIPHTHERIA TOXIN (DT) MEDIATED CELL ABLATION IN CLEC9A$^{CRE/DTR}$ROSA^{DTR} MICE

Clec9a$^{cre/cre}$Rosa^{DTR} mice were injected with 25ng per gram body weight diphtheria toxin (DT) (SIGMA) intraperitoneally (i.p.). 24h after the injection the spleens were harvested and analysed using flow cytometry.

3.13 *IN VITRO* CYTOKINE PRODUCTION

Splenocytes were enriched for CD11c^{+} cells as described above. 10^5 cells were seeded in a round bottom plate (Sarstedt) and stimulated with either LPS (100ng/ml, R151-*E.coli*, Sigma of CpG (0.5ng/ml, CpG 1668, Sigma). The cells were incubated at 37°C 1ith 5% CO_2 in a humid atmosphere for 2h. Then, brefeldin A (5µg/ml, Biolegend) was added and the cells were incubated for another 4h. Cells were harvested and stained intracellular for cytokine production as described above.

3.14 POLYMERASE CHAIN REACTION FOR DJ-REARRANGEMENTS OF THE HEAVY CHAIN LOCUS

Genomic DNA was isolated from sort purified populations that were digested for 2h with proteinase K (0.2mg/ml, Sigma, in lysis buffer containing 0.5M Tris-HCl, 0.5M EDTA, 5M NaCl, 20% SDS) by phenol-chloroform extraction. Two different approaches were used for the PCR for the IgH locus. One PCR approach targets the Dfl16 and Dsp2 D gene families. This PCR was split into two reactions for Germline (J3 & Mu0) and DJ-rearrangement (DH L & J3) with 20ng input DNA each (Schlissel et al., 1991).

DHL-GGAATTCG(AorC)TTTTTGT(CorG)AAGGGATCTACTACTGTG;

Mu0-CCGCATGCCAAGGCTAGCCTGAAAGATTACC;

J3-GTCTAGATTCTCACAAGAGTCCGATAGACCCTGG.

The alternative PCR approach to assess DJ-rearrangements targets the DHQ52 element. The following primers were used for two sequential PCRs as previously described (Bar-On et al., 2010).

PCR-1: DHQ52-1-CACAGAGAATTCTCCATAGTTGATAGCTCAG;
DHQ52-2GCCTCAGAATTCCTGTGGTC TCTGACTGGT;

PCR-2: JH4-1-AGGCTCTGAGATCCCTAG ACAG;
JH4-2- GGGTCTAGACTCTCAGCCGGCTCCCTCAGGG

3.15 MICROSCOPIC ANALYSIS OF *IN VITRO* CHEMOTACTIC MIGRATION OF DENDRITIC CELLS

In vitro chemotactic migration was adapted from the protocol published by Michael Sixt and Tim Lämmermann (Sixt & Lämmermann, 2011). Here, however, DC2 were sort purified from CD11c enriched splenocytes as $CD64^{-}CD11c^{+}MHCII^{+}CD11b^{+}CD24^{-}$ cells and cultured in complete medium with and without LPS (200ng/ml, Enzo) and GM-CSF (20ng/ml; PeproTech) for 18h at 37°C in 5% CO_2 to activate the cells. The cells were then resuspended in bovine collagen (Purecol, final concentration 1.67%; Advanced Biomatrix) and seeded into prepared migration chambers in a 6 well cell culture plate to image 6 conditions simultaneously. After the collagen matrix was polymerized, CCL19 (100ng/ml, PeproTech) was added on top of the gel to form a gradient. Images were taken in brightfield at an inverted motorized live-cell fluorescence microscope (Leica DMi8) at 37°C every minute for 5h. The analysis was performed using FIJI (ImageJ) software and manual tracking.

3.16 IMMUNOFLUORESCENCE STAINING OF LYMPH NODES

Mouse lymph nodes were carefully isolated from the mice and snap-frozen in OCT on dry ice. 12µm thin sections were cut at a cryostat at -20°C (Leica CM3050S), rehydrated in PBS for 5min, then fixed in ice-cold acetone for 5min and washed again in PBS for 5min. The tissue was circled with a Hydrophobic barrier PAP pen (Kisker Biotech GmbH) and blocked for 1h at RT with 100ul blocking solution (PBS 10% goat serum). After blocking the buffer was removed by tilting the slide and the tissue was stained with 100µl antibody staining mix in blocking buffer for 2h at RT in a humidified staining chamber in the dark. After the staining the slides were washed 3 times for 5min in PBS and the sections were stained with a secondary antibody with an analogous procedure if necessary. Finally, the tissue was mounted with ProLong™ Diamond Antifade Mountant (Thermo Fisher Scientific) at RT for 24h and stored at 4°C until imaging. LNs were imaged with a Leica SP8X WLL microscope, equipped with 405nm laser, WLL2 laser (470 - 670nm) and acusto-optical beam splitter. Tile scans were acquired with a

20x0.75 objective and signal was recorded with hybrid photodetectors. The following channels were used: BV421 (excitation 405nm; emission 415-470nm), AF488/GFP (500; 510-542), AF594 (592; 605-640) and AF647 (646; 656-718). Recording was done sequentially to avoid bleed-through and finished tile-scans were merged in LAS X (Leica, version 3.4.1.17670).

3.17 Statistical Analyses

Statistical analyses were performed using PRISM software (TreeStarInc.) Statistical significance was assessed by unpaired student's *t*-test with a value of $p < 0.05$ considered to be statistically significant.

3.18 Table of Antibodies

ANTIGEN	CLONE	CONJUGATE	COMPANY
CD3	145-2C11	Pacific Blue (PB), Fluorescein isothiocyanate (FITC), Brilliant violet 421 (BV421)	Biolegend
CD4	RM4-5	PB	Biolegend
CD4	GK1.5	FITC	Biolegend
CD8	53-6.8	FITC, PB, BV605	eBioscience
CD11b	M1/70	FITC, PB, Allophycocyanin-Cyanine7 (APC-Cy7)	Biolegend
CD11b	M1/70	Brilliant Ultraviolet 737 (BUV737)	BD-Bioscience
CD11C	N418	Peridinin-chlorophyll- protein complex Cyanine5.5 (PerCpCy5.5), APC/Cy7, BV785	Biolegend
CD16/32	2.4G2	Purified (Fc-Block)	BD-Bioscience
CD16/32	93	FITC	Biolegend
CD19	ID3	Phycoerythrin (PE), PB	BD-Bioscience
CD24	M1/69	BV605, BV510	Biolegend
CD25	3C7	PE	Biolegend
CD40	3/23	BV421	BD-Bioscience
CD43	1B11	PeCy7	Biolegend
CD45.1	A20	PB	Biolegend
CD45.2	104	Phycoerythrin-Cyanine7 (Pe-Cy7)	Biolegend
CD45.2	104	AF700	eBioscience
B220 (CD45R)	RA3-6B2	FITC, PE, PB	Biolegend
CD64	X54-5/7.1	PE, Pe-Cy7, APC	Biolegend

CD86	GL-1	BV605	Biolegend
CD90.2 (Thy1.1)	OX-7	APC-Cy7	Biolegend
CD103	2E7	PE	eBioscience
CD103	M290	BUV395	BD-Bioscience
CD115	AFS98	BV605, APC	Biolegend
CD117	2B8	PerCpCy5.5, Pe-Cy7	Biolegend
CD135	A2F10	PE, APC, purified	Biolegend
NK1.1 (CD161c)	PK136	PB, FITC	Biolegend
CD172A	P84	Pe-Cy7, APC, PerCP-Cy5.5	Biolegend
CD197 (CCR7)	4B12	PE	Biolegend
CD205	NLDC-145	APC	Biolegend
DNGR-1 (CD370)	1F6	PE	Custom conjugated
anti-RAT	Poly4054	AF594	Biolegend
CCR7 (CD197)	4B12	PE	Biolegend
CLEC4A4	33D1	Purified, APC	Biolegend
EPCAM	G8.8	AF647, AF594	Biolegend
ESAM	1G8	APC	Biolegend
F4/80	BM8	AF647, APC	Biolegend
IFNγ	XMG1.2	APC	eBioscience
IL7R/CD127	SB/199	BUV737	eBioscience
IL-12/IL-23 p40	C15.6	PeCy7	Biolegend
IRF4	M-17	purified	Santa Cruz
IRF8	V3GYXCH	PE	eBioscience
ISOTYPE RAT IgG2a, κ	RTK2758	PE, BV421, BV605	Biolegend
LY6C	HK1.4	AF700, PB, BV421, PerCPCy5.5, FITC	Biolegend
LY6G	1A8	FITC AF700	Biolegend
anti-mMer (MerTK)	polyclonal	Biotinylated	R&D Systems
MHCII I-A/I-E	M5/114.15.2	AF700, BV421, aF488	Biolegend
SCA-1 (LY-6A/E)	D7	PE	eBioscience
SiglecH	551	PerCPCy5.5	Biolegend

SiglecH	eBio440	eF660	eBioscience
STREPTAVIDIN	-	PE, APC	Biolegend
TER119	Ter119	PB, FITC	Biolegend
TNFA	MP6-XT22	PE	Biolegend
ZBTB46	U4-1374	PE	BD Pharmingen

4. RESULTS

4.1 IDENTIFICATION OF POTENTIAL REGULATORS FOR TRAFFICKING OF DENDRITIC CELL PROGENITORS IN STEADY-STATE

4.1.1 ANALYSES ON PRE-cDC SUBSET DISTRIBUTION IN THE TISSUES REVEALS NO DIRECT CORRELATION WITH DENDRITIC CELL SUBSETS

The aim of this study was to identify which factors are relevant for the trafficking of pre-cDCs. With regard to recent publications showing pre-committed DC subpopulations in the BM, it became interesting to investigate if pre-committed precursors are differentially recruited to the peripheral tissues (Grajales-Reyes et al., 2015; Schlitzer et al., 2015). For this purpose, pre-cDCs were identified in lymphoid and non-lymphoid organs using multicolour flow cytometric analyses and the pre-committed subsets were identified based on the expression of the surface markers Ly6C and SiglecH as (Schlitzer et al., 2015). The pre-cDCs were further distinguished in Ly6C$^-$SiglecH$^+$ pre-DC, which are most unrestricted and have been shown to have both cDC and pDC potential, Ly6C$^+$SiglecH$^+$ pre-cDCs, which are restricted to the cDC lineage, Ly6C$^+$SiglecH$^+$ pre-cDC2 and Ly6C$^+$SiglecH$^-$ pre-cDC1 (Schlitzer et al., 2015). To be able to investigate tissue-specific differences in recruitment, lymphoid as well as non-lymphoid organs were analysed. As lymphoid organs, the spleen, mesenteric LN (mLN) and thymus were chosen due to their well-investigated DC populations. Kidney, lung and lamina propria of the small intestine were chosen for non-lymphoid organs due to their differential but defined DC subset distribution. As reference population, cDCs were gated in the spleen as depicted in **Figure 6 A.** For all flow cytometric analyses on spleen, leukocytes were first defined by size and granularity, then doublets were gated out and the following gate restricts the cell population on living cells by excluding dead cells. DCs are further identified as CD11c$^+$MHCII$^+$ cells that were lacking the monocyte marker CD64 and are not auto-fluorescent (**Figure 6**, **A)**. DC subsets are furthermore defined as CD24$^+$CD11b$^-$ cDC1 and CD24$^-$CD11b$^+$ cDC2 (**Figure 6**, **A)**. Splenic pre-cDCs were identified as lineage$^-$ (Lin, CD3, CD4, CD8, Ter119, NK1.1, B220), CD11b^{low}CD11c$^+$MHCII$^-$CD43$^+$CD135$^+$CD172a^{int} cells. The gating strategy for BM pre-cDCs is very similar but does not gate on CD43. **Figure 6 B and C** show the representative gating on BM and spleen respectively. In the non-lymphoid organs, kidney, small intestine and lung, pre-cDCs were identified by gating on CD45$^+$ cells first and then lineage$^-$ (Lin, CD3, CD4, CD8, Ter119, NK1.1, B220), CD11b^{low}CD11c$^+$MHCII$^-$CD135$^+$CD172a^{int} cells. The identification of pre-committed pre-cDCs in the published organs BM, blood, and spleen could be largely reproduced, but the frequency of the Ly6C$^-$SiglecH$^-$ pre-cDC1 population was diminished in comparison to published data (Schlitzer et al., 2015).

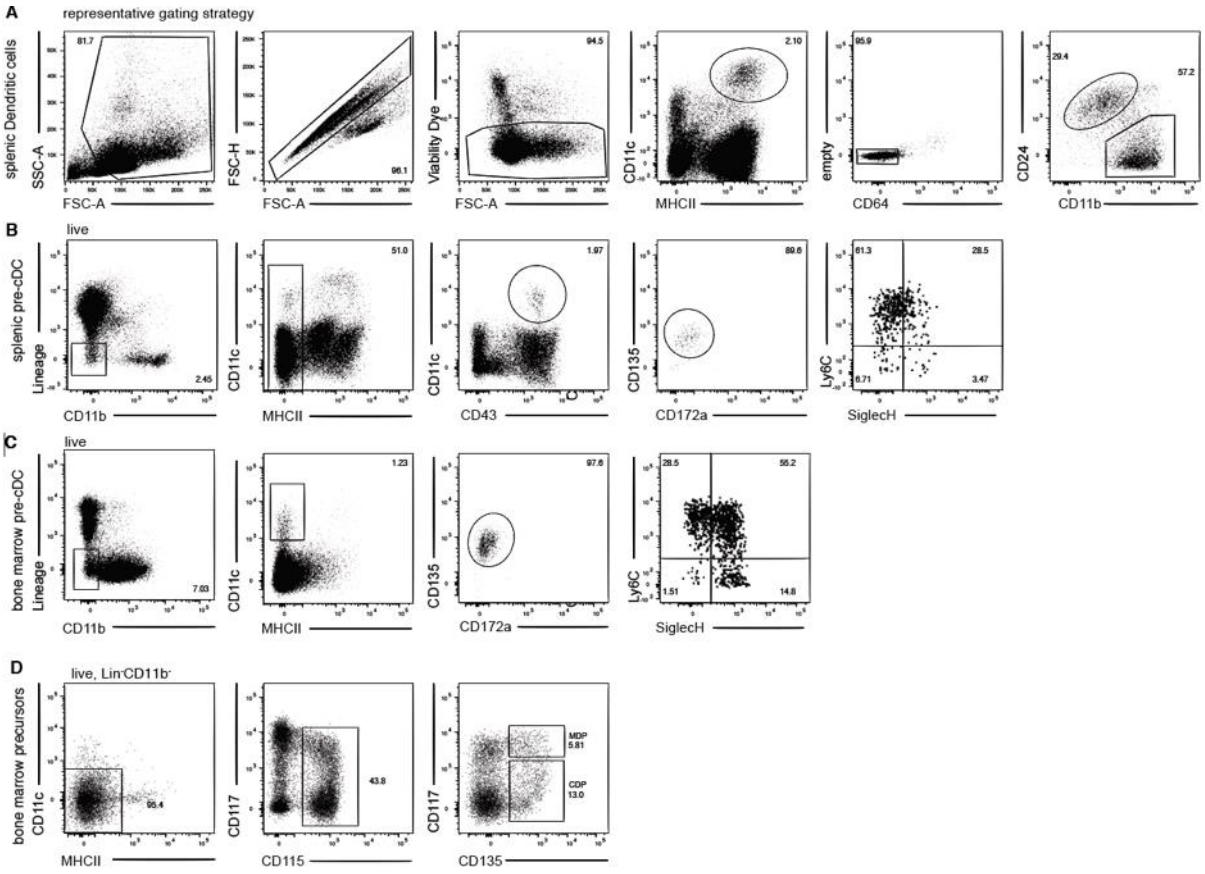

Figure 6: Representative gating strategy of DCs and their precursors. A. representative gating of DCs in the spleen. **B+C.** representative gating of pre-cDCs in the spleen **(B)** and BM **(C)** with further dividing in pre-committed subsets by gating on SiglecH and Ly6C. **D.** representative gating of MDP and CDP in the BM of wildtype mice.

To understand the differences in pre-cDC subset distribution in comparison to published data, further analyses to improve the gating strategy led to the conclusion that a more inclusive gating on cells with an intermediate expression of MHCII increases the frequency of the pre-cDC1 gate, as also shown by (Grajales-Reyes et al., 2015), but also increases the risk of including differentiated DCs. Therefore, a strict gating on MHCII negative cells remained the basis of the pre-cDC identification in the various tissues. Finally, cells that share the marker expression of pre-cDCs were identified in the thymus, lung, and mesenteric lymph node but also in the kidney, and lamina propria of the small intestine. Furthermore, the pre-committed subsets were identified based on Ly6C and SiglecH expression. To find a correlation between the pre-committed pre-cDC subsets and the differentiated DC subsets in the peripheral organs the subset distribution in was compared to published ratios of DC subset distribution and is shown here in representative plots (**Figure 7**). DCs were identified as in **Figure 6**, **A**. The DC subsets were identified based on the surface markers CD24 and CD11b as $CD24^{+}CD11b^{-}$ cDC1 and $CD11b^{+}CD24^{-}$ cDC2 or based on the expression of CD103 and CD11b in the small intestine as $CD103^{+}CD11b^{-}$ cDC1, $CD103^{+}CD11b^{+}$ double-positive cDC2, and $CD103^{-}CD11b^{+}$ single positive cDC2. (**Figure 7**, **A**). As it has also been published, DC subset distribution shows a predominance of the cDC2 in all organs except the thymus (Pakalniškytė & Schraml,

2017). The pre-cDC subset distribution in the thymus, however, shows a predominance of the pre-cDC2 whereas it shows an equal distribution of pre-cDC1 and pre-cDC2 in the kidney, which does not reflect the DC subset distribution in the respective tissue (**Figure 7**). These analyses suggest that the DC network is generated by the tissue microenvironment and not by differential recruitment of the progenitor.

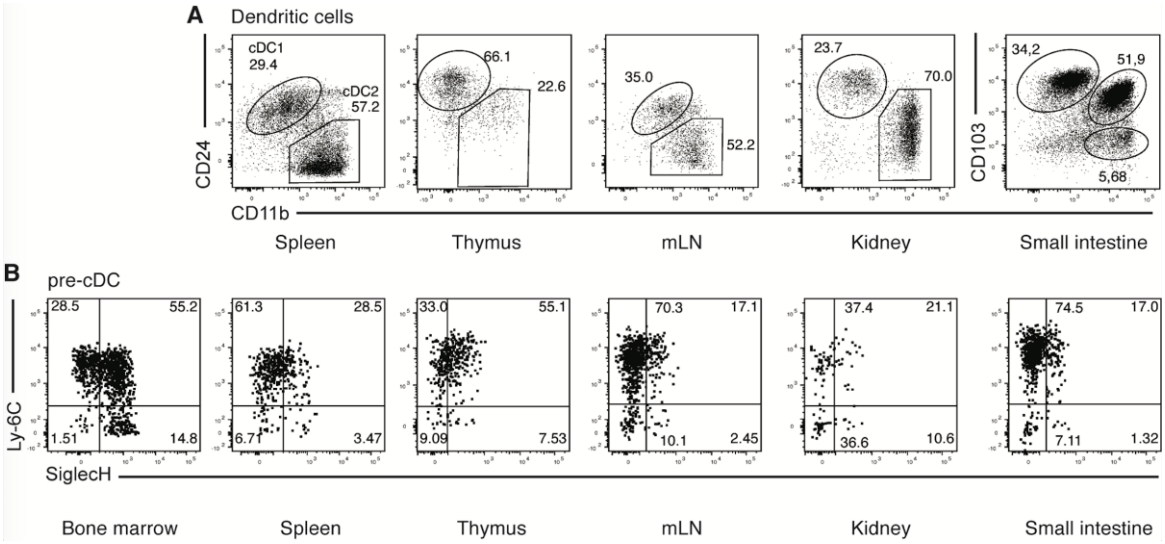

Figure 7: DC and pre-cDC subset distribution across lymphoid and non-lymphoid organs. A. DC subset distribution of $CD24^+CD11b^-$ cDC1 and $CD11b^+CD24^-$ cDC2 in the spleen, thymus, mLN and kidney of wildtype mice after pre-gating on live, $CD11c^+MHCII^+CD64^-$ cells ($CD45^+$ cells in the kidney and small intestine). In the small intestine, DCs were subset into $CD103^+CD11b^-$ cDC1, $CD103^+CD11b^+$ double positive cDC2 and $CD103^-CD11b^+$ single positive cDC2. **B.** pre-cDCs were identified in the indicated populations as live, Lin-(CD3, CD4, CD8, Ter119, NK1.1, B220) $CD11c^+MHCII^-CD172a^{int}CD135^+$ cells and further pre-committed subsets were identified by Ly6C and SiglecH expression. Shown are representative plots.

4.1.2 Multiplex qPCR screen for migration-related receptors reveals 39 trafficking receptors to be expressed on pre-cDCs in peripheral tissues

To identify migration-related receptors that are important for the trafficking of bulk pre-cDCs to different peripheral organs, a quantitative real-time PCR based method was employed. Fluidigm provides the technology that facilitates the screening of 96 targets against 96 samples by running a 96x96 delta gene plate in one run on a Biomark machine. This method has the advantage of a high throughput screening with a low amount of input RNA. For the 96 target genes, a list of migration related-receptors was created including chemokine receptors, IL-receptors, integrin chains, and intracellular adhesion molecules as well as control genes for sort precision and normalization (**Table 3**).

Table 3 List of target migration related receptors

Ccr1	Cxcr6	Il2ra	Notch2	ITGA6	ITGB4
Ccr1l1	Cx3cr1	Il2rb	Id2	ITGA7	ITGB5
Ccr2	Aplnr	Il2rg	TCF4	ITGA8	ITGB6
Ccr3	Cmklr1	Il4ra	Zeb2	ITGA9	ITGB7
Ccr4	Csf1r	Il5ra	IRF8	ITGA10	ITGB8
Ccr5	Csf2ra	Il6ra	IRF4	ITGA11	SELL
Ccr6	Csf3r	Il6st	Batf3	ITGAD	SELP
Ccr7	Tnfrsf1a	Il18r1	Klf4	ITGAE	SELPLG
Ccr8	Tnfrsf1b	Il9r	SiglecH	ITGAL	ICAM-3
Ccr9	Trem1	Il10ra	Ly6C	ITGAM	ICAM-1
Ccr10	Xcr1	Il10rb	GAPDH	ITGAV	ICAM-2
Cxcr1	GPR1	Il13	ITGA1	ITGA2B	ICAM4
Cxcr2	Il1r1	Il13ra1	ITGA2	ITGAX	ICAM5
Cxcr3	Il1r2	Il15ra	ITGA3	ITGB1	PECAM-1
Cxcr4	Il1rapl2	Il21r	ITGA4	ITGB2	GPR183
Cxcr5	Il1rapl1	Sigirr	ITGA5	ITGB3	CDH1

For this screening, pre-cDCs were sorted from BM, spleen, mLN, thymus, and lung to cover both lymphoid and non-lymphoid organs and to gain sufficient yield of pre-cDCs to isolate RNA. As also in the chosen organs the frequency of pre-cDCs is very low (**Table 4**) an enrichment technique was established based on magnetic enrichment of CD135 positive cells using biotinylated CD135 antibody and anti-biotin beads, which gave better results than gradient-based enrichment techniques as well as a lineage depletion approach and CD11c enrichment.

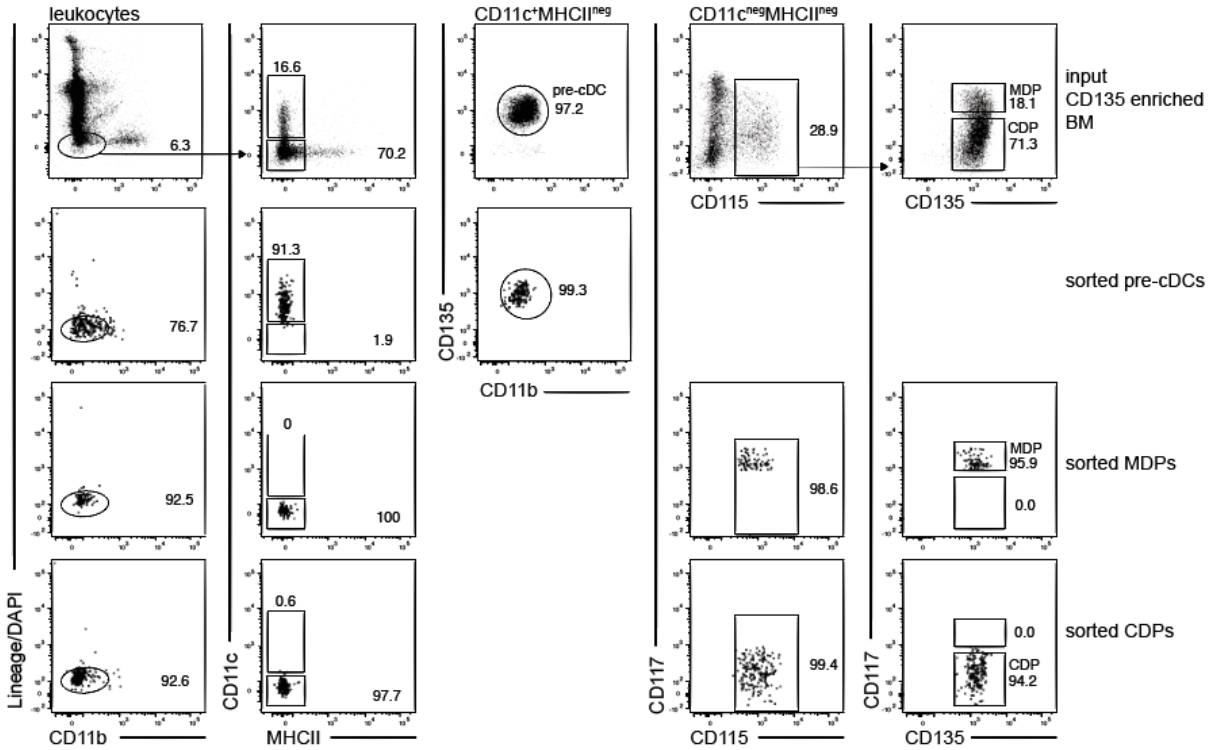

Figure 8: Sort purity of bone marrow DC progenitors. BM cells were stained with biotinylated CD135 antibody and enriched using anti-biotin beads and magnetic separation. The first row shows the gating strategy to sort lineage$^-$ (Lin, CD3, CD4, CD8, Ter119, NK1.1, B220), CD11b^{low}CD11c$^+$MHCII$^-$CD135$^+$CD172a^{int} pre-cDCs, lineage$^-$ (Lin, CD3, CD4, CD8, Ter119, NK1.1, B220), CD11b^{low}CD11c$^-$MHCII$^-$CD115$^+$CD135$^+$CD117^{hi} MDPs and lineage$^-$ (Lin, CD3, CD4, CD8, Ter119, NK1.1, B220), CD11b^{low}CD11c$^-$MHCII$^-$CD115$^+$CD135$^+$CD117^{low} CDPs. The following rows show samples of sorted pre-cDCs, MDPs and CDPs, respectively.

Table 4 pre-cDC sorts from selected lymphoid and non-lymphoid organs

Cell type	Organ	Sorted cells	Frequency of pre-cDCs among living cells
MDP	BM	3563	0.19%
		3395	
		4705	
CDP		18505	0.42%
		22751	
		26075	
Pre-cDC		30014	0.07%
		31934	
		44750	
	Spleen	14164	0.02%
		14465	
		11160	
	mLN	1055	0.012%

		1671	
		3380	
	Thymus	2368	0.001%
		3782	
		4179	
	lung	2352	0.31%
		3787	(of leukocytes)
		4750	

Pre-cDCs from BM, spleen, thymus, mLN, and lung were sorted in biological triplicates from steady-state wildtype mice (**Table 4**). In addition, earlier progenitors namely MDPs and CDPs were sorted from the BM to compare expression levels of trafficking receptors between migratory and non-migratory stages of DC development. The purity of the sort was controlled by flow cytometry on the sorted sample and is exemplified on the sort of BM progenitors in **Figure 8**. The qPCR screen revealed 39 candidate trafficking receptors that were detectable in pre-cDCs from all tissues (**Figure 9**). Out of this list, most receptors are higher expressed in the peripheral organs compared to the progenitors that have not emigrated from the BM yet.

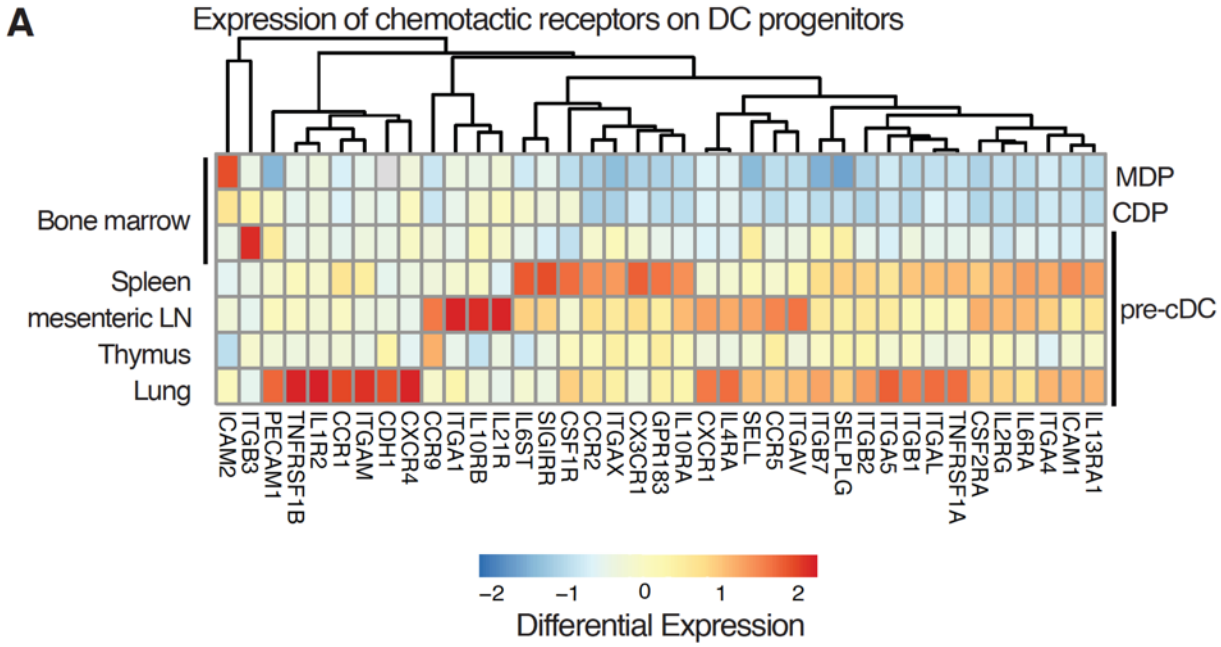

Figure 9: Candidate receptors for pre-cDC migration. Expression of chemotactic receptors on DC progenitors from different tissues. Pre-cDCs, CDPs (lin$^-$B220$^-$CD11c$^-$MHCII$^-$CD11b$^-$CD135$^+$CD115$^+$CD117$^{low\text{-}int}$) and MDPs (lin$^-$B220$^-$CD11c$^-$MHCII$^-$CD11b$^-$CD135$^+$CD115$^+$CD117^{hi}) were sorted from indicated tissues. Expression of the indicated receptors was quantified by real time PCR using Fluidigm technology, normalized to GAPDH and scaled per target. Heatmap shows relative expression of receptors with detectable expression in pre-cDC.

4.1.3 *In vitro migration of pre-cDCs in transwell assay as a basic tool for the verification of relevance for trafficking receptors in pre-cDC migration*

A further step to verify the influence of the identified candidate receptors is to access their relevance on pre-cDC migration *in vitro*. For this purpose, an *in vitro* migration experiment for pre-cDC migration, which is based on the CCR2-CCL2 axis that, had been published before has been successfully reproduced (H. Nakano et al., 2017; **Figure 10**). This assay can further be used to validate the influence of the candidate receptors on pre-cDC migration by manipulating them or by analysing differential migration of pre-cDCs from different tissues.

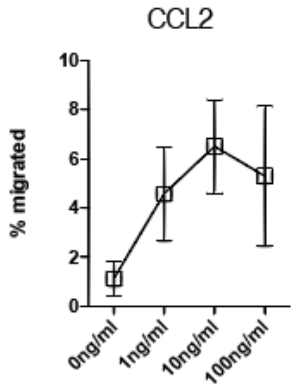

Figure 10: CCL2 induced migration of bone marrow pre-cDCs. 1x10^5 total bone marrow cells were seeded to the 5µm pore size transwell inlets which have been preincubated with indicated concentrations of CCL2. After two hours, migrated cells were harvested from the lower well and pre-cDCs were quantified by flow cytometry (n=3).

4.2 *Clec9a*-mediated ablation of conventional dendritic cells suggests a lymphoid path to generating dendritic cells *in vivo*

4.2.2 *Myeloproliferation in* Clec9a$^{cre/cre}$Rosa^{DTA} *mice*

Clec9a$^{cre/cre}$Rosa^{DTA} mice were generated to serve as a mouse model to specifically deplete DCs. Available DC depletion models are not specific to the cDCs but also deplete other cells that express CD11c, such as monocyte-derived DCs and macrophages (CD11c-DTR (Rombouts et al., 2017). Here, *Clec9a^{cre}* mice were crossed to Rosa26-STOP-floxed-

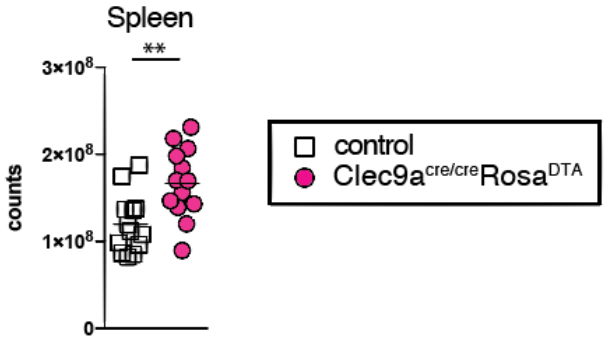

Figure 11: *Clec9a$^{cre/cre}$Rosa^{DTA}* mice show splenomegaly. Total number of leukocytes in the spleen of *Clec9a$^{cre/cre}$Rosa^{DTA}* and control mice is shown. Each symbol represents one mouse; n=13, **p < 0.01

diphtheria toxin (DT) mice (*Clec9a*^{Cre}*Rosa*^{DTA}) with the aim to deplete all cells deriving from CDPs as they are the first progenitor with *Clec9a* expression (Schraml et al., 2013). In this study, most experiments were performed on mice that were homozygous for the cre locus as it has been published that homozygosity increases the cre mediated recombination but does not affect the specificity in the reporter mice *Clec9a*^{cre}*Rosa*^{EYFP} experiments, in which mice with different genotypes were used, are explicitly marked (Schraml et al., 2013). As comparisons throughout the experiments, littermate control mice were used that had either only *Clec9a*^{cre} *or Rosa*^{DTA} or that were wildtype in both loci. For the shown analyses, adult mice between the age of 8 and 17 weeks were used.

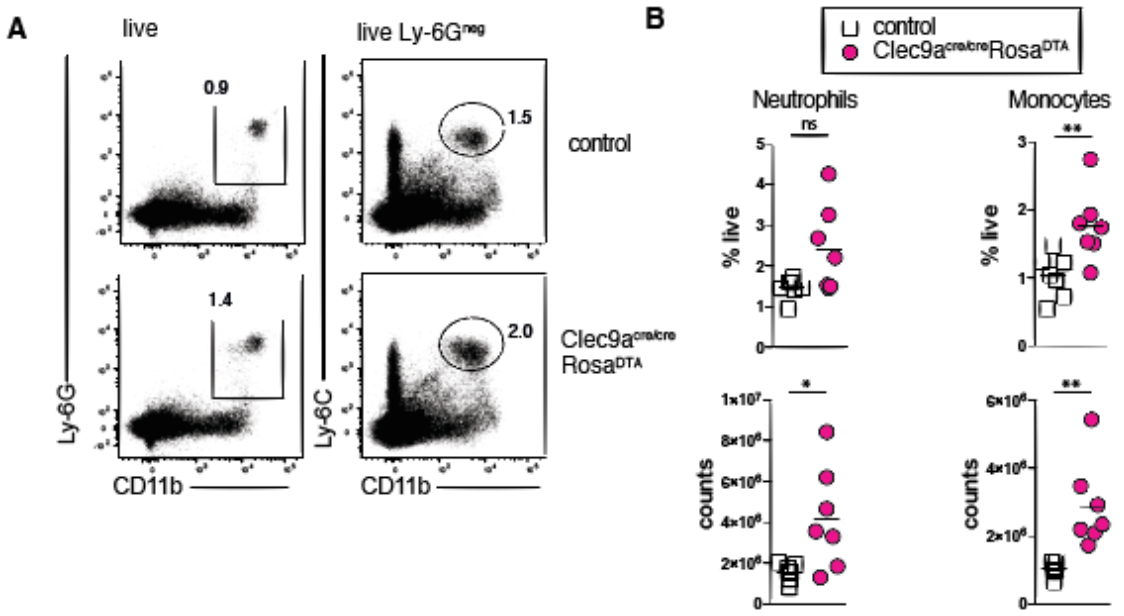

Figure 12: *Clec9a*$^{cre/cre}$*Rosa*^{DTA} mice exhibit neutrophilia and monocytosis. A. representative gating strategy for the flow cytometric identification of neutrophils and monocytes in the spleen of *Clec9a*$^{cre/cre}$*Rosa*^{DTA} and control mice neutrophils were identified among live cells by the marker expression of Ly6G and CD11b and monocytes were identified as Ly6G^{-}Ly6C^{+}CD11b^{+} cells**. B.** neutrophils and monocytes were quantified in the spleens of *Clec9a*$^{cre/cre}$*Rosa*^{DTA} and control mice. Each symbol represents one mouse; n=7; ns: not significant; * p<0.05; ** p< 0.01.

In existing DC depletion models it has been shown that these mice develop a systemic neutrophilia and monocytosis (Birnberg et al., 2008; Finger Stadler et al., 2017; Hochweller et al., 2008; Jiao et al., 2014; Meredith et al., 2012; Rombouts et al., 2017; Sichien et al., 2016; Tittel et al., 2012; van Blijswijk et al., 2014). One symptom caused by myeloproliferation is an increased spleen. **Figure 11** shows that, indeed, the total cellularity of the spleen is increased in *Clec9a*$^{cre/cre}$*Rosa*^{DTA} mice compared to control mice. Specifically, neutrophilia and monocytosis can also be found in *Clec9a*$^{cre/cre}$*Rosa*^{DTA} mice by an increase of neutrophil (Ly6G^{+}CD11b^{+}) and monocyte (Ly6G^{-}Ly6C^{+}CD11b^{+}) counts in the spleen of adult *Clec9a*$^{cre/cre}$*Rosa*^{DTA} mice compared to littermate controls (**Figure 12**). Myeloproliferation in DC depletion mice is considered a secondary effect of increased Flt3L levels in the serum of these mice (Birnberg et al., 2008). Therefore, the FLt3L levels in the serum of *Clec9a*$^{cre/cre}$*Rosa*^{DTA} mice were measured by ELISA and indeed elevated Flt3L levels were found in comparison to control mice (**Figure 13**). To study if additional growth factors or chemokines that are responsible for the neutrophil and monocyte homeostasis were dysregulated in *Clec9a*$^{cre/cre}$*Rosa*^{DTA} mice ELISA and bead array were performed to detect differences in the serum levels of G-CSF, CXCL9, CCL22, CCL5, and CCL17. From the detected chemokine ligands none was found significantly altered in *Clec9a*$^{cre/cre}$*Rosa*^{DTA} mice compared to control mice and also the growth factor G-CSF was found at equal levels in the compared serum samples (**Figure 14).**

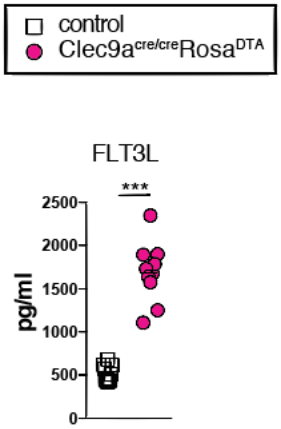

Figure 13: *Clec9a*$^{cre/cre}$*Rosa*^{DTA} mice have increased serum levels of Flt3L. Flt3L concentrations in the serum of Clec9a$^{cre/cre}$Rosa^{DTA} and control mice were measured using ELISA. Each symbol represents one mouse; n=10; *** p< 0.001

Increased Flt3L concentrations and DC depletion can influence the T-cell homeostasis (Fry et al., 2004; Stolley & Campbell, 2016). To analyse if the lymphoid compartment in *Clec9a*$^{cre/cre}$*Rosa*^{DTA} mice shows differences in the homeostasis of lymphoid cells, B-cells as well as CD4$^+$ and CD8$^+$ T-cells were quantified in the spleen of *Clec9a*$^{cre/cre}$*Rosa*^{DTA} mice. No difference was observed in the frequency of CD19$^+$B220$^+$MHCII$^+$ B-cells, and CD3$^+$CD4$^+$ T-cells, Unexpectedly though, also the counts of CD19$^+$B220$^+$MHCII$^+$ B-cells, and CD3$^+$CD4$^+$ T-cells are not significantly different between *Clec9a*$^{cre/cre}$*Rosa*^{DTA} and control mice although the cellularity of the spleen in *Clec9a*$^{cre/cre}$*Rosa*^{DTA} mice is significantly higher as shown in **Figure 11**. This can be explained by a trend to lower frequency of CD3$^+$CD4$^+$ T-cells in *Clec9a*$^{cre/cre}$*Rosa*^{DTA} mice on the one hand, and a generally high spread of total cell counts in this experiment on the other hand. Interestingly, however, CD3$^+$CD8$^+$ T-cells were diminished by a third both in counts and frequency. Taken together, *Clec9a*$^{cre/cre}$*Rosa*^{DTA} mice show myeloproliferation and increased Flt3L concentrations as well as a decreased CD8$^+$ T-cell compartment in the spleen. These systemic differences have to be considered when performing functional analyses on these mice, which can therefore not be considered as steady-state mice.

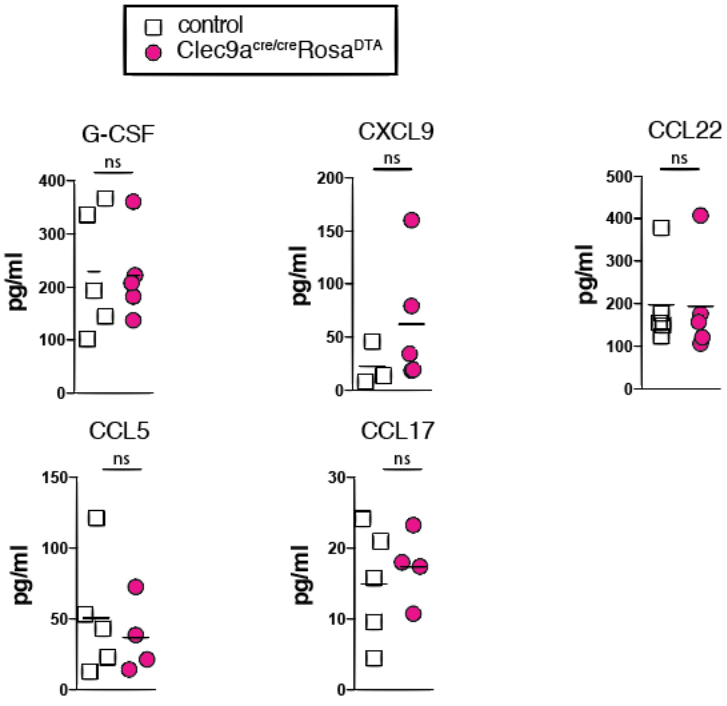

Figure 14: *Clec9a*$^{cre/cre}$*Rosa*^{DTA} mice comparable levels of growth factors and chemokines in the serum. GCSF was measured using ELISA on the serum of *Clec9a*$^{cre/cre}$*Rosa*^{DTA} and control mice; CXCL9, CCL22, CCL5 and CCL17 were measured using cytometric bead array on the serum collected from *Clec9a*$^{cre/cre}$*Rosa*^{DTA} and control mice. Each symbol represents one mouse; n=4-5; ns: not significant.

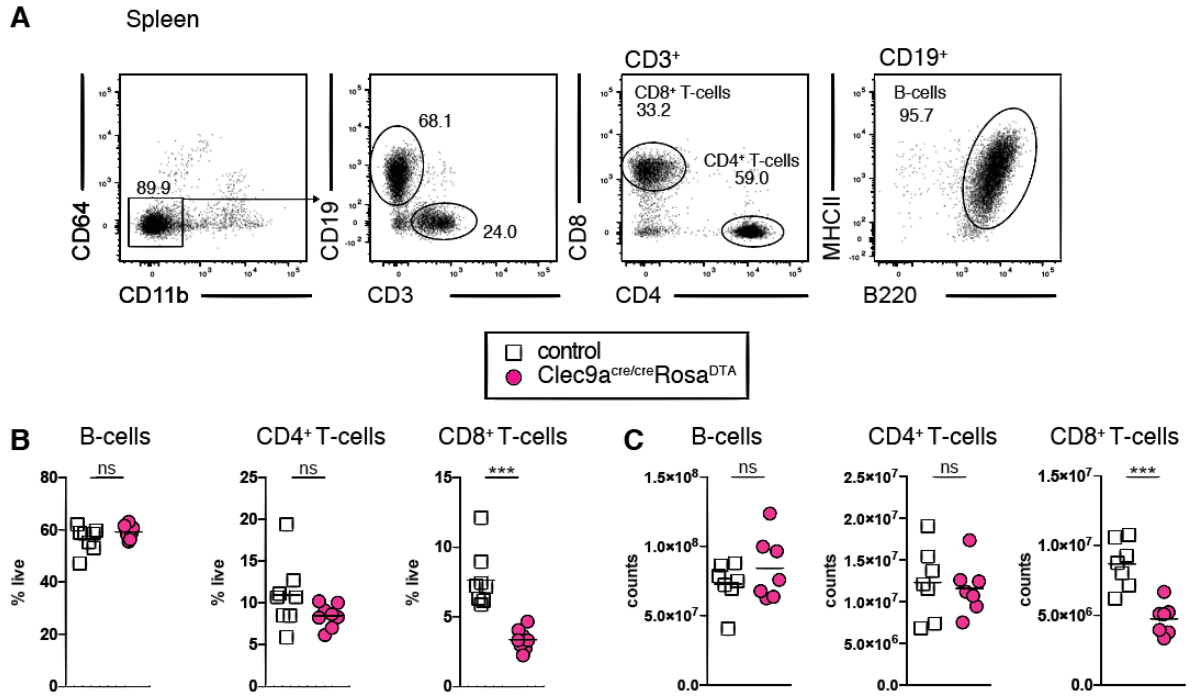

Figure 15: CD8+ T-cells are diminished in the spleen of *Clec9a$^{cre/cre}$Rosa^{DTA}* mice. A. Representative gating strategy of B-cells and CD4$^+$ and CD8$^+$ T-cells on control mouse splenocytes. First, CD64$^+$ and CD11b$^+$ cells were excluded and then B-cells were further gated as CD19$^+$CD3$^-$B220$^+$MHCII$^+$ cells. T-cells were identified as CD19$^-$ CD3$^+$ and further subset in CD8$^+$ and CD4$^+$ T-cells. **B.** Frequency of B-cells, CD4$^+$ and CD8$^+$ T-cells in the spleen of *Clec9a$^{cre/cre}$Rosa^{DTA}* and control mice as identified in (A). **C.** Total counts of B-cells, CD4$^+$ and CD8$^+$ T-cells in the spleen of *Clec9a$^{cre/cre}$Rosa^{DTA}* and control mice. Data of 2 independent experiments. Each symbol represents one mouse; n=7; ns: not significant; ***p<0.001.

4.2.3 Incomplete depletion of cDC2 in Clec9a$^{Cre/Cre}$Rosa^{DTA} *mice*

Next, the spleen was analysed for the depletion of DCs. Here, the frequency of CD64$^-$ CD11c$^+$MHCII$^+$ DCs (**Figure 16**, **A**) was reduced *Clec9a$^{cre/cre}$Rosa^{DTA}* mice but not fully depleted and not even reduced when comparing total DC counts (**Figure 16**, **B**). The analysis of the two main subsets of DCs in the spleen showed that the cDC1 subset, which was identified as CD64$^-$CD11c$^+$MHCII$^+$CD24$^+$ cells, was lost in *Clec9a$^{cre/cre}$Rosa^{DTA}* mice (**Figure 16**, **C**). It is expected that the cDC1 population is lost in *Clec9a$^{cre/cre}$Rosa^{DTA}* mice because the progenitor as well as the differentiated population expresses the *Clec9a* gene and therefore expresses the Cre that excises the STOP codon in front of the Rosa^{DTA} locus and therefore enables the expression of the toxin that kills the cell. The idea behind the depletion of cDC2 *Clec9a$^{cre/cre}$Rosa^{DTA}* mice, on the other hand, does not rely on the expression of Clec9a in the differentiated population as the cDC2 do not express *Clec9a*, but the depletion would solely depend on the depletion of the *Clec9a* expressing progenitors. The fate-mapping model *Clec9a^{cre}Rosa^{YFP}* also underlines that this *Clec9a* expression in the progenitor population is sufficient to label the cDC2 efficiently (Schraml et al., 2013). Interestingly the frequency cDC2, which were identified as CD64$^-$CD11c$^+$MHCII$^+$CD11b$^+$ cells (**Figure 16**, **A**) by flow cytometry, was only slightly reduced from 1.30±0.06% to 0.88±0,08% (Mean±SEM) of living cells in the

spleens of *Clec9a*$^{cre/cre}$*Rosa*^{DTA} mice (**Figure 16**, **B**). The total counts of cDC2 was not diminished in the spleen of *Clec9a*$^{cre/cre}$*Rosa*^{DTA} mice due to the increased spleen sizes in comparison to control mice (**Figure 16**, **C**). The difference in frequency only can hereby be explained by the proportional increase of monocytes and neutrophils in the spleen of *Clec9a*$^{cre/cre}$*Rosa*^{DTA} mice.

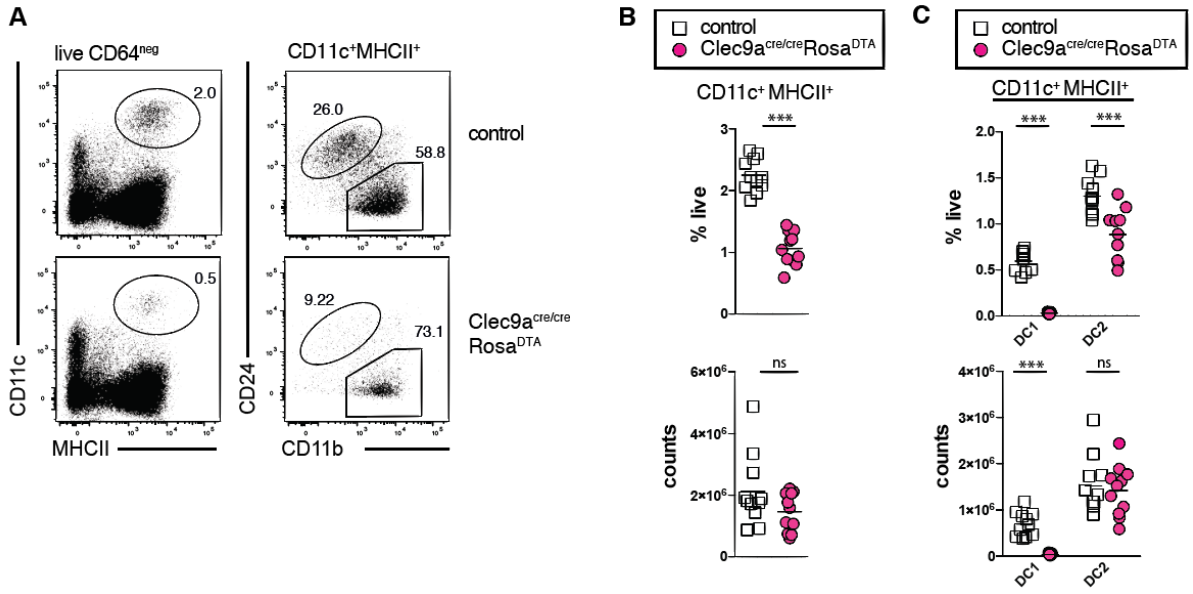

Figure 16: Depletion of cDC1 but not cDC2 in *Clec9a*$^{cre/cre}$*Rosa*^{DTA} mice. A. Representative FACS plots on splenic live CD64$^-$ cells from *Clec9a*$^{cre/cre}$*Rosa*^{DTA} and control mice showing gating on CD11c$^+$MHCII$^+$ DCs and gating to identify the CD24$^+$CD11b$^-$ cDC1 and CD11b$^+$CD24$^-$ cDC2. **B.** Frequency and counts of total CD11c$^+$MHCII$^+$ DCs in the spleen of *Clec9a*$^{cre/cre}$*Rosa*^{DTA} and control mice. **C.** Frequency and counts of the DC subsets cDC1 and cDC2 as identified in (A). Each symbol represents one mouse; n=11; ns: not significant; *p<0.05; **p<0.01; *** p< 0.001.

Plasmacytoid DCs also express DNGR-1 at low levels in their differentiated state, therefore a depletion of pDCs was likely in *Clec9a*$^{cre/cre}$*Rosa*^{DTA} mice although they do not derive from DNGR-1$^+$ progenitors. pDCs were quantified in the spleen of *Clec9a*$^{cre/cre}$*Rosa*^{DTA} mice, however no difference in frequency or counts was detected (**Figure 17, A**). Interestingly though, whereas pDCs from control mice express low levels of DNGR-1, pDCs isolated from *Clec9a*$^{cre/cre}$*Rosa*^{DTA} mice show reduced expression of DNGR-1 on the surface, even though DNGR-1 is still slightly expressed as the biological negative control (knockout for DNGR-1) shows lower background staining (**Figure 17, B**). Red pulp macrophages are an abundant subset of APCs in the spleen. Due to the expressional overlap with DCs, they are also depleted in the CD11c depletion model CD11c-DTR (Meredith et al., 2012). To show the specificity of the DC depletion in *Clec9a*$^{cre/cre}$*Rosa*^{DTA} mice RPMs were quantified in *Clec9a*$^{cre/cre}$*Rosa*^{DTA} mice. RPMs were found in equal frequencies and counts in the spleen of *Clec9a*$^{cre/cre}$*Rosa*^{DTA} and control mice (**Figure 17, C**).

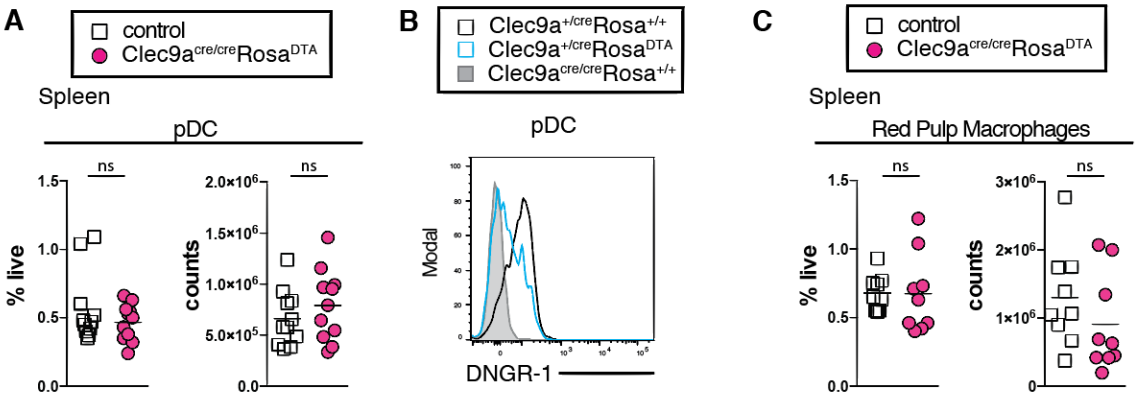

Figure 17: Equal quantification of pDCs and RPMs in the spleens of *Clec9a$^{cre/cre}$Rosa^{DTA}* and control mice. **A.** Frequency and counts of pDC in the spleen of *Clec9a$^{cre/cre}$Rosa^{DTA}* and control mice identified as SiglecH^{+}B220^{+} cells. **B.** DNGR-1 expression level of pDCs from heterozygous *Clec9a^{Cre}Rosa^{DTA}* and control mice that were determined by flow cytometry are shown as a representative histogram. Mice homozygous for the *Cre* locus served as a negative control for DNGR-1 expression; n=11. **C.** Frequency and counts of red pulp macrophages in the spleen of *Clec9a$^{cre/cre}$Rosa^{DTA}* and control mice identified as either auto-fluorescent CD64^{+} cells or CD64^{+}F4/80^{+} cells; n=9. Each symbol represents one mouse; ns: not significant.

4.2.4 Loss of dendritic cell progenitors in *Clec9a^{Cre}Rosa^{DTA}* mice

As the DC2 population was not found to be decreased in *Clec9a$^{cre/cre}$Rosa^{DTA}* mice, the next step was to verify that the cDC progenitors are indeed depleted. For this purpose, the frequencies and counts of MDPs, CDPs, and pre-cDCs in the BM, as well as pre-cDCs in the spleen of *Clec9a$^{cre/cre}$Rosa^{DTA}* mice, were analysed in comparison to control mice. **Figure 18**, **A** shows the gating strategy for DC progenitors in the BM and **Figure 18**, **C** the identification of pre-cDCs in the spleen of both *Clec9a$^{cre/cre}$Rosa^{DTA}* and control mice. The quantification shows no difference in the MDP population, as expected, but a reduction in CDP and a loss in pre-cDCs both from BM and spleen (**Figure 18**, **B and D**). This shows that the DC progenitors are indeed depleted in *Clec9a$^{cre/cre}$Rosa^{DTA}* mice indicating that the development of cells that resemble DC2 in *Clec9a$^{cre/cre}$Rosa^{DTA}* mice is independent of conventional DC progenitors.

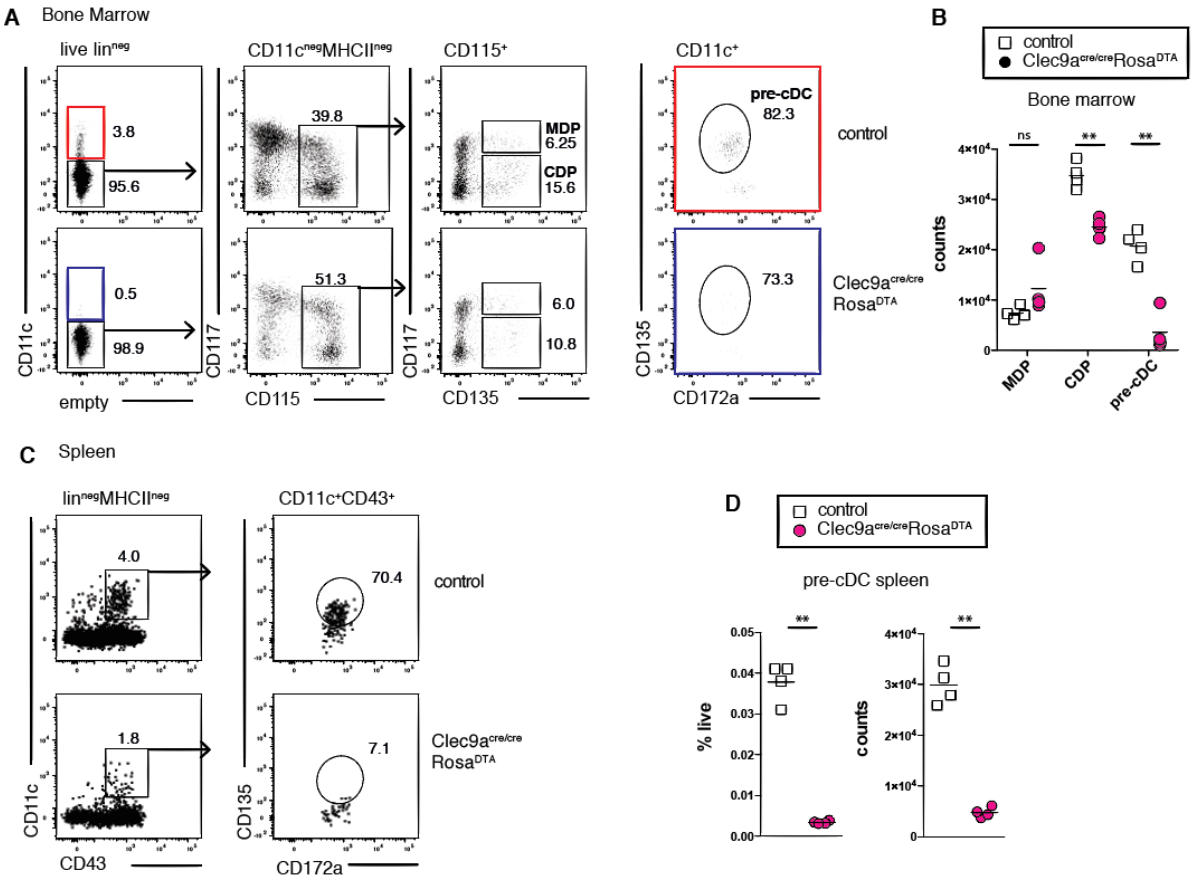

Figure 18: Loss of DC precursors in *Clec9a$^{cre/cre}$Rosa^{DTA}* mice. A. Representative FACS plots on BM cells from Clec9a$^{cre/cre}$Rosa^{DTA} and control mice pre-gated as live, lineage negative (Lin: CD3, CD4, CD8, Ter119, NK1.1, B220, CD11b) cells. Pre-cDCs were then identified as CD11c^{+}MHCII^{-}CD135^{+}CD172a^{int} cells. MDPs were identified as CD11c^{-}MHCII^{-}CD115^{+}CD135^{+}CD117^{hi} cells and CDPs as CD11c^{-}MHCII^{-}CD115^{+}CD135^{+}CD117$^{low-int}$ cells. **B.** Quantification of DC progenitors in the BM of *Clec9a$^{cre/cre}$Rosa^{DTA}* and control mice identified as in **(A). C.** Representative FACS plots on splenocytes from *Clec9a$^{cre/cre}$Rosa^{DTA}* and control mice pre-gated as live, lineage negative (Lin: CD3, CD4, CD8, Ter119, NK1.1, B220, CD11b) MHCII^{-} cells. Pre-cDCs were then identified as CD11c^{+}CD43^{+}CD135^{+}CD172a^{int} cells. **D.** Quantification of pre-cDCs in the spleen of *Clec9a$^{cre/cre}$Rosa^{DTA}* and control mice identified as in **(C).** Each symbol represents one mouse; n=4; ns: not significant; ** p<0.01.

4.2.5 Loss of dendritic cells and their progenitors upon DT treatment of Clec9a$^{cre/cre}$Rosa^{DTR} mice

To verify that *Clec9a^{cre}* mice can be used to deplete DCs we turned to Clec9a$^{cre/cre}$Rosa^{DTR} mice. In the transient depletion model in Clec9a^{Cre}Rosa^{DTR} mice, cells which express *Clec9a* express *Cre* recombinase, which excises the floxed STOP sequence before the DTR gene. Therefore, all cells that express Clec9a but also all its progeny will express the DTR because the edited sequence in the genome is inherited. The DTR expression is a useful tool to induce the depletion of the DTR expressing cells at a given time point and for a short period of time (van Blijswijk et al., 2014). Clec9a$^{cre/cre}$Rosa^{DTR} mice were injected intraperitoneally (i.p.) with 25ng/g of body weight of diphtheria toxin and the splenocytes were analysed after 24h. After

this short time of DC depletion, there is no increase monocyte or neutrophil frequencies or counts in the spleen of Clec9a$^{cre/cre}$Rosa^{DTR} mice compared to control mice (**Figure 19**).

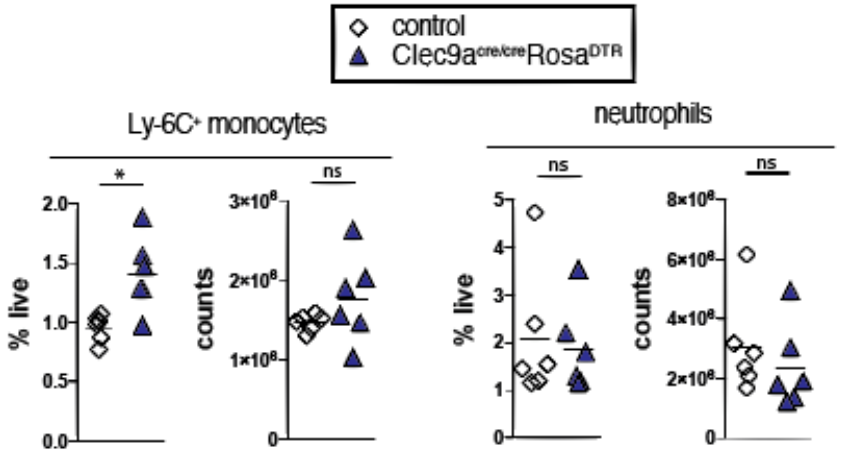

Figure 19: No manifestation of neutrophilia and monocytosis in *Clec9a$^{cre/cre}$Rosa^{DTR}* mice 24 hours after DT injection. *Clec9a$^{cre/cre}$Rosa^{DTR}* and control mice were injected i.p. with 25ng/g diphtheria toxin. After 24h the spleens were analysed with flow cytometry. Monocytes were identified as Ly6G$^-$Ly6C$^+$CD11b$^+$ cells, neutrophils as Ly6G$^+$CD11b$^+$ cells. Each symbol represents one mouse; n=6; ns not significant; *p<0.05.

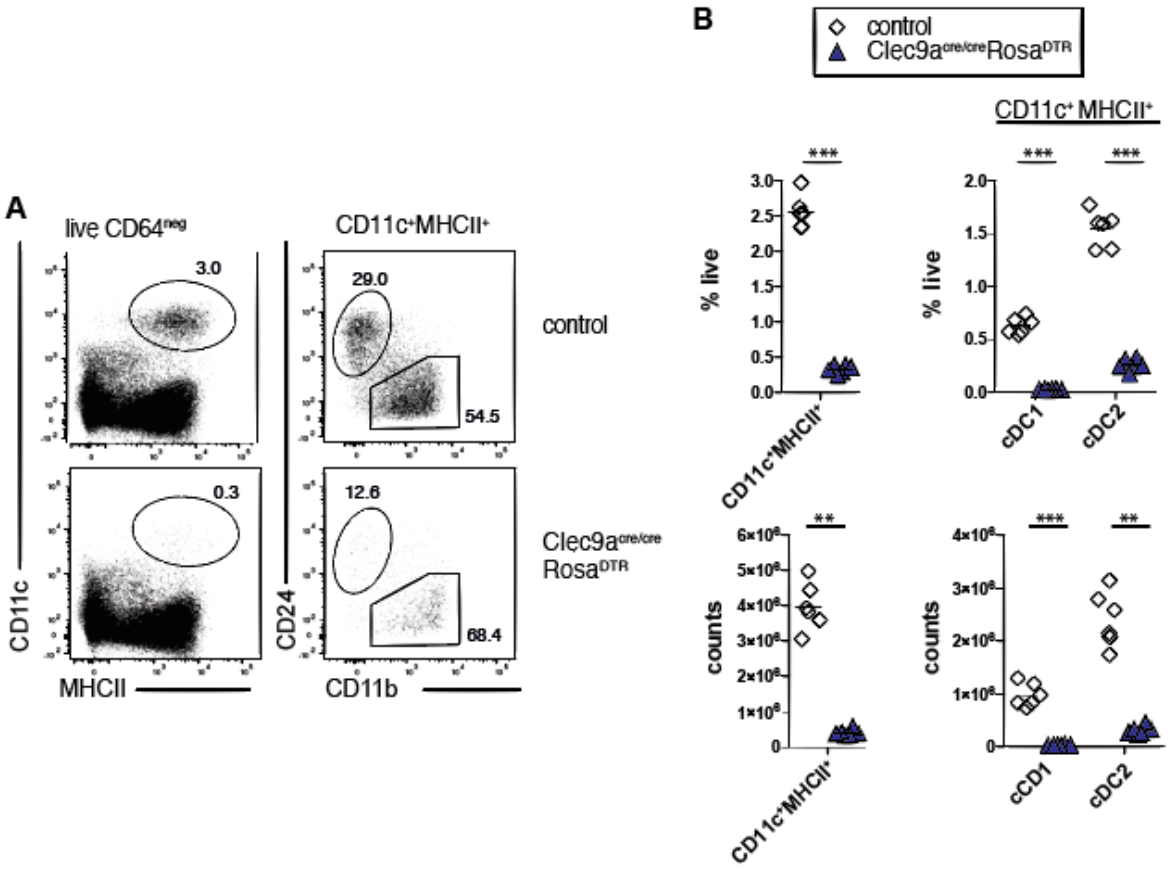

Figure 20: Efficient depletion of DCs in *Clec9a$^{cre/cre}$Rosa^{DTR}* mice. A. Representative FACS plots on splenic live CD64$^-$ cells from *Clec9a$^{cre/cre}$Rosa^{DTR}* and control mice showing gating on CD11c$^+$MHCII$^+$ DCs and gating to identify the CD24$^+$CD11b$^-$ cDC1 and CD11b$^+$CD24$^-$ cDC2. **B.** Frequency and counts of total CD11c$^+$MHCII$^+$ DCs in the spleen of *Clec9a$^{cre/cre}$Rosa^{DTR}* and control mice. **C.** Frequency and counts of the DC subsets cDC1 and cDC2 as identified in (A). Each symbol represents one mouse; n=6; **p<0.01; *** p< 0.001.

As expected, cDC1 were lost in the spleens of Clec9a$^{cre/cre}$Rosa^{DTR} mice (**Figure 20**). In contrast to the constitutive depletion in *Clec9a$^{cre/cre}$Rosa^{DTA}* mice, in the short-term inducible depletion in Clec9a$^{cre/cre}$Rosa^{DTR} mice, also the cDC2 cells were lost proving that the Cre expression in the progenitor population is sufficient to deplete the progeny although it does not express *Clec9a* in the differentiated state (**Figure 20**). Additionally, also pre-cDCs were quantified in the spleens of Clec9a$^{cre/cre}$Rosa^{DTR} mice and found to be lost (**Figure 21**). Therefore, *Clec9a^{cre}* mice are a valid tool that efficiently depletes cDCs as well as cDC progenitors in a short-term depletion.

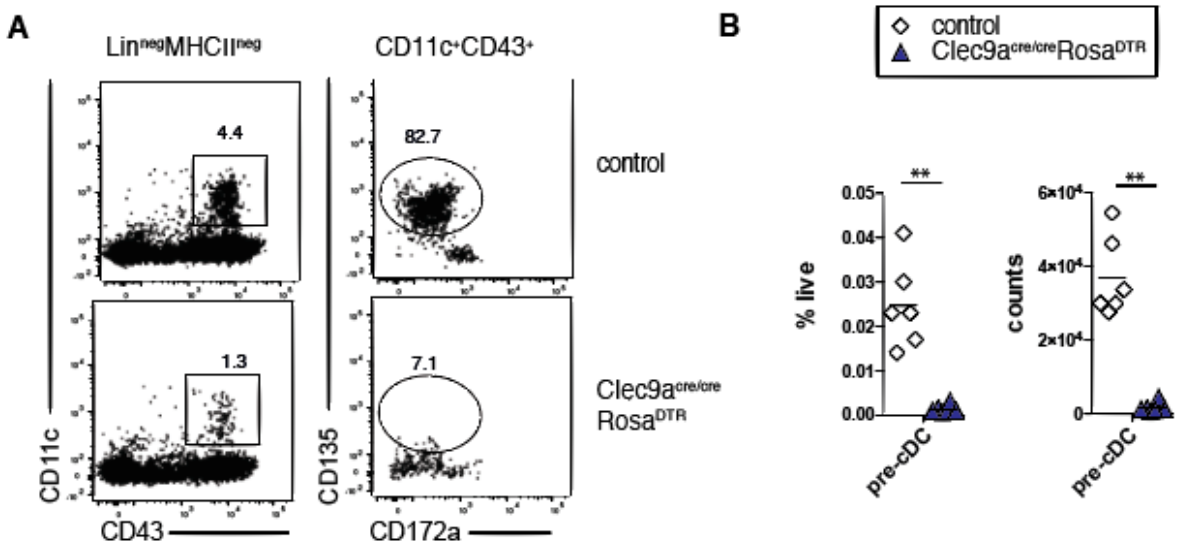

Figure 21: Loss of pre-cDCs in *Clec9a$^{cre/cre}$Rosa^{DTR}* mice. A. Representative FACS plots on splenocytes from *Clec9a$^{cre/cre}$Rosa^{DTR}* and control mice pre-gated as live, lineage negative (Lin: CD3, CD4, CD8, Ter119, NK1.1, B220, CD11b) MHCII^{-} cells. Pre-cDCs were identified as CD11c^{+}CD43^{+}CD135^{+}CD172a^{int} cells. **B.** Quantification of pre-cDCs in the spleen of *Clec9a$^{cre/cre}$Rosa^{DTR}* and control mice identified as in **(A).** Each symbol represents one mouse; n=6; ** p<0.01.

4.2.6 Progenitors of dendritic cells in Clec9a$^{cre/cre}$Rosa^{DTA} mice are inefficient in producing dendritic cells in vitro

To additionally rule out the fact that the reduced population of CDPs and the few remaining pre-cDCs that are still present in *Clec9a$^{cre/cre}$Rosa^{DTA}* mice escape depletion and develop into DC2, the remaining progenitor cells were cultured to analyse their potential to produce progeny. For this purpose, sort purified progenitors were cultured in a FLT3L ligand DC-differentiation culture system. In detail, total BM (TBM), MDPs, CDPs, and pre-cDCs from the bone marrow of *Clec9a$^{cre/cre}$Rosa^{DTA}* and control mice were cultured in the presence of FLT3. Additionally, CD45.1 congenic feeder BM cells, were used in the culture to ensure equal culture conditions despite differences in starting cells due to poor yield resulting from the severe reduction of pre-cDCs in *Clec9a$^{cre/cre}$Rosa^{DTA}* mice. Seven days later, the output of the

cultures was analysed by flow cytometry. Despite low cell numbers put in culture, culturing equal numbers of pre-cDCs from control mice generated CD11c^{+}MHCII+ cells, whereas no pre-cDC from DTA mice generated equivalent cells (**Figure 22**). While gating for pre-cDC in *Clec9a$^{cre/cre}$Rosa^{DTA}* mice it became obvious that the few remaining cells that fall into the pre-cDC gate remain on the lower corner of the gate for CD135 which becomes obvious in the

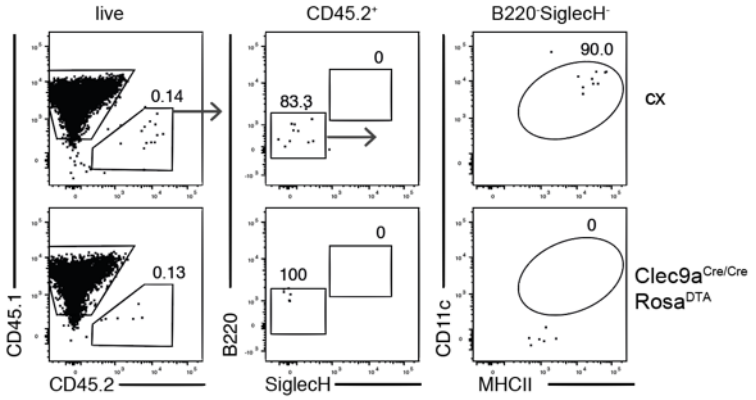

Figure 22: Remaining pre-cDCs from Clec9a$^{cre/cre}$Rosa^{DTA} mice do not generate cDC *in vitro*. Sort purified pre-cDCs (Lin^{-}MHCII^{-}CD11c^{+}CD135^{+}CD172^{int}) from the BM of control and Clec9a$^{cre/cre}$Rosa^{DTA} mice were cultured in FLT3L and the presence of congenic CD45.1^{+} bone marrow for 7 days. On Day 7 cultures were analysed by flow cytometry. Shown is the representative gating strategy for the DC outcome of the culture after 7 days. Pre-cDC progeny is gated on CD45.2 and gated for B220^{+}SiglecH^{+} pDCs or B220^{-}SiglecH^{-}CD11c^{+}MHCII^{+} DCs.

spleen as visible in **Figure 18**, **C**. The low CD135 expression on splenic cells is shown in **Figure 23** by comparing CD135 levels from the previous gate. It is, therefore, possible that the failure to expand pre-cDCs from *Clec9c$^{cre/cre}$Rosa^{DTA}* mice in response to FLT3L was due to lower expression of the receptor CD135. CD135 expression was not found to be different in MDPs and CDPs coming from *Clec9c$^{cre/cre}$Rosa^{DTA}* and control mice as becomes evident in the representative gating for MDPs and CDPs in **Figure 18, A**. Therefore, also these cells were cultured with FLT3L and compared to TBM cells in culture. TBM FLT3L culture gave substantial amounts of progeny from *Clec9c$^{cre/cre}$Rosa^{DTA}* and control mice, but yet, *Clec9c$^{cre/cre}$Rosa^{DTA}* BM gave significantly less CD11c+MHCII+ cells (**Figure 24**, **A**). MDPs, and CDPs from control mice readily expanded in FLT3L cultures and generated CD11c^{+}MHCII^{+} cells of both cDC1 and cDC2 subtypes. In contrast, the same progenitor populations from *Clec9a$^{cre/cre}$Rosa^{DTA}* mice exhibited significantly reduced output in response

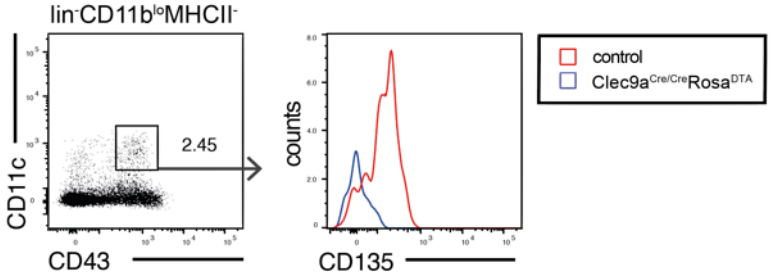

Figure 23: Lower expression of CD135 on cells resembling pre-cDCs in the spleen of *Clec9a$^{cre/cre}$Rosa^{DTA}* mice. Representative gating of pre-cDC gating without final gating on CD135 in splenocytes from a control mouse and overlaid histogram of these cells from *Clec9a$^{cre/cre}$Rosa^{DTA}* and control mice shown the expression of CD135.

to FLT3L compared to control progenitor outcome to which it was normalized for quantification in **Figure 24**, **C**. Looking at the DC subsets, the cultures with TBM, MDPs and CDPs generated no CD24$^+$ cDC1 equivalents and only few CD11b$^+$ cDC2 equivalents (**Figure 24**, **C**).

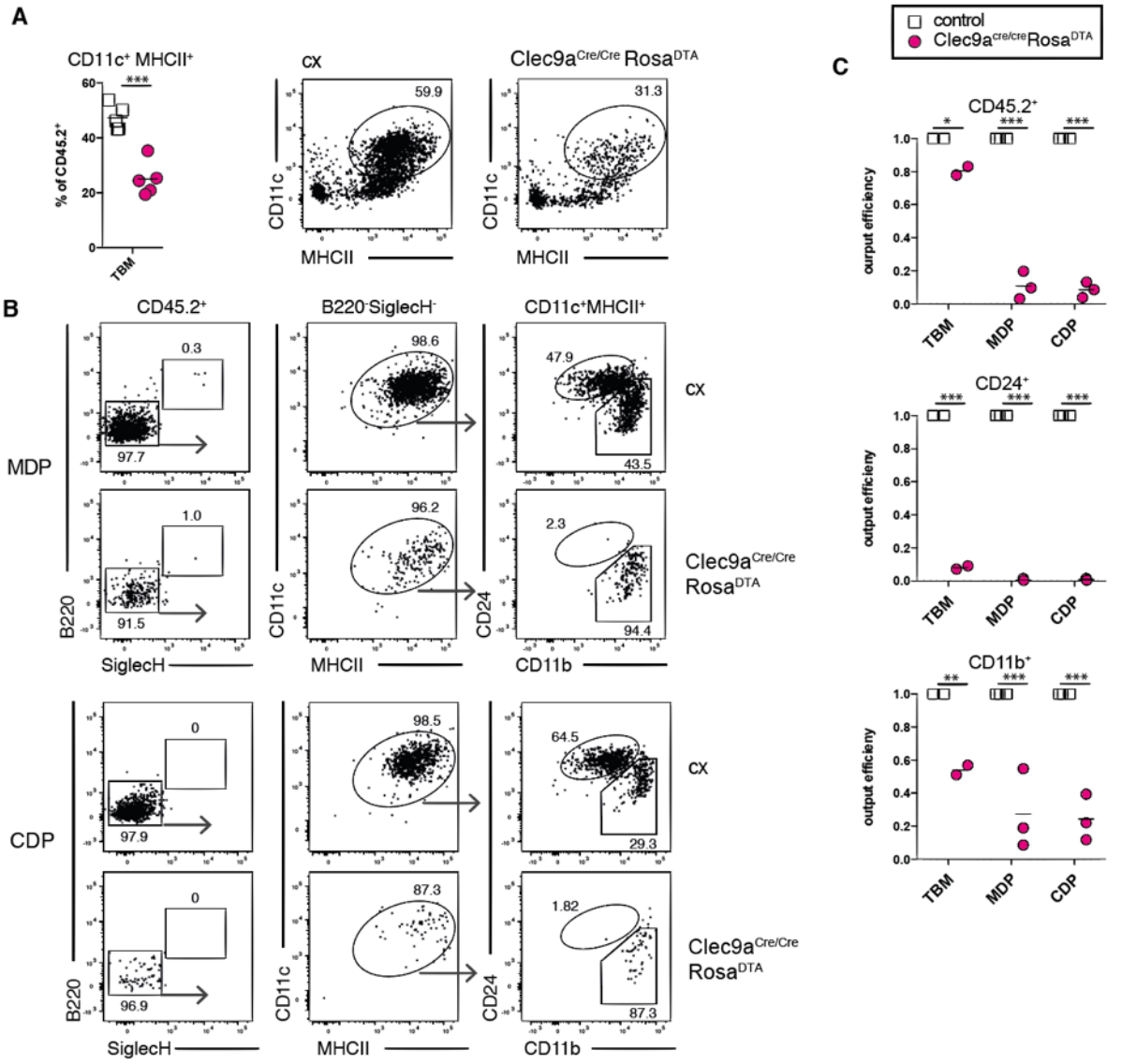

Figure 24: Bone marrow progenitors from *Clec9a$^{cre/cre}$Rosa^{DTA}* mice do not generate cDC in Flt3L cultures *in vitro*. A. Total bone marrow (TBM) from control and *Clec9a$^{cre/cre}$Rosa^{DTA}* mice was cultured with Flt3L for 7 days. On Day 7 cultures were analysed by flow cytometry. Shown is the representative gating for and the frequency of CD11c$^+$MHCII$^+$ cells in all CD45.2$^+$ cells in the culture **B**. Sort purified MDPs (Lin$^-$MHCII$^-$CD11c$^-$CD115$^+$CD135$^+$CD117^{hi}) and CDPs (Lin$^-$MHCII$^-$CD11c$^-$CD115$^+$CD135$^+$CD117$^{low\text{-}int}$) from the BM of control and *Clec9a$^{cre/cre}$Rosa^{DTA}* mice were cultured with Flt3L in the presence of congenic BM cells (CD45.1$^+$) for 7 days. On Day 7 cultures were analysed by flow cytometry. Shown is the representative gating for and the frequency of CD11c$^+$MHCII$^+$ cells in all CD45.2$^+$ cells in the culture. **C**. The output efficiency of cultured BM, MDPs and CDPs from **A** and **B** was calculated as the number of cells generated at the end of the culture period divided by the number of input cells normalized to the control. Each symbol represents one mouse. * p<0.05, ** p<0.01, *** p<0.001.

Taking into account that Flt3L is not the only growth factor that stimulates DC progenitors to differentiate into DCs, additionally also cultures with GM-CSF were prepared. GM-CSF

cultures are known to produce cells resembling either macrophages (GM-MACs) or DCs (GM-DCs) or other CD11c^{+}MHCII^{+} cells (GM-DN, double negative), which can be distinguished by the marker expression of MHCII, CD115, and CD135, where MHCII^{hi}CD11b^{lo}CD115^{-}CD135^{+} cells are termed GM-DCs, MHCII^{lo}CD11b^{hi}CD115^{-}MerTK^{+} cells are termed GM-MACS and MHCII^{hi}CD11b^{lo}CD115^{-}CD135^{-} are termed GM-DN cells (Helft et al., 2015). When total BM (TBM) of *Clec9a$^{cre/cre}$Rosa^{DTA}* and control mice was cultured in the presence of GM-CSF, less GM-DCs developed compared to the culture of TBM form control mice (**Figure 25, A**). However, the frequency of CD115^{-}CD135^{-} GMDNs and CD115^{+}CD135^{-}MerTK^{+} GM-MACs was unchanged between *Clec9a$^{cre/cre}$Rosa^{DTA}* and control mice (**Figure 25, A**). Additionally, also sort purified CDPs gave reduced output of GM-DCs when cultured in the presence of GM-CSF and also here the frequency of GM-DN cells was comparable between *Clec9a$^{Cre/Cre}$Rosa^{DTA}* and control mice (**Figure 25, B**).

Considering that the few DC progenitors that are left in *Clec9a$^{cre/cre}$Rosa^{DTA}* mice are inefficient in giving progeny *in vitro* in BM-cultures, the hypothesis was further supported that DC2 in *Clec9a$^{cre/cre}$Rosa^{DTA}* mice do not derive from myeloid DC progenitors but derive from alternative progenitors in the absence of bona fide progenitors.

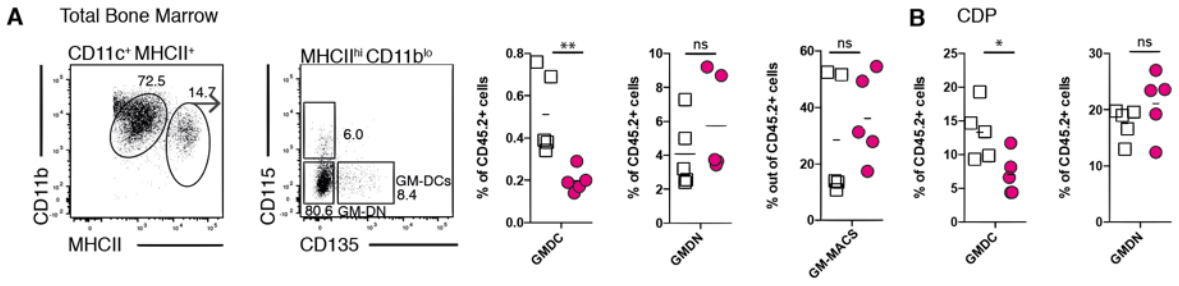

Figure 25: Bone marrow progenitors from *Clec9a$^{cre/cre}$Rosa^{DTA}* mice do not generate cDC in GM-CSF cultures *in vitro*. A. and B. TBM from control and *Clec9a$^{cre/cre}$Rosa^{DTA}* mice (CD45.2^{+}) in the presence of GM-CSF for 6 days. **A.** Representative gating on cells harvested from GM-CSF culture of BM from control mice to identify GM-CSF-derived CD45.2^{+}CD11c^{+}CD11b^{+}MHCII^{hi}CD115^{-}CD135^{+} GM DCs and CD45.2^{+}CD11c^{+}CD11b^{+}MHCII^{hi}CD115^{-}CD135^{-} GM-DNs. Frequency of GM-DC and GM-DN as well as CD45.2^{+}CD11c^{+}CD11b^{hi}MHCII^{+}CD115^{+}MerTK^{+} GM MACs. **B.** Sort purified CDPs (Lin^{-}MHCII^{-}CD11c^{-}CD115^{+}CD135^{+}CD117$^{low\text{-}int}$) from the BM of control and *Clec9a$^{cre/cre}$Rosa^{DTA}* mice were cultured with GM-CSF in the presence of congenic BM cells (CD45.1^{+}) for 6 days. On Day 6 cultures were analysed by flow cytometry. Shown is the representative gating for and the frequency of GMDC and GMDN cells in all CD45.2^{+} cells in the culture as identified in (**A**). Each symbol represents one mouse; n=5; ns: not significant; * p<0.05, ** p<0.01.

4.2.7 DC2 FROM CLEC9A$^{CRE/CRE}$ROSA^{DTA} MICE PHENOTYPICALLY RESEMBLE BONA FIDE DENDRITIC CELLS

DC2 that have been found to unexpectedly arise in *Clec9a$^{cre/cre}$Rosa^{DTA}* mice were identified as such based on the expression of confined markers as CD64^{-}CD11c^{+}MHCII^{+}CD11b^{+} cells. However, based on the hypothesis that these cells have a distinct origin than bona fide DC2, phenotypic differences were analysed to provide evidence of different origins or functions that explain the reason for this additional DC development pathway. For this purpose, surface

markers that are commonly used to identify DC2 were analysed by flow cytometry. However, most markers showed a similar expression profile on cells resembling DC2 in *Clec9a*$^{cre/cre}$*Rosa*^{DTA} mice compared to control mice like CD11c, MHCII, Clec4a4, ESAM, CD172a (**Figure 26**, **A**). CD4, however, showed a decreased expression on some but not all the cells resembling DC2 in *Clec9a*$^{cre/cre}$*Rosa*^{DTA} mice (**Figure 26**, **A**). Another marker that was analysed on the cells of interest was the receptor for Flt3L, CD135, which was found to be decreased on the cells that resemble DC2 in *Clec9a*$^{cre/cre}$*Rosa*^{DTA} mice. In addition to surface markers also transcription factors that are known to be required for the development of DCs were analysed by intranuclear staining and flow cytometry (Kashiwada et al., 2011; Satpathy et al., 2012; Schlitzer et al., 2013). The analysed transcription factors IRF4 and Zbtb46 showed overlapping expression whereas IRF8 was not expressed in both bona fide DC2 from control mice and cells resembling DC2 in *Clec9a*$^{cre/cre}$*Rosa*^{DTA} mice (**Figure 26**, **A**). The characteristic phenotype of DCs are the dendrites, which DCs use to patrol their surroundings for antigens. For the comparison of the microscopical structure, cytospins of sort purified CD11c^{+}MHCII^{+}CD24^{-}CD11b^{+} cells from the spleens of *Clec9a*$^{cre/cre}$*Rosa*^{DTA} as well as heterozygous *Clec9a*$^{+/cre}$*Rosa*^{DTA} and control mice were analysed. Both cytospins showed characteristic dendrites and no microscopic differences of any kind were detected between cells resembling DC2 from *Clec9a*$^{cre/cre}$*Rosa*^{DTA}, *Clec9a*$^{+/cre}$*Rosa*^{DTA} mice and cDC2 from control mice (**Figure 26**, **B**). From the phenotype of the cells, therefore, no definite distinction can be made between DC2 in *Clec9a*$^{cre/cre}$*Rosa*^{DTA} and control mice.

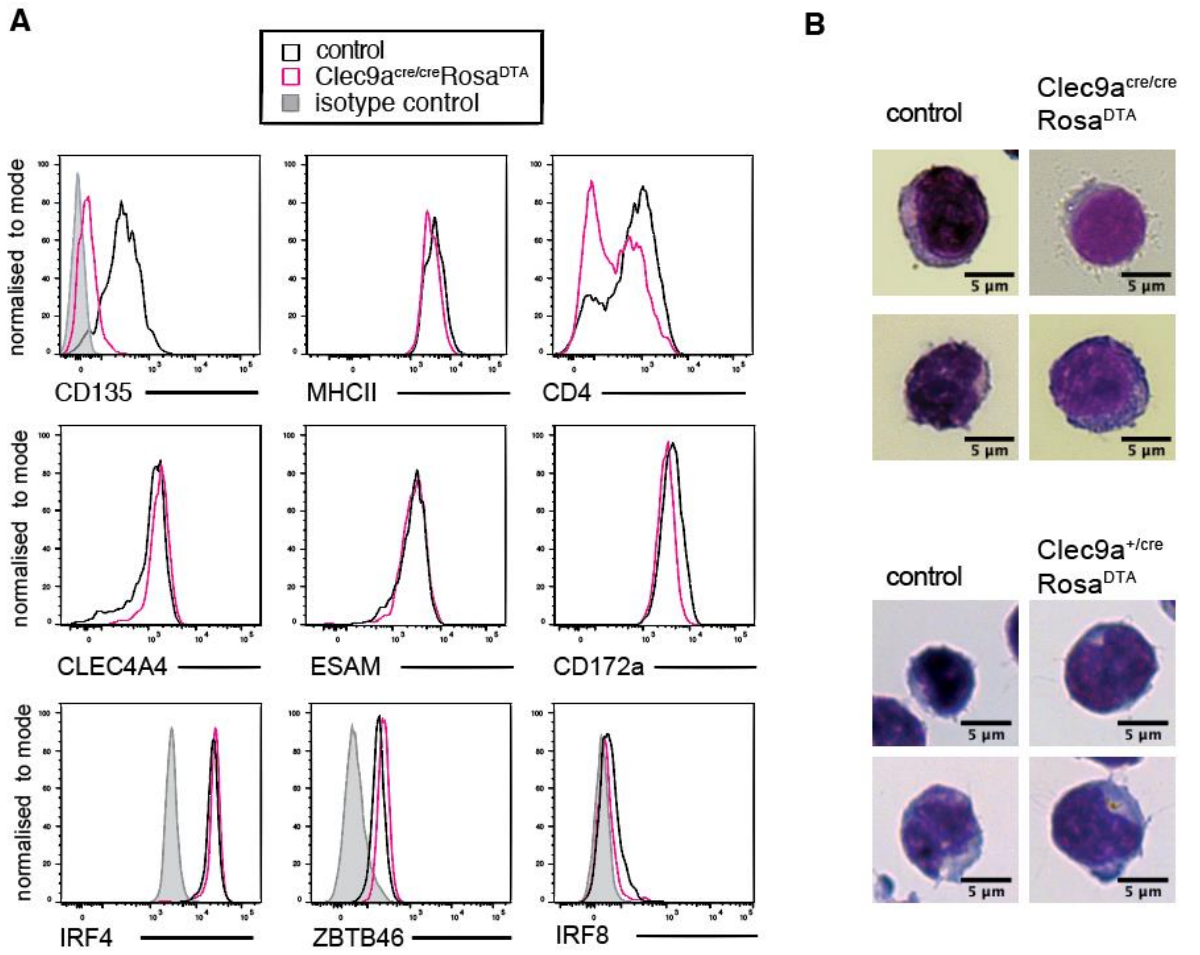

Figure 26: Phenotypic comparison of DC2 from of *Clec9a$^{cre/cre}$Rosa^{DTA}* and control mice. A. Splenic DC2 (CD64^{-}CD11c^{+}MCHII^{+}CD24^{-}CD11b^{+}) were analysed for the expression of typical DC2 surface markers (first two rows) as well as intranuclear staining of typical DC transcription factors by flow cytometry. Shown are representative overlays. Representative gating of pre-cDC gating without final gating on CD135 in splenocytes from a control mouse and overlaid histogram of these cells from *Clec9a$^{cre/cre}$Rosa^{DTA}* and control mice shown the expression of CD135. **B.** Cytospins of sort purified DC2. DC2 were sorted from homozygous *Clec9a$^{cre/cre}$Rosa^{DTA}* (upper panel) and heterozygous *Clec9a$^{+/cre}$Rosa^{DTA}* (lower panel) as well as control mice as CD64^{-}CD11c^{+}MCHII^{+}CD24^{-}CD11b^{+} cells spun on a microscope slide and stained with Giemsa. Representative cells were imaged.

4.2.8 DC2 *FROM* *CLEC9A$^{CRE/CRE}$ROSA^{DTA}* *MICE PRODUCE CYTOKINES IN RESPONSE TO* *CPG* *AND* *LPS* *IN COMPARABLE FREQUENCIES TO* *CDC2 FROM CONTROL MICE*

To test whether DC2 from *Clec9a$^{cre/cre}$Rosa^{DTA}* and control mice share the same function despite differences in origin, functional analyses were performed to gain more insights into the reason for the existence of DC2 of a different origin. A hallmark function of DCs is their ability to secrete cytokines to stimulate T cells responses. In comparative functional analyses, splenocytes were enriched for DCs and stimulated with TLR ligands in the presence of the Golgi inhibitor brefeldin A to block secretion of the cytokines. After 6h, cytokine expression was measured by intracellular cytokine staining and flow cytometry in the cells resembling DC2 from *Clec9a$^{cre/cre}$Rosa^{DTA}* mice and bona fide cDC2 from control mice. As expected DC2

produced IL12 and TNF after stimulation with either LPS or CpG in comparison to unstimulated cells (**Figure 27**). Equal frequencies of cDC2 from control mice and cells resembling DC2 from *Clec9a*$^{cre/cre}$*Rosa*^{DTA} mice produced TNF and/ or IL12 in response to CpG (**Figure 27**, lower panel). When stimulated with LPS, however, a lower percentage of DC2 from *Clec9a*$^{cre/cre}$*Rosa*^{DTA} mice produced TNF alone and also the percentage of TNF^{+}IL12^{+} DC2 was lower in *Clec9a*$^{cre/cre}$*Rosa*^{DTA} mice compared to DC2 from control mice, whereas no difference was observed in the frequency of only IL-12 producing cells after LPS stimulation (**Figure 27**, upper panel).

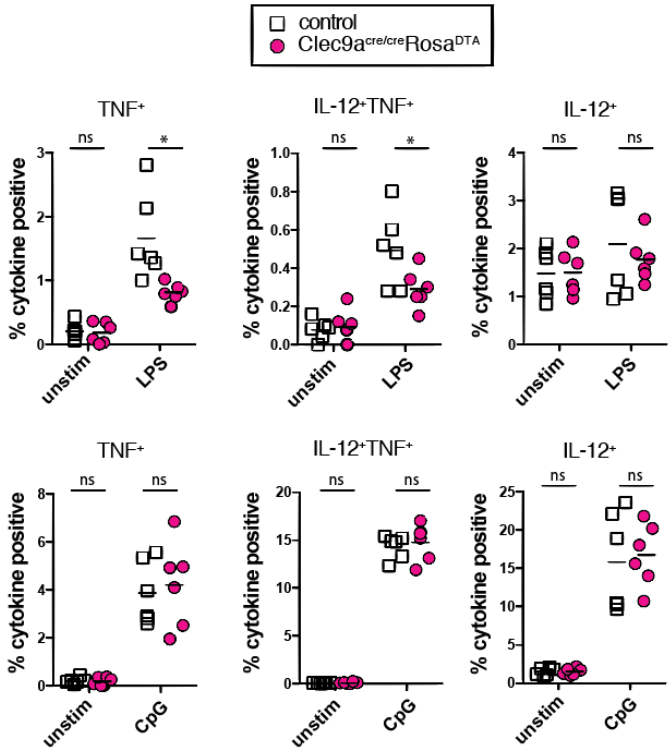

Figure 27: Cytokine production of DC2 from of *Clec9a*$^{cre/cre}$*Rosa*^{DTA} and control mice after stimulation. A. Splenocytes from *Clec9a*$^{cre/cre}$*Rosa*^{DTA} and control mice were enriched for CD11c^{+} cells using magnetic separation. CD11c enriched cells were stimulated with either LPS (100ng/ml) or CpG (0.5µg/ml) for 6h in the presence of brefeldin A. From the harvested cells DC2 were identified as CD64^{-}CD11c^{+}MCHII^{+}CD24^{-}CD11b^{+} cells and analysed for the expression of IL12 and TNF by intracellular cytokine staining and flow cytometry. The frequency of either single or double-positive cells for each cytokine among the DC2 population are shown. Each symbol represents one mouse; n=6; ns: not significant; * p<0.05.

4.2.9 DC2 FROM CLEC9A$^{CRE/CRE}$ROSA^{DTA} MICE HAVE SOMATIC REARRANGEMENTS IN THE IGH LOCUS SUGGESTING A LYMPHOID ORIGIN

Although the current opinion in the field is, that DCs derive from myeloid progenitors in steady-state (Auffray et al., 2009; Manz, Traver, Akashi, Merad, Miyamoto, Engleman, et al., 2001a), studies also showed that common lymphoid progenitors have the potential to give rise to DCs *in vitro* and also in adoptive transfer studies (Izon et al., 2001; Manz, Traver, Miyamoto, Weissman, & Akashi, 2001b; Welner et al., 2008; Wu et al., 2001). Considering the hypothesis that the cells that resemble cDC2 in *Clec9a*$^{cre/cre}$*Rosa*^{DTA} mice have an alternative origin, a

potential lymphoid origin was further investigated. RAG1 is expressed in common lymphoid progenitors and leads to the somatic rearrangement of the D- and J- segments of the heavy chain locus (IgH) in the B-cell receptor gene (Borghesi et al., 2004; **Figure 28**, **A**). The D-J rearrangement of the IgH locus was analysed by PCR on genetic DNA isolated from sort purified cDC2 from control mice and equivalent cells from *Clec9a*$^{cre/cre}$*Rosa*^{DTA} mice. Neutrophils, which served as a negative control due to their myeloid origin, were sorted as Ly6G^{+} cells from control splenocytes and showed no bands at the height of D-J rearrangements but only the germline band whereas pDC, which have been under discussion for having a dual myeloid and lymphoid origin and are known to have D-J rearrangement of the IgH locus, did show rearrangements in the PCR and served as a positive control (**Figure 28**, **B**). As expected cDC2 from control mice did not show bands at the height of somatic rearrangements of the IgH locus but indeed the cells that resemble DC2 in *Clec9a*$^{cre/cre}$*Rosa*^{DTA} mice showed D-J rearrangements control (**Figure 28**, **B**). This shows a history of RAG1 expression in the DC2 in *Clec9a*$^{cre/cre}$*Rosa*^{DTA} mice indicating a lymphoid origin and clearly shows a difference to cDC2 from control mice. Therefore, the *Clec9a*$^{cre/cre}$*Rosa*^{DTA} mouse model suggests that upon blockade of normal cDC development, cDC can arise from a lymphoid progenitor and these cells will from here on be termed lymphoid DC2.

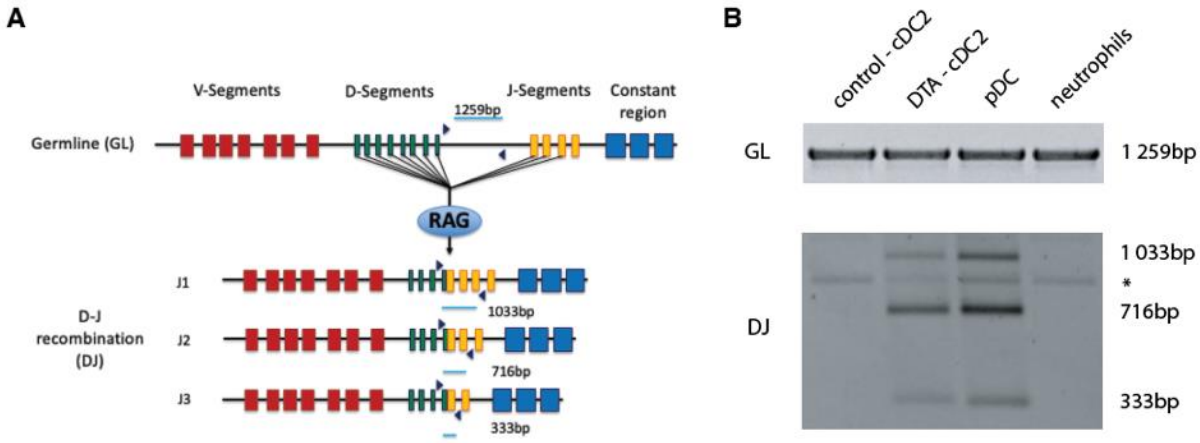

Figure 28: DC2 from *Clec9a*$^{cre/cre}$*Rosa*^{DTA} mice show D-J rearrangements. A. Schematic display of RAG1 induced rearrangements in the IgH locus. **B.** Genomic PCR of sort purified populations from *Clec9a*$^{cre/cre}$*Rosa*^{DTA} and control mice for germline (GL) locus and D–J rearrangements of the IgH chain using primer mixtures homologous for regions of the Dfl16 and Dsp2 D gene families. pDCs (SiglecH^{+}B220^{+}) served as positive control and neutrophils (Ly-6G^{+}) as negative control. Representative of 3 independent experiments. * unspecific band.

4.2.10 Clec9a$^{cre/cre}$Rosa^{DTA} mice show a trend to increased Common Lymphoid Progenitors (CLP)

As it has been shown that CLPs can give rise to DCs in *in vitro* studies and also in adoptive transfer experiments into irradiated mice, and CLPs are known to have RAG1 expression leading to D-J rearrangements as they have been found in the lymphoid DC2 of *Clec9a*$^{cre/cre}$*Rosa*^{DTA} mice, they were considered a potential progenitor for the lymphoid DC2

that arise independent of CDPs in *Clec9a*$^{cre/cre}$*Rosa*^{DTA} mice. The CLPs in the BM of control and *Clec9a*$^{cre/cre}$*Rosa*^{DTA} mice were quantified since a potential increase in a progenitor population was reasoned to be indicative of an increased demand for the population to fill an empty niche. Indeed, CLPs identified as CD117^{int}Sca-1$^{low-int}$CD135^{+}IL7R^{+} cells seemed increased in frequency and in counts in the BM of 2 analysed *Clec9a*$^{cre/cre}$*Rosa*^{DTA} mice in comparison to 2 control mice (**Figure 29**). This provides a hint towards a dysregulation of the CLP population however does not prove the CLP to be the progenitor of the lymphoid DC2 in *Clec9a*$^{cre/cre}$*Rosa*^{DTA} mice.

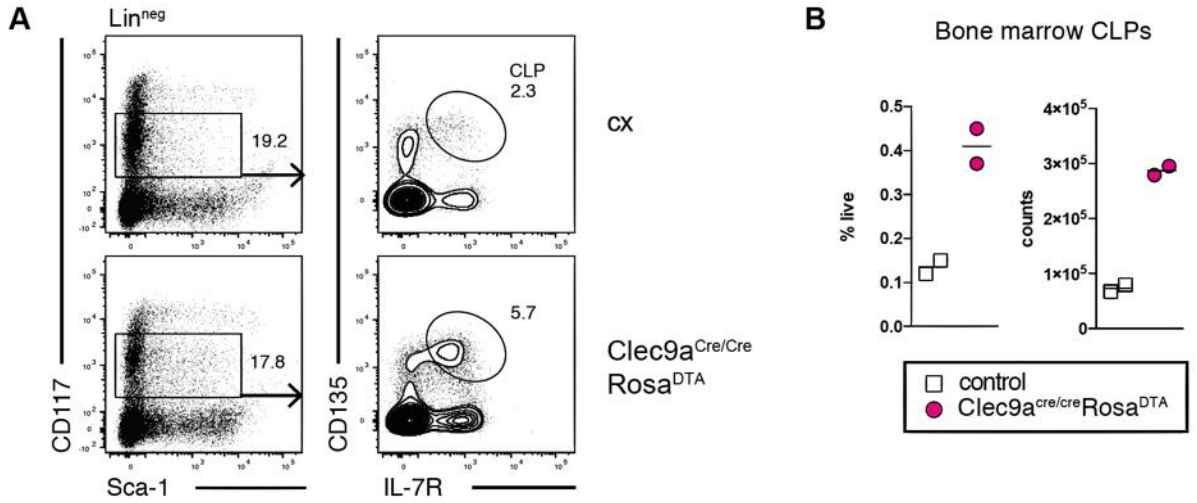

Figure 29: Quantification of Common Lymphoid Progenitors (CLPs) in the BM of *Clec9a*$^{cre/cre}$*Rosa*^{DTA} and control mice. A. Representative gating strategy of CLPs identified as Lineage negative (Lin: CD3, CD4, CD8, CD19, GR-1, Ter119, NK1.1) CD117^{int}Sca-1$^{low-int}$CD135^{+}IL7R^{+} cells in the BM of *Clec9a*$^{cre/cre}$*Rosa*^{DTA} and control mice. **B.** Frequency and counts of CLPs in the BM *Clec9a*$^{cre/cre}$*Rosa*^{DTA} and control mice as identified in (**A**). Each symbol represents one mouse; n=2.

4.3 CLEC9A$^{CRE/CRE}$ROSA^{DTA} MICE SHOW A POTENTIAL REDUCTION IN DC2 MIGRATION COMPARED TO BONA FIDE DC2

4.3.2 REDUCED MIGRATORY DC2 IN THE SKIN DRAINING BUT NOT MESENTERIC LYMPH NODES FROM CLEC9A$^{CRE/CRE}$ROSA^{DTA} MICE COMPARED TO BONA FIDE CDC2

To gain further insight into differences between *Clec9a*$^{cre/cre}$*Rosa*^{DTA} and control mice outside of the spleen, lymph nodes that drain different organs were analysed by flow cytometry. The analysis in this chapter shows the inguinal LN (iLN) and the ear draining LN (auricular LN, aLN) representing 2 skin draining LNs and the mesenteric LN that drains the intestine. The analysis of the spleen showed that *Clec9a*$^{cre/cre}$*Rosa*$^{DTA\ A}$mice do not fully represent a steady-state model and depletion of CDP derived cells leads to myeloproliferation and neutrophilia (**Figure 12**). The total cellularity of the analysed iLN, aLN and mLNs however, in contrast to the spleen has not been found increased. Interesting in the context of myeloproliferation

though, a population of CD64^{+}CD11b^{+} cells that are likely monocyte-derived cells based on the expression of CD64 was found to be increased in the LNs of *Clec9a$^{cre/cre}$Rosa^{DTA}* mice (**Figure 30**). The DC compartment in LNs is divided into resident DCs, that are constantly replenished from bone marrow precursors and migratory DCs that have migrated from the drained organ to the lymph node. These populations can be distinguished by the level of the markers CD11c and MHCII in steady-state.

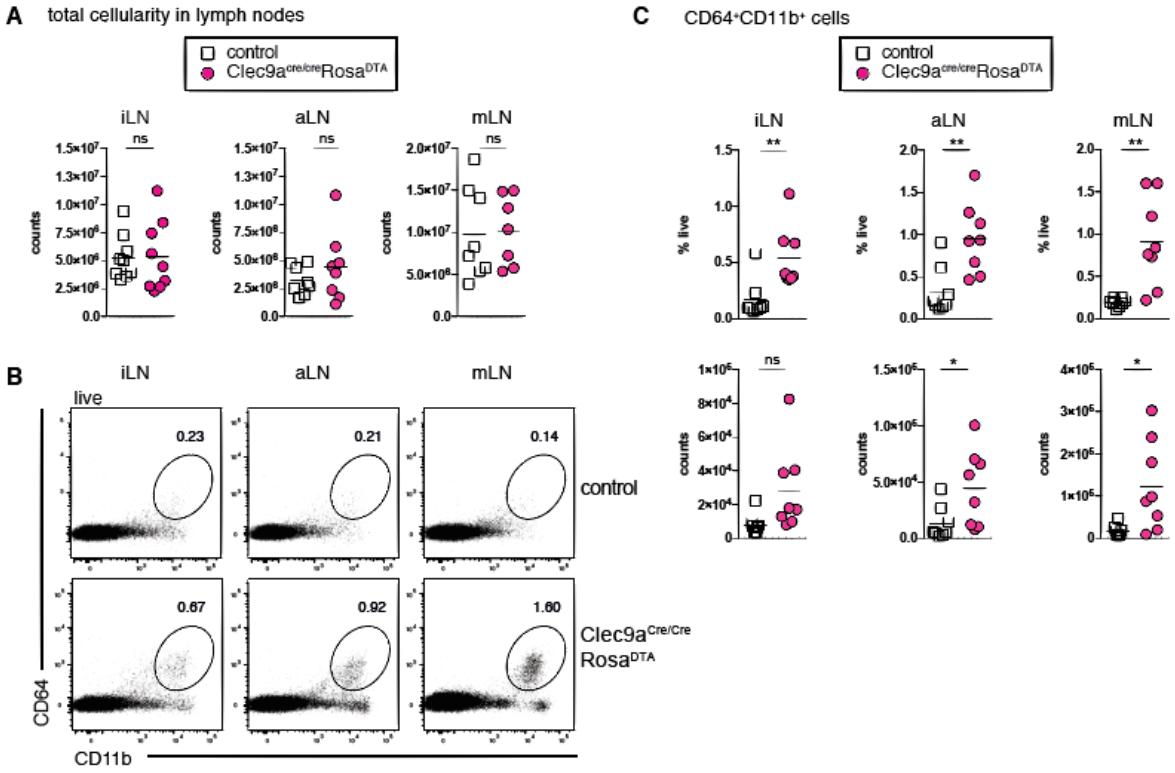

Figure 30: Comparable cellularity but increase of a CD64^{+}CD11b^{+} population in different LNs in *Clec9a^{cre}Rosa^{DTA}* mice. **A.** Total cellularity of iLN, aLN and mLN in *Clec9a$^{cre/cre}$Rosa^{DTA}* and control mice. **B.** Representative FACS plots of live cells in the different LNs showing gating on a CD64^{+}CD11b^{+} population. **C.** Quantification of the CD64^{+}CD11b^{+} population identified as in (**B**). Each symbol represents one mouse; n=8; ns: not significant; * p<0.05; ** p<0.01.

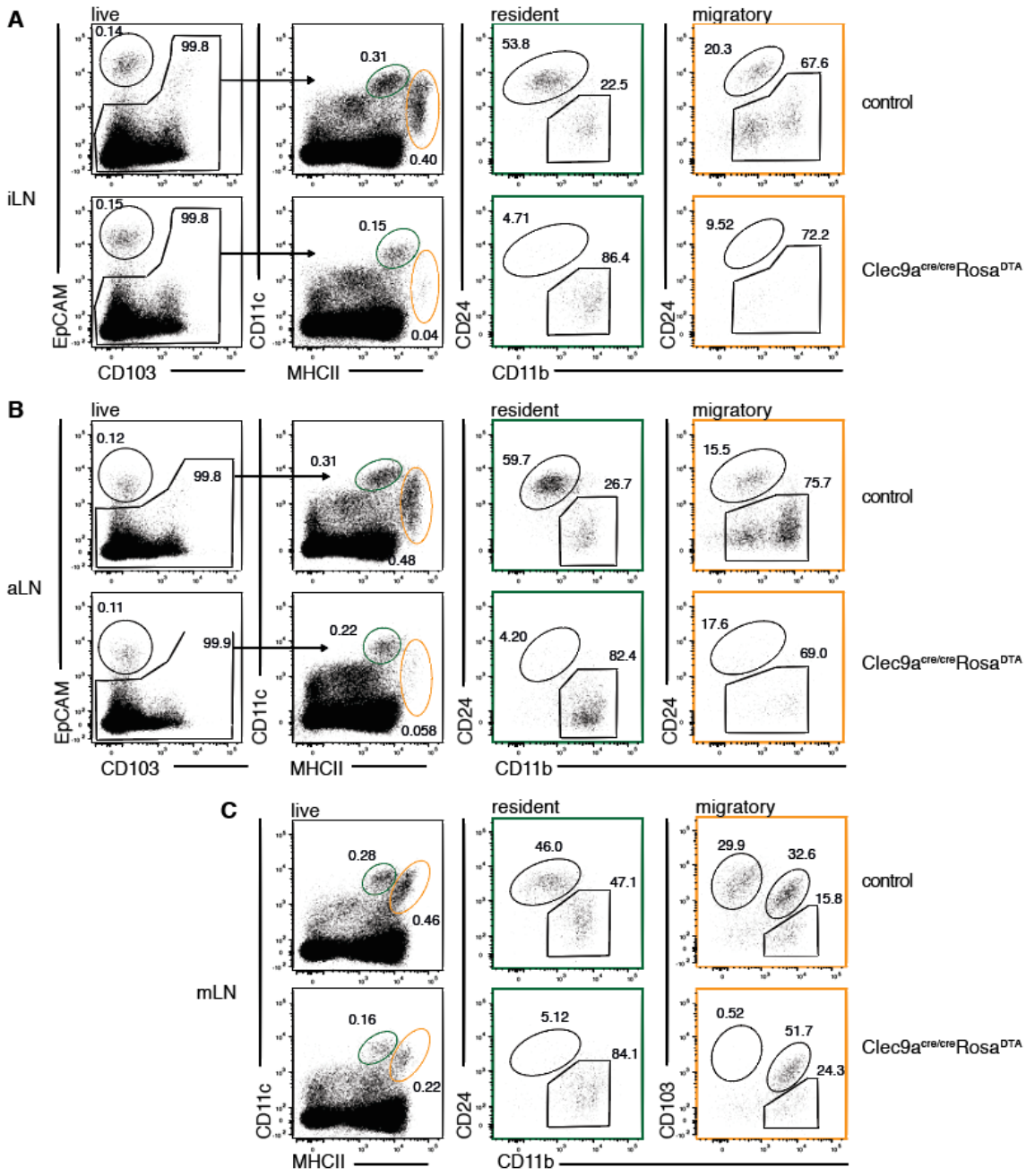

Figure 31: Representative gating of resident and migratory DC subsets as well as LC in different of *Clec9a*$^{cre/cre}$*Rosa*^{DTA} and control mice. Cells were isolated from the skin draining inguinal LN (iLN, **A**), auricular LN (aLN, **B**) and mesenteric LN (mLN; **C**) of control mice (upper row) and *Clec9a*$^{cre/cre}$*Rosa*^{DTA} mice (lower row) and analysed by flow cytometry. **A. and B.** Skin draining LN were gated for EpCAM^{+}CD103^{-} Langerhans cells (further gating ensured them to be CD11c^{+}MHCII^{+}, not shown) the remaining non-Langerhans cells were further gated for CD11c and MHCII and CD11c^{hi}MHCII^{+} resident DCs were distinguished from CD11c^{+}MHCII^{hi} migratory DCs. Both resident and migratory DC subsets were further subset in CD24^{+} cDC1 and CD11b^{+} DC2. **C.** Living cells from the mLN of control mice (upper row) and *Clec9a*$^{cre/cre}$*Rosa*^{DTA} mice (lower row) were gated for CD11c^{hi}MHCII^{+} resident DCs and CD11c^{+}MHCII^{hi} migratory DCs. Resident DCs were further subset into CD24^{+} cDC1 and CD11b^{+} DC2 whereas among migratory DCs CD103^{+}CD11b^{-} cDC1, CD103^{+} CD11b^{+} double-positive (DP) DC2 and CD103^{-} CD11b^{+} single-positive (SP) DC2 were distinguished.

As shown in **Figure 31** this discrimination can still be applied in *Clec9a*$^{cre/cre}$*Rosa*^{DTA} mice. In the skin draining iLN and aLN. Langerhans cells (LCs) that also migrate from the skin to the draining LN under steady state conditions have to be distinguished from DCs. Therefore, LCs

were gated separate as EpCAM^{+}CD103cells and excluded from further DC gating (**Figure 31**). The remaining cells were gated as CD11c^{+}MHCII^{hi} migratory DCs and CD11c^{hi}MHCII^{hi} resident DCs (**Figure 31**). Both DC compartments can again be dissected into cDC1 and cDC2 based on gating on CD24^{+} and CD11b^{+} cells respectively (**Figure 31**). In mesenteric lymph nodes, the migratory DC compartment is composed of the DCs that have migrated from the intestine. Therefore, the migratory DC population can be divided into the 3 main DC populations that can be identified in the gut, namely CD103^{+}CD11b^{-}, CD103^{+}CD11b^{+} and CD103^{-}CD11b^{+} cells (**Figure 31**, **C**). When comparing the quantification of the different populations in the skin draining LNs between *Clec9a*$^{cre/cre}$*Rosa*^{DTA} and control mice, it became evident that cDC1 were depleted from both resident and migratory DC compartments, as expected. Also, resident DC2 were not diminished in counts in *Clec9a*$^{cre/cre}$*Rosa*^{DTA} mice, which compares to the observation in the spleen in **Figure 16**. Migratory DC2, however, were significantly decreased in the skin draining lymph nodes in *Clec9a*$^{cre/cre}$*Rosa*^{DTA} mice compared to control mice. This implies that the migration of lymphoid DCs is impaired. A decrease in migratory DC2 was not found in the mLN of *Clec9a*$^{cre/cre}$*Rosa*^{DTA} mice, which suggests a tissue-specific defect that affects the migration from the skin to the skin draining LNs specifically. To exclude that the discrepancy in migratory DC2 is derived from cell-extrinsic effect like a dysregulation of the CCL7 gradient deposition in *Clec9a*$^{cre/cre}$*Rosa*^{DTA} mice, also Langerhans cells were quantified. Langerhans cells are not affected by the *Clec9a*$^{cre/cre}$*Rosa*^{DTA} system, as they derive from embryonic precursors and do not express *Clec9a* (Schraml et al., 2013). In addition, Langerhans cells also migrate from the skin to the in steady-state using similar mechanisms (Ohl et al., 2004). In the quantification of Langerhans cells in the iLN and aLN, equal frequencies and counts were found for *Clec9a*$^{cre/cre}$*Rosa*^{DTA} and control mice (**Figure 31**, **A and B**). Therefore, the hypothesis that lymphoid DC2 show an intrinsic cell migration defect from the skin to the draining LNs was stated.

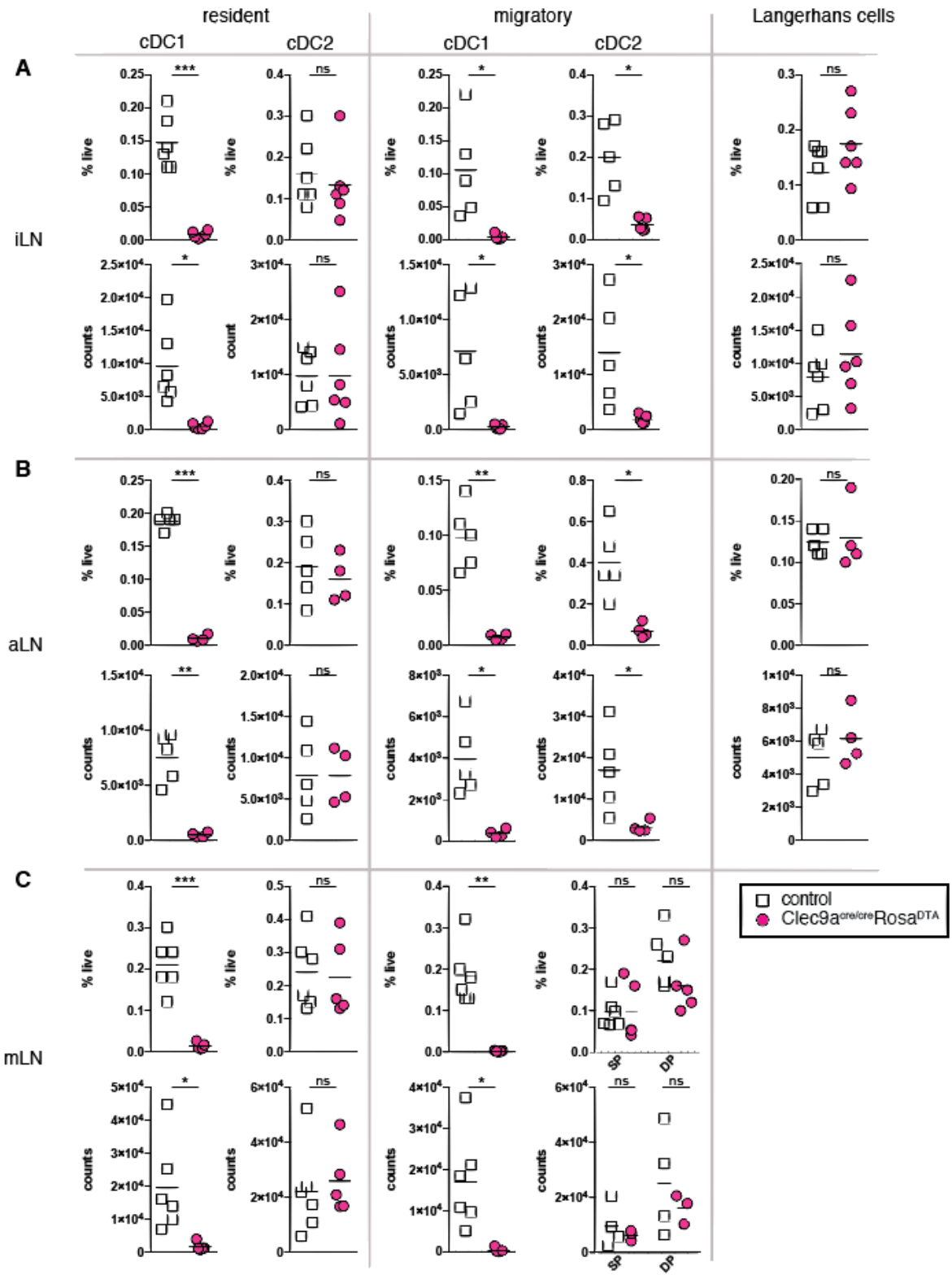

Figure 32: Quantification of migratory DC2 in the inguinal (A) and auricular (B) and mesenteric (C) LN of *Clec9a*$^{cre/cre}$*Rosa*^{DTA} and control mice in both frequency and counts. Resident and migratory DC2 were analysed by flow cytometry and gated as in **Figure 31** were *Clec9a*$^{cre/cre}$*Rosa*^{DTA} and control mice. Each symbol represents one mouse; n=4-6; ns: not significant; * p<0.05; ** p<0.01; *** p<0.001.

One possible reason for reduced migration in lymphoid DC2 is a difference in CCR7 receptor expression as this is necessary to facilitate the migration. Therefore, the expression of CCR7 on DC2 in the inguinal LNs from *Clec9a*$^{cre/cre}$*Rosa*^{DTA} and control mice was analysed by surface antibody staining and flow cytometry. In the LNs migratory DCs have high CCR7 expression, compared to resident DCs (Lee et al., 2009; **Figure 33**). The level of CCR7 on both resident and migratory DC2 was not altered between DC2 from *Clec9a*$^{cre/cre}$*Rosa*^{DTA} and control mice (**Figure 33**, **A**) and also the percentage of CCR7 positive cells among the resident and migratory DC2 populations was comparable between lymphoid DC2 and cDC2 (**Figure 33**, **B**). This shows that lymphoid DC2 can express CCR7 upon migration to the draining LN at the same level as cDC2 and also the baseline expression of CCR7 in the resident DC2 population is comparable between *Clec9a*$^{cre/cre}$*Rosa*^{DTA} and control mice and therefore differences in upregulation of CCR7 in migratory DCs is not defective in lymphoid DC2 and thus cannot account for the reduced migratory DC cell numbers found in skin draining LN in *Clec9a*$^{cre/cre}$*Rosa*^{DTA} compared to control mice.

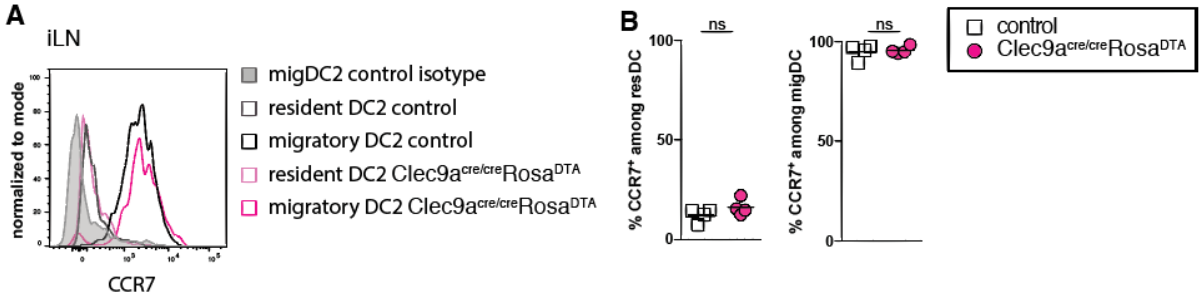

Figure 33: Equal CCR7 expression on migratory and resident DC2 in the inguinal LN of *Clec9a*$^{cre/cre}$*Rosa*^{DTA} and control mice. A. Overlaid histograms of CCR7 expression in resident, CD11c^{hi}MHCII^{+} (light traces) and migratory, CD11c^{+}MHCII^{hi} (dark traces) CD11b^{+}CD24^{-} DC2 subsets in the inguinal LN of *Clec9a*$^{cre/cre}$*Rosa*^{DTA} (pink traces) and control mice (black traces). The grey trace shows the isotype stained migratory DC2 population of a control mouse. **B**. Frequency of CCR7^{+} cells among the indicated population gated based on isotype control staining. Each symbol represents one mouse; n=4; ns: not significant.

4.3.3 Reduced numbers of DC2 after migration from the skin of from Clec9a^{cre}*Rosa*^{DTA} *mice but also in the isolation from the skin*

To confirm the hypothesis that lymphoid DC2 have a defect in the migration from the skin, an experiment was performed that analyses the migration from the skin of the ear *in vitro*. For this purpose, ears from *Clec9a*^{cre}*Rosa*^{DTA} and control mice were split into dorsal and ventral halves and incubated for 24h on either medium only, as a negative control, or medium containing CCL19 that induces CCR7 mediated DC migration. The migration towards CCL19 gave a great advantage over cell migration to medium proving that the cells migrate directed toward the chemokine in a CCR7 dependent manner. In the quantification of the DC2 in the medium after 24h using flow cytometry, about 10 times less lymphoid DC2 were found to have migrated out of the ear of *Clec9a*$^{cre/cre}$*Rosa*^{DTA} mice compared to cDC2 that migrated out of the

ears of control mice (**Figure 34, A**). Langerhans cells served again as control for CCR7 directed movement and showed no difference between *Clec9a*$^{cre/cre}$*Rosa*^{DTA} and control mice (**Figure 34, A**). Of note, this experiment was performed in both heterozygous a *Clec9a*$^{+/Cre}$*Rosa*^{DTA} and homozygous *Clec9a*$^{Cre/Cre}$*Rosa*^{DTA} mice giving similar results (**Figure 34, B**). The reduced counts of lymphoid DCs after the migration out of the ear towards CCL19 indicate that indeed lymphoid DCs have a defect in the migration from the skin.

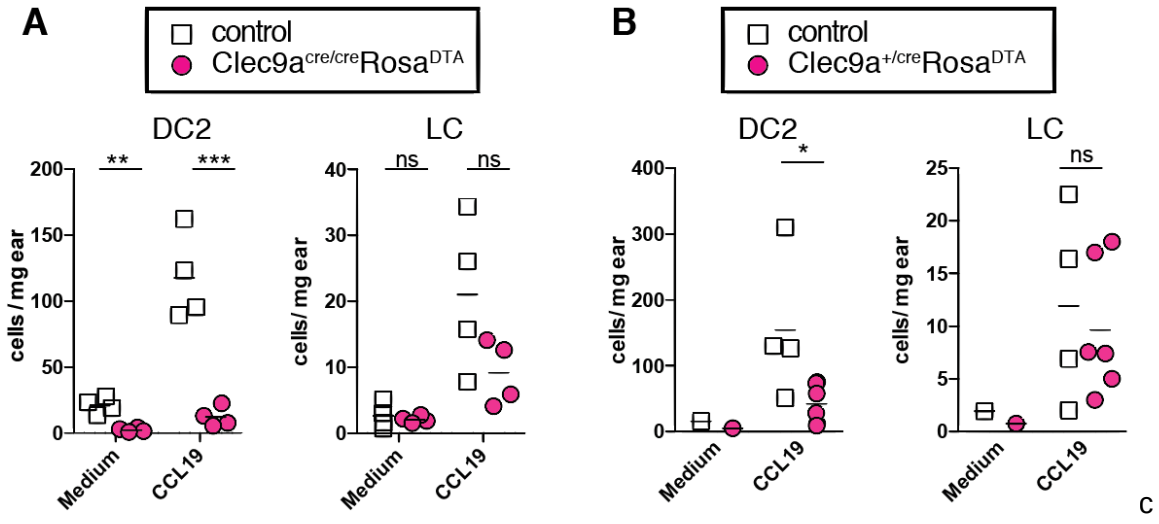

Figure 34: Reduced migration of lymphoid DC2 but not LC out of ear from heterozygous *Clec9a*$^{+/cre}$*Rosa*^{DTA} and homozygous *Clec9a*$^{cre/cre}$*Rosa*^{DTA} mice. Ears from heterozygous *Clec9a*$^{+/cre}$*Rosa*^{DTA} (**B**, n=6), homozygous *Clec9a*$^{cre/cre}$*Rosa*^{DTA} (**A,** n=4) and control mice (A: n=4 B: n=1) were placed on medium alone or containing 100ng/ml CCL19. 24 hours later the number of lymphoid and myeloid DC2 was quantified by flow cytometry and calculated back to the initial weight of the ear placed in culture. Each symbol represents one mouse; ns: not significant. * p<0.05; ** p<0.01; *** p<0.001.

The data from both, the reduced migration of lymphoid DC2 and the reduced quantification after migration out of the ear in the *in vitro* crawl out assay relies on the fact that the numbers of DC2 in the skin are not reduced as has been also shown for the spleen and the resident DC2 in the LNs. To prove that lymphoid DC2 numbers are equal in the skin of *Clec9a*^{cre}*Rosa*^{DTA} and control mice, leukocytes were isolated from the dermis and epidermis of the ears of these mice. The gating strategy for DCs and Langerhans cells, which are mainly found in the epidermis, is depicted in **Figure 35 A.** for the dermis and **B.** for the epidermis and includes CD45^{+}CD11c^{+}MHCII^{+}CD64^{-}EpCAM^{+}CD103^{-} cells. Dendritic cells, which can only be found in the dermis, were gated as CD45^{+}CD11c^{+}MHCII^{+}CD64^{-} cells that were not EpCAM^{+}CD103^{-} and were further subset in CD24^{+} cDC1 and CD11b^{+} cDC2 (**Figure 35**, **A**) (Henri, Poulin, et al., 2010b; Tamoutounour et al., 2013).

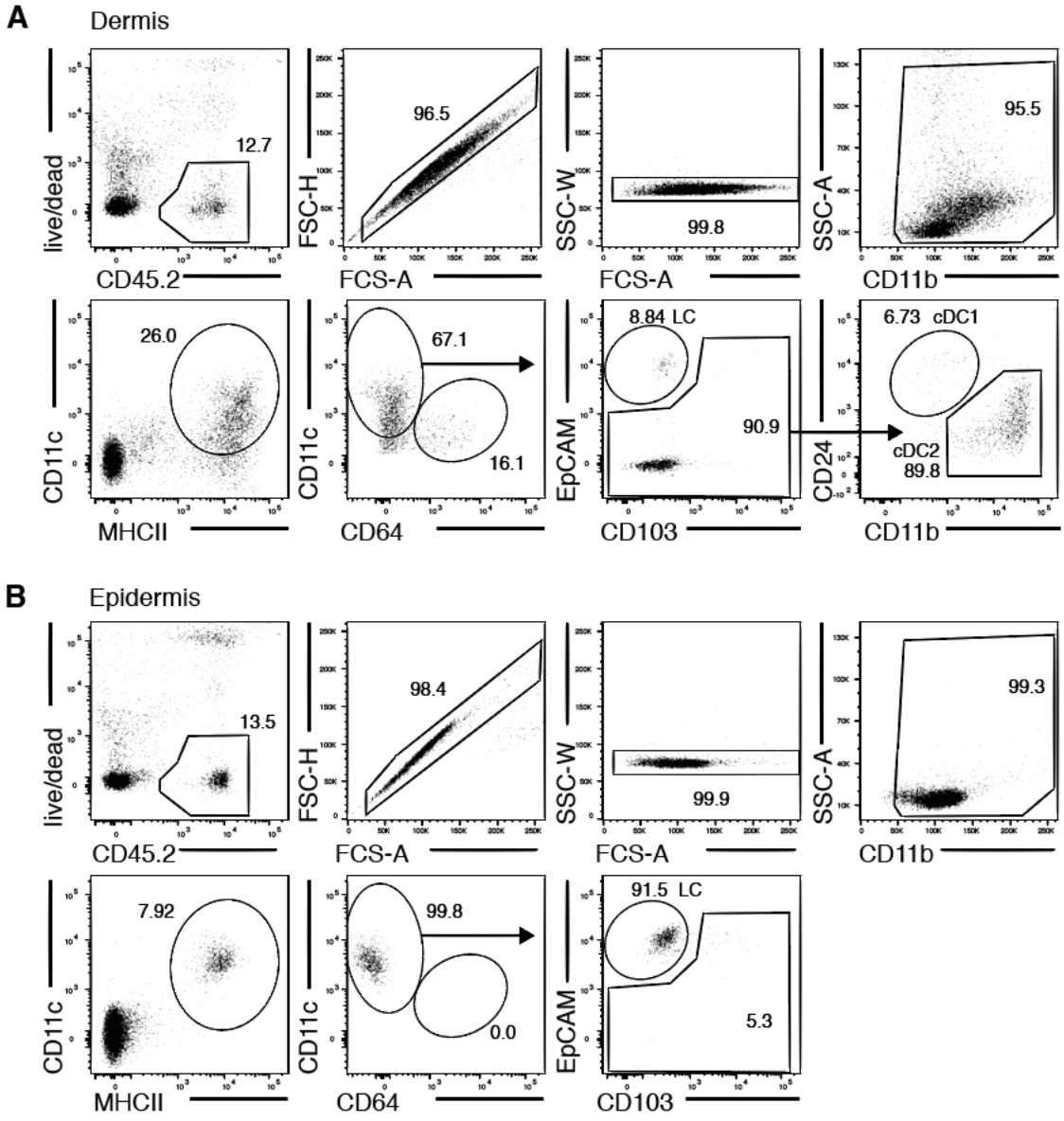

Figure 35: Representative gating of DC subsets in the dermis as well as LC in the epidermis of the ear. Cells were isolated from the skin of a control mouse, split into dermis (**A**) and epidermis (**B**), stained and analysed by flow cytometry. **A and B.** Cells were gated on CD45.2 positive, then doublets were excluded from the analysis. Single cells were gated based on size and granularity for leukocytes and these were further gated on $CD11c^{+}MHCII^{+}$ cells. In the next step, cells were divided into $CD64^{+}$ and $CD64^{-}$ cells. CD64- cells were gated for $EpCAM^{+}CD103^{-}$ Langerhans cells and the remaining non-Langerhans cells were considered DCs and further subset in $CD24^{+}$ cDC1 and $CD11b^{+}$ DC2 in the dermis (**A**).

In contrast to the quantification in the spleen, however, reduced numbers of lymphoid DC2 and cDC2 were found per mg ear tissue from both heterozygous *Clec9*$^{+/cre}$*Rosa*^{DTA} and homozygous *Clec9a*$^{cre/cre}$*Rosa*^{DTA} mice compared to control mice (**Figure 36, A and B**). Noticeable however is that the difference in DC2 numbers between *Clec9a*$^{+/cre}$*Rosa*^{DTA} and the control mouse are more marginal than between homozygous *Clec9a*$^{cre/cre}$*Rosa*^{DTA} mice and thus was not detected with fewer repetitions. These findings question the hypothesis of reduced migration based on the finding of reduced numbers of migratory lymphoid DC2 in the skin draining LNs and in the ear-crawl out assay in homozygous mice, however higher

differences in the crawl out assays compared to the skin quantification of DC2 still point towards a migration defect of lymphoid DC2 in the skin.

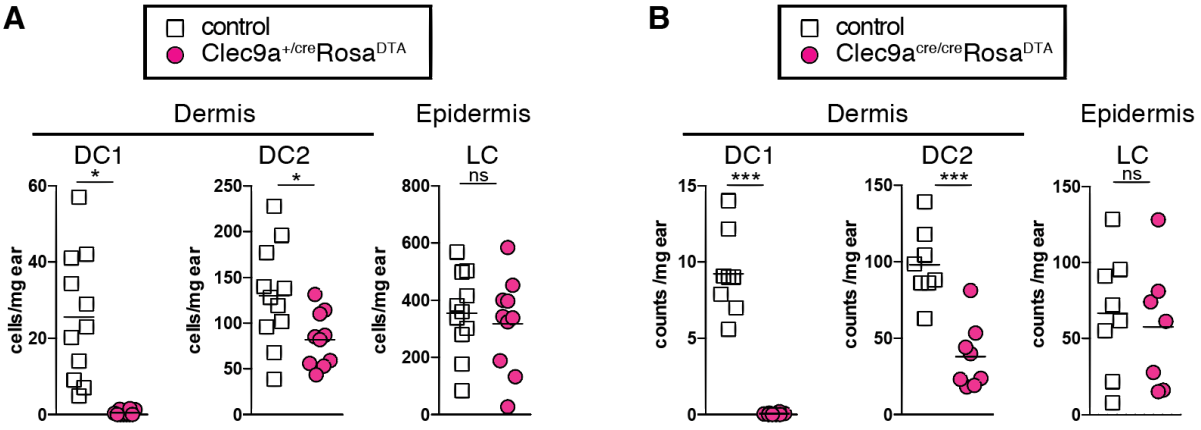

Figure 36: Quantification of Langerhans cells and DC2 in the skin of heterozygous *Clec9a$^{+/cre}$Rosa^{DTA}* (A) and homozygous *Clec9a$^{cre/cre}$Rosa^{DTA}* (B) mice. Cells were isolated from the skin of a control mouse, split into dermis and epidermis, and analysed by flow cytometry. Cells were quantified using counting beads and the counts were divided by the weight of the ear, to control for different amounts of input material. The cells were gated as described in **Figure 35**. Each symbol represents one mouse; n=7-8; ns: not significant; * p<0.05; ** p<0.01; *** p<0.001.

4.3.4 Splenic Lymphoid DC2 migrate less towards CCR7 ligands in vitro in steady-state but not upon activation

To further test the migration of the lymphoid DC2 in general, independent of the skin, splenic DCs were tested for their migratory capacity in an *in vitro* assay. Migration of splenic DC2 does not occur from a non-lymphoid tissue but takes place only within the spleen from the bridging channels into the white pulp, where they carry out their function as activators of T-cells (Calabro et al., 2016; Lu, Dang, McDonald, & Cyster, 2017; Yi & Cyster, 2013). Therefore, the migration of DCs within the spleen is important for their function as only the correct positioning to the zones of action facilitates their function. To analyse the migration capacity of splenic DC2 from *Clec9a$^{cre/cre}$Rosa^{DTA}* and control mice, total splenocytes were enriched for CD11c^{+} cells using magnetic separation and the enriched cells were applied to a transwell inlet with a polycarbonate membrane of 5µm pore size. The DC2 that had migrated to the lower well containing either medium or medium supplemented with CCR7 ligands were quantified using flow cytometry and calculated back to the percentage of input cells. Interestingly, the splenic lymphoid DC2 from *Clec9a$^{cre/cre}$Rosa^{DTA}* mice showed a reduced percentage of migration compared to the cDC from control mice although both lymphoid DC2 and bona fide cDC2 showed enhanced migration towards CCR7 stimuli in comparison to medium only (**Figure 37**). These findings suggest that, in steady-state, splenic lymphoid DC2 migrate less efficient towards CCR7 ligands (independent of the ligand), which further raises

the hypothesis that antigen-presenting function of DC2 could be impaired due to incorrect positioning of the cells within the organs.

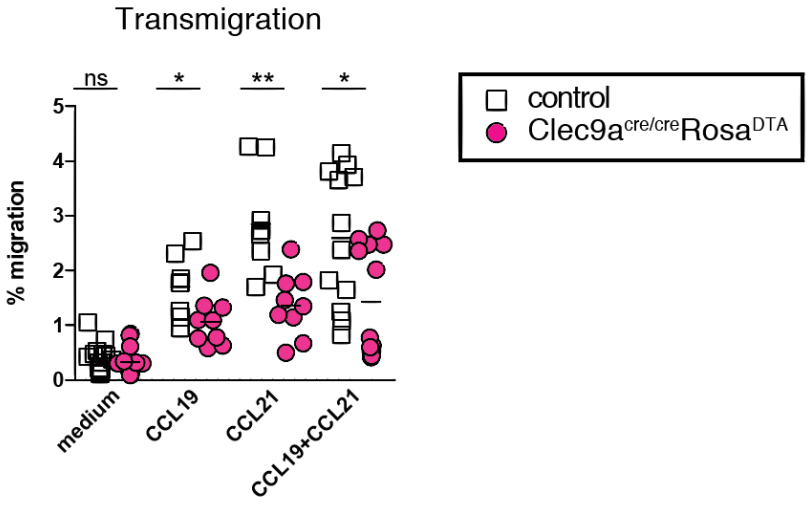

Figure 37: Reduced migration of splenic lymphoid DC2 to CCR7 ligands. CD11c enriched splenocytes from *Clec9a*$^{cre/cre}$*Rosa*^{DTA} and control mice were tested for their ability to migrate towards CCL19 (100ng/ml), CCL21 (100ng/ml) or a combination of both in transwells with 5µm pore size. Cell migration of DC2 to the lower chamber was quantified after 2 hours using flow cytometry and counting beads (n=9). ns, not significant; * p<0.05; ** p<0.01.

To further examine the mechanism that is impaired and leads to decreased migration of the DC2 an *in vitro* microscopic approach was applied. With this method, different parameters of the migration can be visualized, such as the velocity, directionality and shape of the cells. *In vitro* imaging approaches to visualize DC migration have been published for BM-derived DCs produced by culture with GM-CSF and activated with LPS but have not been shown on *ex vivo* isolated cells. The "*in vitro* analysis of chemotactic Leucocyte migration in 3D environments" approach has been chosen to provide an overview of the migration (Sixt & Lämmermann, 2011). For the purposes of this thesis, it was, however, necessary to perform the assay on ex vivo isolated cells, as only these have been validated and have been demonstrated do be of distinct origin *Clec9a*$^{cre/cre}$*Rosa*^{DTA} compared to control mice, whereas in GM-CSF cultures likely monocytes produce the DC outcome. In addition, the frequency of migrating cells in the transwell assay was with only up to 5% very low to possibly give enough data for the analysis of the imaging approach. Therefore, for this assay, DC2 were sort purified from the spleens of *Clec9a*$^{cre/cre}$*Rosa*^{DTA} and control mice and cultured in the presence of either medium only or medium containing LPS for 18h for the cells to rest or to become activated before seeding them in a collagen gel to improve the percentage of migrating cells. After the collagen had polymerized, a CCL19 gradient was applied and the cells were imaged every minute for 5h at 37°C using brightfield microscopy. The analysis of the videos by tracking of single cells as shown in **Figure 38**, **A** revealed no striking difference between *Clec9a*$^{cre/cre}$*Rosa*^{DTA} and control mice in either of the parameters, such as velocity,

accumulated distance and directionality (**Figure 38**). Of note, there was no difference observed comparing medium cultured and LPS cultured cells, except the percentage of migrating cells in LPS cultured cells was increased (**Figure 38**, **B**). This finding contradicts the fact that less splenic lymphoid DC2 have migrated in the transwells towards CCR7 ligands, but also cannot directly be compared as the transwell migration showed cells in steady-state condition.

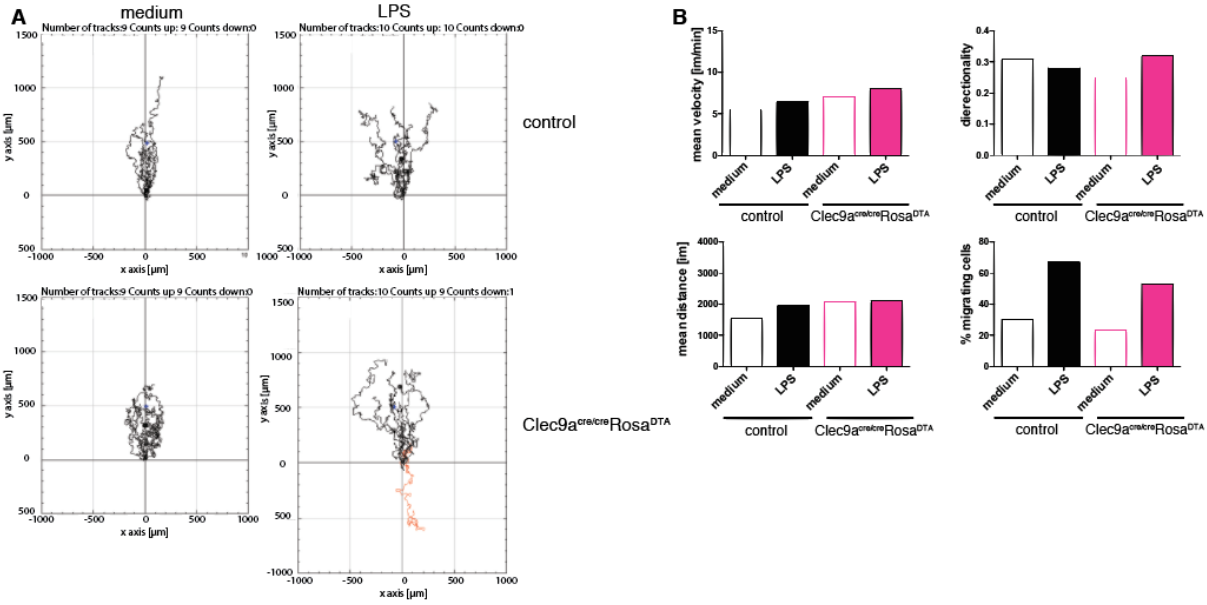

Figure 38: Comparable *in vitro* chemotactic migration of DC2 from *Clec9a*$^{cre/cre}$*Rosa*^{DTA} and control mice in 3D environments. DC2 were sort purified from the spleens of *Clec9a*$^{cre/cre}$*Rosa*^{DTA} and control mice and cultured in medium alone of medium containing 200ng/ml LPS for 18h. Cells were harvested and seeded in bovine collagen and stimulated with CCL19 to induce migration. Cells were imaged for 5h in 1min intervals. For the analysis 9-10 cells were tracked manually. **A.** Single-cell tracks of migrated splenic DC2 from *Clec9a*$^{cre/cre}$*Rosa*^{DTA} and control mice. **B.** Analysis of migration parameters was calculated automatically from the tracks of the individual cells. The frequency of migrating cells was calculated by dividing counts of migrating cells by counts of motionless cells while analysing at least 85 cells.

To analyse if the activation in the 3D migration assay has an impact on the abrogation of differences in migration capacity between lymphoid DC2 and cDC2, the activation status of lymphoid DC2 and control cDC2 was compared and the transwell migration experiment was repeated using CD11c enriched cells that have been activated with LPS for 18h prior to seeding them on the transwell.

The activation status of the DC2 was analysed to compare if lymphoid DC2 and cDC2 are differentially activated by LPS, which can impact their migration capacity. DCs upregulate co-stimulatory molecules on their surface after like CD40 CD80, CD83 and CD86 but also the chemokine receptor CCR7, which is a prerequisite for the migration towards CCR7 ligands. Therefore, the activation factors CD40 and CD86, as well as CCR7 were stained on the surface of the CD11c enriched cells after 18h culture with either medium or LPS and analysed by flow cytometry. All analysed markers, CD40, CD86 and CCR7 were highly upregulated on

DC2 after the culture with both LPS and medium only. The level of CD40, however, was yet increased in DC2 cultured with LPS compared to cells cultured with medium only whereas CCR7 staining intensity was even increased on cells cultured with medium only compared to LPS activated cells (**Figure 39**). The level of the activation markers CD40 and CD86 were not different between DC2 from *Clec9a*$^{cre/cre}$*Rosa*^{DTA} and control mice suggesting that both cells were equally activated after the culture (**Figure 39**). Additionally, also the CCR7 levels were comparable between DC2 from *Clec9a*$^{cre/cre}$*Rosa*^{DTA} and control mice (**Figure 39**). Lymphoid DC2, therefore, behave similarly to activation in culture with or without LPS in terms of upregulation of activation markers and CCR7 and therefore a possible defect in migration is not dependent on the differential activation status of the mice.

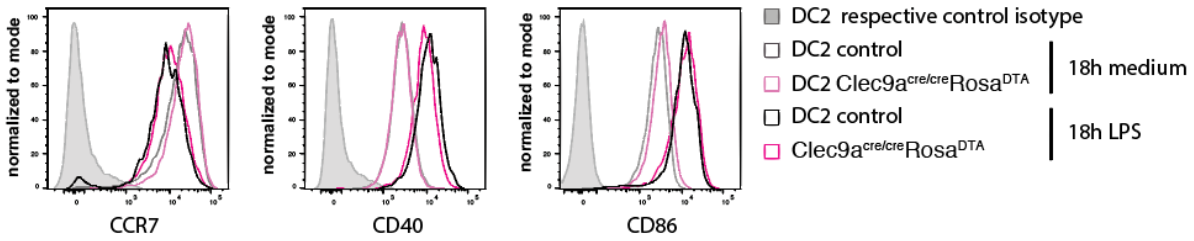

Figure 39: Comparable regulation of activation markers on splenic DC2 from *Clec9a*$^{cre/cre}$*Rosa*^{DTA} and control mice after culture for 18h. CD11c enriched splenocytes from *Clec9a*$^{cre/cre}$*Rosa*^{DTA} and control mice were cultured in complete medium with or without LPS (200ng/ml) for 18h. Shown are overlaid histograms of DC2 gated as CD64^{-}CD11c^{+}MHCII^{+}CD11b^{+}CD24^{-} cells for the markers CCR7, CD40 and CD86 for both conditions each. Grey traces represent the respective isotype control for the activation marker that has been stained on a control sample cultured with LPS.

In a transwell experiment that was performed as described above with the difference that cells were seeded after culturing them for 18h in either medium alone or medium containing LPS, the cells migrated about 10 times more efficiently towards CCR7 ligands, independent of LPS however also the migration towards medium is highly increased implying a higher random migration after activation (**Figure 40**). In line with the fact that DC2 cultured for 18h in medium alone show similar activation markers as DCs stimulated with LPS in addition, cells from both conditions migrated at the same frequency (**Figure 40**). Interestingly, the lymphoid DC2 and cDC2 from *Clec9a*$^{cre/cre}$*Rosa*^{DTA} and control mice respectively migrated at a similar frequency. (**Figure 40**). Therefore, the migration defect that has been observed in freshly isolated steady-state lymphoid DCs has been abrogated after activation in culture.

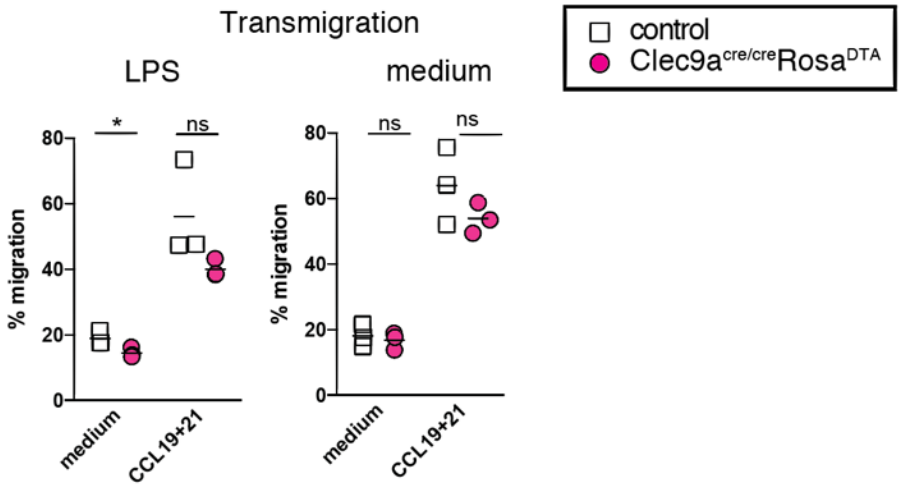

Figure 40: Comparable migration of splenic lymphoid DC2 to CCR7 ligands after activation with LPS. CD11c enriched splenocytes from *Clec9a*$^{cre/cre}$*Rosa*^{DTA} and control mice were cultured in complete medium with or without LPS (200ng/ml) for 18h. After the culture, cells were harvested and 10^5 cells were seeded into a transwell with 5µm pore size to test their ability to migrate towards a combination of both CCL19 and CCL21 (100ng/ml, each). Cell migration to the lower chamber was quantified after 2 hours using flow cytometry and counting beads (n=3). Each symbol represents one mouse; ns, not significant; * $p<0.05$.

4.3.5 *Lymphoid DC2 show increased necrosis in culture and increased Apoptosis after transmigration in the presence of CCR7 ligands*

Given the fact that the migration differences that have been observed in the crawl out assay and in the transwell migration of freshly isolated splenic DC2 were both depending on quantification of migrated cells after a certain time period and in the presence of CCR7 ligands, the differences can also be an artefact of increased cell death of lymphoid DC2 compared to cDC2 either due to faster turnover or due to their reaction to CCR7 ligands. Therefore, the frequency of apoptotic and necrotic cells was measured CD11c enriched cells that have been cultured for 2h in complete medium or in the presence of CCR7 ligands as well as in cells that have migrated through a transwell towards medium only, or medium containing CCR7 ligands using annexinV and propidium iodide (PI) staining. In this assay, double-negative cells are considered viable, whereas cells that stain for annexinV but not PI are apoptotic and double-positive cells are necrotic (**Figure 41, A)** (Schutte, Nuydens, Geerts, & Ramaekers, 1998). The DC2 that have been cultured with medium with or without CCR7 ligands showed a higher frequency of apoptotic cells compared to freshly isolated cells (**Figure 41, B)**. No difference was however observed between *ex vivo* isolated lymphoid DC2 and cDC2 from *Clec9a*$^{cre/cre}$*Rosa*^{DTA} and control mice (**Figure 41, B)**. Interestingly among the cells that have migrated through a transwell towards CCR7 ligands more apoptotic cells were found percentage-wise among the lymphoid DC2 (17.13±2.4%) compared to control cDC2 (9.54±1.59%) (Mean±SEM; **Figure 41, B)**. These cells, however, were still quantified in the transwell migration assay, as they did not (yet) stain as dead cells and therefore do not explain the differences in migration frequency. Cells cultured with CCR7 ligands serve as the control

for the input cells to the transwell inlet. Here the percentages of apoptotic cells is very high after 2h in culture compared to *ex vivo* isolated cells, but no difference can be observed in apoptotic cells between lymphoid DC2 and cDCs (**Figure 41, C)**. However, the percentage of necrotic cells is slightly increased in lymphoid DC2 cultured with medium or CCR7 ligands from 14.92±1.13% to 19.02±1.26% and 16.55±1.39% to 21.55±1.69%, respectively (Mean±SEM; **Figure 41, C)**. Therefore, it appears that lymphoid DC2 are more susceptible to cell death in culture compared to control cDC2.

The results of the increased cell death of lymphoid DC2 *in vitro* impact the results of the previously shown experiments. Although the differences in cell death induction between DC2 from *Clec9a*$^{cre/cre}$*Rosa*^{DTA} and control mice are not as pronounced as the differences observed in DC migration, they still have to be considered to impact the outcome of assays that include culturing. Therefore, the previously shown reduction in migration of not activated splenic lymphoid DC2 can be explained by the increased cell death in the assay and not by a migration defect after all.

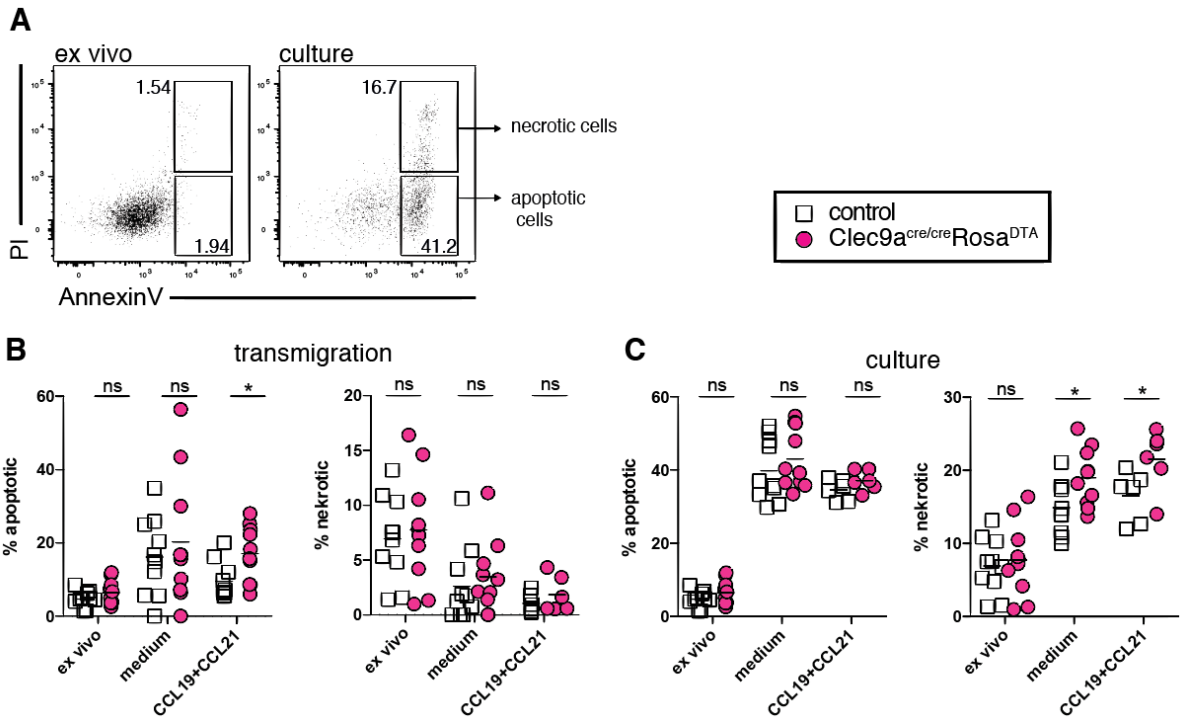

Figure 41: Splenic lymphoid DC2 show increased apoptosis after transwell migration towards CCR7 ligands and increased necrosis in lymphoid DC2 after culture. A. Representative gating on CD11c$^+$MHCII$^+$CD11b$^+$CD24$^-$ cDC2 from ex vivo cells and CD11c enriched splenocytes cultured for 2h in complete medium to identify annexinV$^+$PI$^-$ apoptotic and annexinV$^+$PI$^+$ necrotic cells **B.** Frequency of apoptotic and necrotic cells among DC2 from *Clec9a*$^{cre/cre}$*Rosa*^{DTA} and control mice before and after migration through a transwell. CD11c enriched splenocytes from *Clec9a*$^{cre/cre}$*Rosa*^{DTA} and control mice seeded on a transwell and migrated cells (towards medium or CCL19 and CCL21) were harvested after 2h as in the above experiments (**Figure 37**). DC2 were identified by flow cytometry as CD64$^-$CD11c$^+$MHCII$^+$CD11b$^+$CD24$^-$ cells and apoptotic and necrotic cells were identified based on annexinV and PI staining as in (**A**). Freshly isolated splenocytes (*ex vivo*) served as a control sample. **C.** Frequency of apoptotic and necrotic cells among DC2 from *Clec9a*$^{cre/cre}$*Rosa*^{DTA} and control mice before and after or cultured in complete medium with or without both CCL19 and CCL21 for 2h. DC2 were identified by

flow cytometry as CD64$^-$CD11c$^+$MHCII$^+$CD11b$^+$CD24$^-$ cells and apoptotic and necrotic cells were identified based on annexinV and PI staining as in (**A**). Freshly isolated splenocytes (*ex vivo*) served as a control sample. n=9; Each symbol represents one mouse; ns, not significant; * p<0.05.

4.3.6 The localization of the lymphoid DC2 in the inguinal LN appears disturbed in immunofluorescence sections

The migration of DCs is not only important for the transport of antigens from peripheral tissues upon activation, but also for the positioning of DCs within the lymphoid organs at steady state. The finding that freshly isolated, but not activated splenic DC2 migrate less towards CCR7 ligands, therefore, implied that the correct positioning of the lymphoid DC2 is impaired. To analyse the localization of DC2 within the lymphoid organs, inguinal LNs were analysed by confocal fluorescence microscopy. To visualize the T-cell zone, T-cells were stained with CD3 and to identify DC2 the markers CD11c, MHCII and Clec4a4 (clone 33D1) were used. Whereas CD11c and MHCII are staining all DCs, Clec4a4 is a specific marker to stain DC2 (Dudziak et al., 2007). Preliminary data of 2 independent experiments show that in the analysed control LN, the T-cells zone can clearly be distinguished by the CD3 staining whereas the B-cells zones can be identified by the absence of CD3 staining and MHCII staining, as B-cells express MHCII. In the control iLN section, clusters of cells that stain for Clec4a4 can be found in the interphase between T- and B-cells zones, which correlates with the published localization of cDC2 to the interfollicular zones in the LNs as indicated by arrows in the Clec4a4 staining in **Figure 42**, **A** (Braun et al., 2011; Gerner et al., 2012; 2015; Schumann et al., 2010). The Clec4a4 staining in the iLNs of *Clec9a$^{cre/cre}$Rosa^{DTA}* mice shows more and smaller clusters compared to the control lymph node that are more spread across the centre of the lymph node in the upper panel of **Figure 42**, **B,** but the second replicate shows comparable Clec4a4 distribution to the control iLNs (indicated by white arrow in each of the Clec4a4 staining panels). Additionally, the T-cell zone in the iLNs of *Clec9a$^{cre/cre}$Rosa^{DTA}* mice shows a more condensed staining pattern which is indicated by arrows in the staining for CD3 in **Figure 42**, **B.** This could be indicative of a deviant organization within the lymph nodes of *Clec9a$^{cre/cre}$Rosa^{DTA}* mice compared to control mice.

From this analysis, it, therefore, appears that the lymph node organization in the *Clec9a$^{cre/cre}$Rosa^{DTA}* mouse is abnormal. This could mean that defective positioning of lymphoid DC2 compared to CDP derived DC2 can have an effect on the LN structure especially in terms of the development of T-cell zones. One has to however also consider that DC migration might not be different between lymphoid DC2 and bona fide DC2 due to increased cell death in the migration assays, but the lymphoid DC2 are simply reduced in the skin of *Clec9a$^{cre/cre}$Rosa^{DTA}* mice and following this, migratory DC2 are diminished in the LNs of *Clec9a$^{cre/cre}$Rosa^{DTA}* mice. Therefore, the reduction of migratory DC2 could affect the LN structure. However, in **Figure 42** a reduction of DC2 does not become evident when

comparing the Clec4a4 staining. On the contrary, the Clec4a4 in the *Clec9a*$^{cre/cre}$*Rosa*^{DTA} iLN appears to stain more cells overall compared to the control iLN, which does not compare to the quantification of DC2 in the flow cytometry data shown in **Figure 32**. A quantification of the Clec4a4+ cells in this assay is however missing. Whether other factors that are relevant to ensure proper LN structure are different between *Clec9a*$^{cre/cre}$*Rosa*^{DTA} and control mice has not been addressed yet and therefore no absolute interpretation can be given.

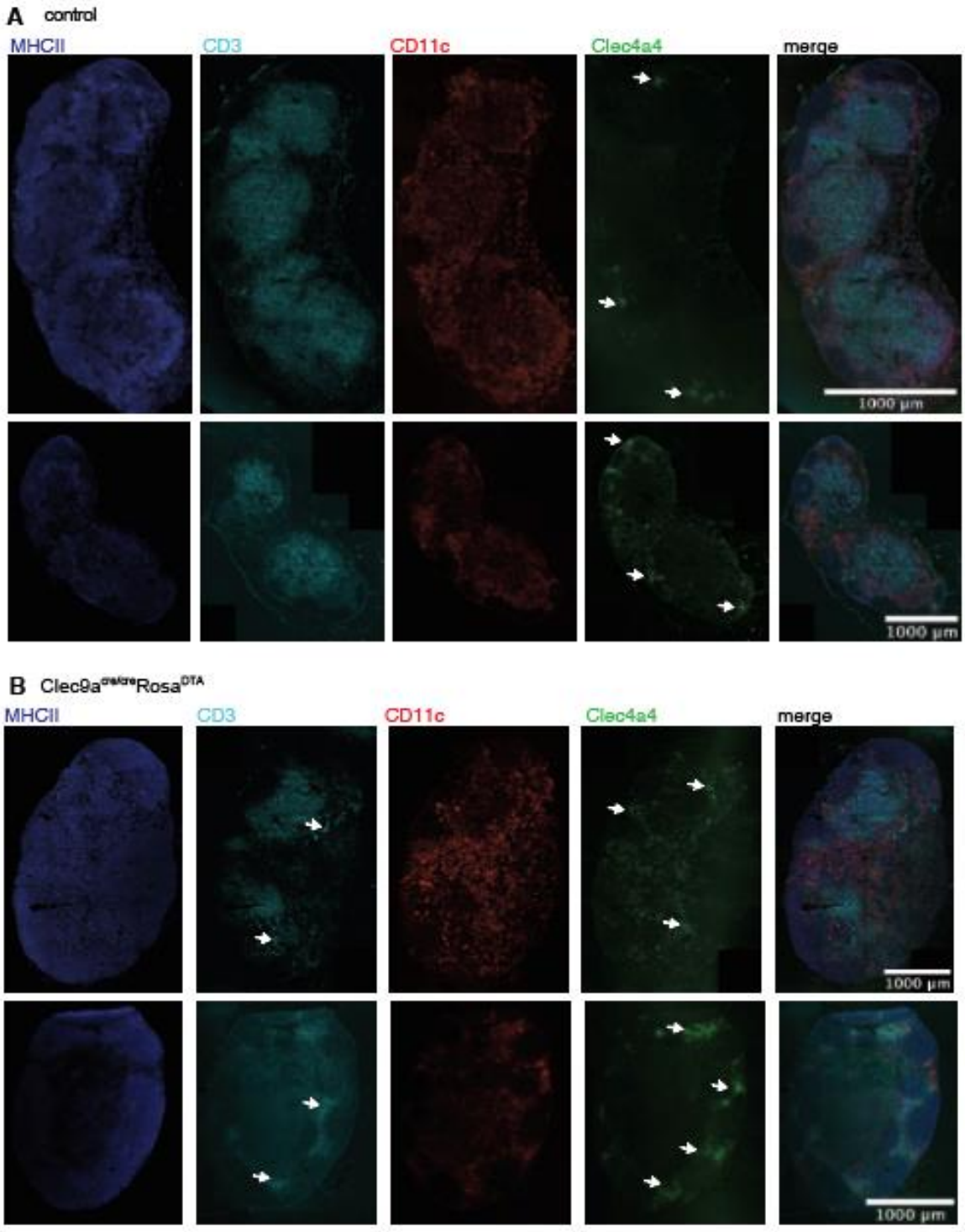

Figure 42: Immunofluorescence images of inguinal LN sections from control and *Clec9a$^{cre/cre}$Rosa^{DTA}* mice.12µm iLN sections from 2 control (**A**) and 2 *Clec9a$^{cre/cre}$Rosa^{DTA}* mice (**B**) were stained with MHCII-AF488 (blue); CD3-BV421 (cyan), CD11c-AF647 (red); Clec4a4-anti-rat-AF594, scale bar 1000/ 500 µm; n=2.

5. DISCUSSION

5.1 PRE-CDC SUBSET DISTRIBUTION DOES NOT ALWAYS CORRELATE TO DC SUBSET DISTRIBUTION IN TISSUES

Recent publications claim that the pre-cDC population contains subpopulations that show pre-commitment towards DC subsets already in the BM (Grajales-Reyes et al., 2015; Schlitzer et al., 2015). One aim of this thesis was to identify regulators of pre-cDC trafficking and to study if the homing of pre-cDCs to different peripheral organs is differentially regulated. Therefore, the existence of pre-committed subpopulations in the pre-cDC population in addition to the knowledge that the ratio of DC subpopulations varies between tissues, has led to the hypothesis that pre-committed pre-cDC subsets are differentially recruited to the different tissues. Differential recruitment could be necessary especially also in inflammation or cancer due to the different functions of the DC subsets and the identification of trafficking receptors that facilitate the migration gives important targets for pharmacological manipulation to improve the outcome of diseases.

Although cells resembling pre-committed pre-cDCs were identified in various peripheral and non-peripheral tissues, the comparison of the pre-cDC subset distribution to the subset distribution found in the differentiated DC population showed no direct correlation in the thymus and in the kidney. These results have led to negate the hypothesis of differential recruitment of the pre-committed pre-cDC to the different tissues because this would include that the ratio of pre-committed pre-cDCs correlates with the DC subset ratioin the respective tissue. One potential critique point for the experiments performed is that the pre-cDCs have been identified based on similar marker expression of pre-cDCs that have been characterized only in lymphoid organs so far. It is, therefore, possible that all cells that were identified as pre-cDCs were in fact not pre-cDCs or contain contamination with other populations, which would erase the ability to judge if the pre-cDC subset distribution differs from the DC subset distribution. In the non-lymphoid organs, especially in the kidney, this is highly probable as the CD135 expression that ultimately defines the pre-cDC population is lower compared to the lymphoid organs, such as the spleen, which hampers proper identification. To ensure the purity of pre-cDCs, the identified gating strategy could be controlled with a differentiation study on sorted pre-cDCs from different tissues. Also, the thymus and kidney could be exceptional organs with different sets of DC subsets. In line with this, cDC1 in the thymus have been shown to have a lymphoid origin, therefore it is possible that the demand for a pre-cDC1 in the thymus is reduced and the subset correlation to the differentiated cDC1 not applicable (Corcoran et al., 2003; Wu et al., 2001). On the other hand, the recruitment of pre-cDCs to the

thymus via the CCR7-CCL21 axis have been shown to be relevant for the cDC1 development in the thymus but cDC2 have been shown to develop extrathymically and migrate to the thymus dependent on CCR2 transporting self-antigens necessary for negative selection (Cosway et al., 2018; Li, Park, Foss, & Goldschneider, 2009; Naik et al., 2005; Wu & Shortman, 2005). This would, therefore, interfere with the hypothesis that pre-committed pre-cDCs have to seed the tissue in the ratio that is found for DCs in the respective tissue. From the correlation of the pre-cDC and DC subsets alone it cannot definitely be judged whether pre-committed pre-cDCs are differentially recruited to the different peripheral tissues. For this reason, but also because pre-cDC subpopulations are even less frequent than the bulk pre-cDC population in the different organs, the hypothesis was declined and further studies on pre-cDC trafficking were performed on bulk pre-cDCs. Interestingly also a recent study that has been published in the course of this thesis has addressed differences in chemokine receptor expression in pre-committed pre-cDC subsets in the BM and indeed found differences in the recruitment of pre-cDC1 and pre-cDC2 (S. J. Cook et al., 2018). They show that CCR5 is highest expressed in uncommitted SiglecH^{+}Ly6C^{+} pre-cDCs, CXCR1 is highest expressed in pre-cDC2 and CXCR3 is highest expressed in pre-cDC1. Furthermore, they show that CXCR3 is important for the recruitment of pre-cDC1 to tumours, but not other tissues, such as spleen, skin, and skin draining LN, by showing a reduction of tumour infiltrating cDC1 in B16 melanomas in CXCR3$^{-/-}$ mice and mixed BM chimeras (S. J. Cook et al., 2018). Cook et al. does however not address differential recruitment of pre-cDCs to different tissue, as this study was aiming at, but concentrates on general differences in the recruitment of pre-cDC1 and pre-cDC2 in tumour development. The fact that differential recruitment is the topic of other publications proves the validity and necessity of studying differences in the regulators for trafficking of pre-committed pre-cDCs as it emphasizes the role for pre-cDC recruitment in fighting diseases, such as cancer here. However, differential recruitment of pre-cDCs seems not to be necessary to establish the DC subset distribution in the peripheral tissues.

5.2 Differential recruitment of pre-cDCs to different peripheral tissues

One aim of this thesis was to identify trafficking receptors that facilitate the migration of pre-cDCs to different peripheral organs following the hypothesis that pre-cDCs are differentially recruited to different tissues. This could provide a target to manipulate recruitment in different types of diseases. For this purpose, BM MDPs, CDPs, and pre-cDCs and well as pre-cDCs from spleen, mLN, thymus, and lung were screened for the expressional profile of 96 targets including mostly trafficking receptors. The organs were chosen to cover both lymphoid and non-lymphoid organs to find potential differences in recruitment. Additionally, blood was

considered a very interesting organ for comparison as well as this is the organ where the pre-cDCs actually traffic though, but the very low frequency and therefore pre-cDC yield did not allow the analysis of this, particularly interesting organ.

Using a high throughput qPCR screening for trafficking receptors comparing pre-cDC from different organs, 39 potentially relevant migration-related receptors were identified in all pre-cDC from different organs. Interestingly some of these identified receptors show expression differences between organs suggesting that they are specifically relevant for the migration to the specific organ. In further experiments, the expression differences of the trafficking receptors will have to be verified on the mRNA level again and furthermore also on the protein level using flow cytometry. Additionally, also their impact on the trafficking of pre-cDC will have to further be proven by *in vitro* and *in vivo* studies using ligands, inhibitors, or receptor/ ligand knock-out mice for the respective receptor. Alternatively, inducible DC depletion and surveillance of DC replenishment with and without receptor blockage can be used. Furthermore, comparing the differences in receptor dependence of pre-cDC recruitment that were found here in steady-state to the recruitment in different kinds of diseases, such as bacterial or viral infections will be especially interesting as in these situations require a faster replenishment of DCs and potential organ-specific recruitment of pre-cDC.

At the beginning of this study, little was known about the trafficking of DC progenitors, however in the course of the study, Nakano et al published a study that identified trafficking receptors that are relevant for pre-cDC trafficking (H. Nakano et al., 2017) and Cook et al show differences in the trafficking of uncommitted pre-cDCs in the BM and pre-cDC1 and pre-cDC2 in the context of tumor infiltration (S. J. Cook et al., 2018). It is therefore already known that CXCR4 is important for the retention of pre-cDC in the BM. This matches the findings for other cell types showing CXCR4 as a retention marker for HSPCs and B-cells in the BM (Ma, Jones, & Springer, 1999; Mazo, Massberg, & Andrian, 2011; Zou, Kottmann, Kuroda, Taniuchi, & Littman, 1998). In the q-PCR screening of CXCR4 in this thesis, CXCR4 was indeed higher expressed in CDPs compared to BM pre-cDCs, which supports the findings of earlier studies as it implies that, once this receptor is lost from the surface in the development from CDP to pre-cDCs, the retention is also lost and the cells can egress from the BM. Interestingly though, the highest expression of CXCR4 in the screening of pre-cDCs from different organs was found in the lung. This implies that the CXCR4 can also be upregulated again and presumably facilitates pre-cDC retention to the lung.

As chemokine receptors that actually facilitate the migration of pre-cDCs, CCR2 and CX3CR1 have been shown to have compensatory roles for accumulation of pre-cDC in the lung in steady-state whereas only CCR2 but not CX3CR1 is important for the migration of pre-cDCs

to the inflamed lung in a LPS inhalation model (H. Nakano et al., 2017). In this thesis, CCR2 and CX3CR1 have been shown to be highest expressed in pre-cDCs of the spleen and only lower expressed in the lung. Nakano et al have also compared the expression of these receptors in the pre-cDCs of spleen and lung, but only proved their expression and did not analyse differences in the expression. However, in their studies on receptor knock out mice or BM-chimeras of CCR2 and CX3CR1, a decrease in pre-cDC numbers was only shown for the lung, but not for the spleen indicating an organ-specific recruitment. This differential recruitment can, for example, be explained by a difference in the gradient establishment and production of the chemokines in the target organ, but this has not been investigated so far.

It has also been shown, that CXCR1 is highest expressed in pre-cDC2 and CXCR3 is highest expressed in pre-cDC1 in comparisons of chemokine receptors on pre-cDC subsets in the BM (S. J. Cook et al., 2018). Furthermore, CXCR1 has been shown to be important for the tumour infiltration of pre-cDC1. In the screening in this study, CXCR1 was also be identified on pre-cDCs in all analysed organs with relatively higher expression in mLN and lung, CXCR3 was not found to be expressed in pre-cDCs of all analysed organs, possibly because the pre-cDC1 are low in frequency among the bulk pre-cDCs, or due to organ differences.

About the recruitment of pre-cDC to the thymus, Cosway et al. have identified pre-cDCs in the thymus and show that the cDC1 pool is dependent on the recruitment of pre-cDCs to the thymus via the CCR7-CCL21 axis (Cosway et al., 2018). CCR7 has not been identified as a receptor that is expressed on pre-cDCs from all analysed organs in this screen and is therefore not included in the list of potential targets. This does not exclude that CCR7 cannot be specifically relevant for the recruitment of pre-cDCs to the thymus and suggests that for finding very specific trafficking receptors, the analysis can be further expanded. The role of the identified migration-related receptors on pre-cDCs has not been investigated so far but the list provides a potential resource for future studies.

5.3 DC DEPLETION IN *CLEC9A$^{CRE/CRE}$ROSA^{DTA}* MICE LEADS TO REPLENISHMENT OF DC2 BY PHENOTYPICALLY SIMILAR CELLS OF LYMPHOID ORIGIN

Although cDCs are generally thought to derive from myeloid progenitors in steady-state (Auffray et al., 2009; Manz, Traver, Akashi, Merad, Miyamoto, Engleman, et al., 2001a), several studies have reported that lymphoid progenitors can give rise to cDCs in vitro as well as in adoptive transfer experiments (Corcoran et al., 2003; Izon et al., 2001; Sathe, Vremec, Wu, Corcoran, & Shortman, 2013; Wu et al., 2001). This study provides additional evidence that cDCs can develop from an alternative path using *Clec9a$^{cre/cre}$Rosa^{DTA}* mice as a model to constitutively deplete cDC progenitors based on the expression of Clec9a. Other than

expected, cells arise in *Clec9a*$^{cre/cre}$*Rosa*^{DTA} mice that resemble cDC2 phenotypically and show only minor differences in cytokine expression after activation. However, the cells that resemble cDC2 in *Clec9a*$^{cre/cre}$*Rosa*^{DTA} mice show somatic rearrangements of the IgH locus, which is indicative of a lymphoid origin and are therefore called lymphoid DC2 here. The working hypothesis is illustrated in **Figure 43**. In general, different ways of defining cell populations can be applied, typically cells are defined as a separate population based on their function, phenotype or origin. One often applied strategy to classify mononuclear phagocytes is to identify them based on their developmental origin. As this study shows that lymphoid DCs do not derive from classical DC progenitors this excludes them from this definition of DCs although they are phenotypically similar to bona fide cDC2 (Ginhoux, Guilliams, & Naik, 2016; Guilliams et al., 2014; Schraml & Reis e Sousa, 2015). Therefore, more research is required for lymphoid DC2 to better understand their developmental origin and function to be able to assign it to a particular cell population.

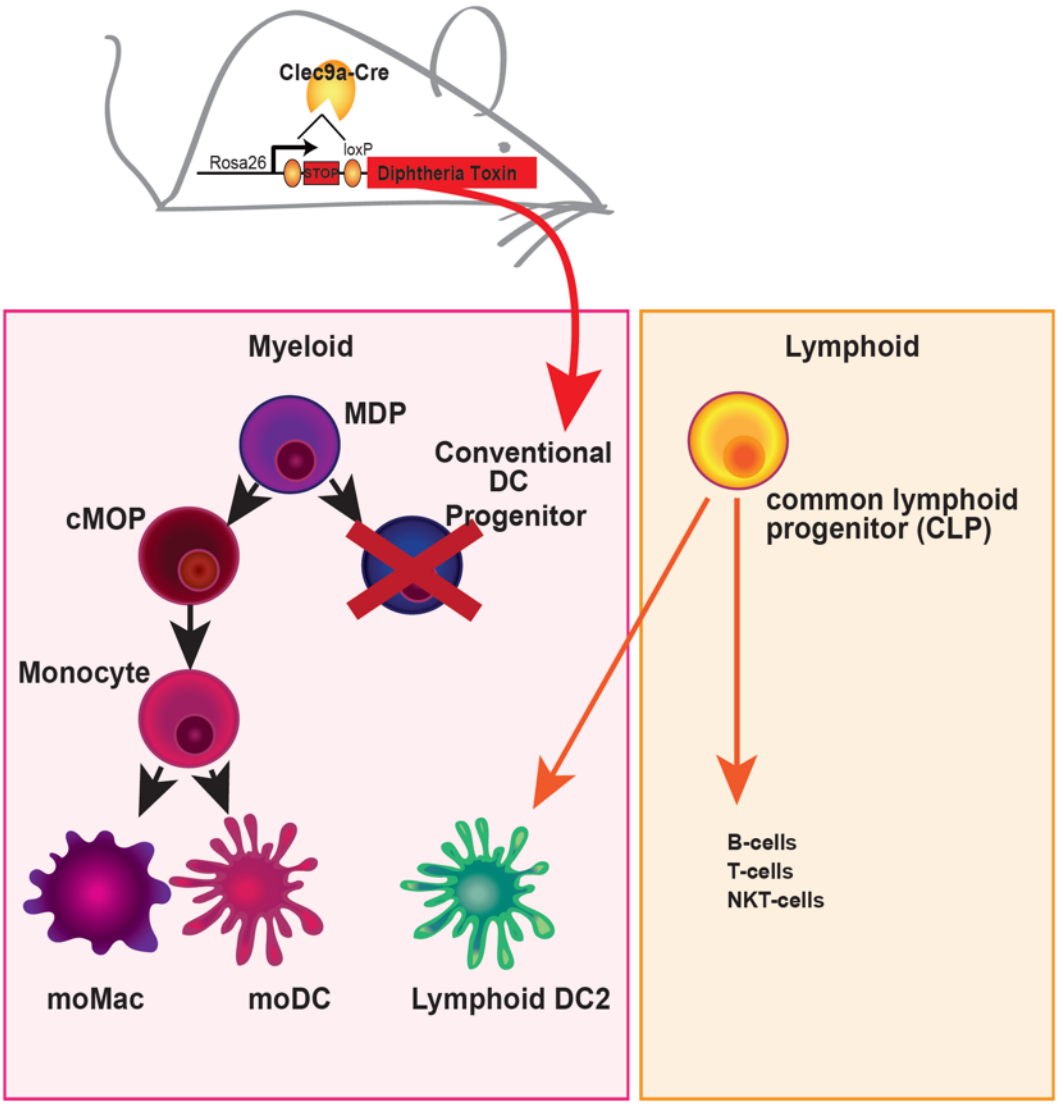

Figure 43: Scheme for lymphoid progenitors filling the cDC2 niche when myeloid DC precursors are lost in Clec9a^{cre}Rosa^{DTA} mice.

Within this study, only the development of cDC2 but not cDC1 can be analysed as cDC1 express *Clec9a* in the differentiated state and therefore cDC1 will be depleted independent on the progenitor in *Clec9a*$^{cre/cre}$*Rosa*^{DTA} mice. Theoretically, lymphoid progenitors could also give rise to cDC1 in *Clec9a*$^{cre/cre}$*Rosa*^{DTA} mice, but they would immediately be depleted after they start expressing Clec9a. To analyse the progenitors with respect to cDC1, other models need to be chosen.

It is still unclear whether lymphoid DC2 develop in *Clec9a*$^{cre/cre}$*Rosa*^{DTA} mice as a consequence of the constitutive depletion of the DC throughout development. It was shown that young

Clec9a$^{cre/cre}$*Rosa*^{DTA} mice still show efficient depletion of cDC2 and the cDC2 in the *Clec9a*$^{cre/cre}$*Rosa*^{DTA} mice only appear with age (Salvermoser et al., 2018). Interestingly, the increase of cDC2 in *Clec9a*$^{cre/cre}$*Rosa*^{DTA} mice goes in line with the establishment of myeloproliferation. To find out if lymphoid DC2 also appear later in life when DC progenitors are depleted over a longer time period, an inducible depletion in *Clec9a*$^{cre/cre}$*Rosa*^{DTR} mice could be utilized. This, however, is not practicable because mice have been shown to produce antibodies against repeated DT doses over time (Rombouts et al., 2017). Ultimately, it will be interesting to find a physiological situation in which lymphoid DC2 develop either to ensure the DC population replenishment with functional redundancy or with functional differences similar to how situation adapted inflammatory monocytes are produced in response to inflammatory stimuli (Yáñez et al., 2017) to mediate specific immune functions. This however also implies that lymphoid DC2 are functionally different from CDP derived cDC2.

5.4 Potential progenitors of DC2 in *Clec9a*$^{cre/cre}$*Rosa*^{DTA} mice

5.4.1 DC progenitors

It has not been fully investigated which progenitor finally gives rise to the lymphoid DC2 in *Clec9a*$^{cre/cre}$*Rosa*^{DTA} mice. Although CDPs were found to be decreased and pre-cDCs almost absent in in the BM and spleen of *Clec9a*$^{cre/cre}$*Rosa*^{DTA} mice, they were not fully depleted and thus it cannot be excluded that CDPs escape the depletion or the remaining pre-cDCs are sufficient to replenish the cDC2 pool. Nevertheless, sorted pre-cDCs from *Clec9a*$^{cre/cre}$*Rosa*^{DTA} mice in contrast to control pre-cDC were unable to produce DC outcome in Flt3L culture. This assay, however, is limited by the very low cell number of pre-cDCs in the DTA mice and furthermore could be influenced by lower CD135 expression in all CD11c^{+}MHCII^{-} cells, which could affect the identification of pre-cDCs in the first place. But also, the response to Flt3L, the ligand for CD135 in the cultures could be affected by lower CD135 levels on cells identified as pre-cDCs in *Clec9a*$^{cre/cre}$*Rosa*^{DTA} mice. TBM gave rise to cDCs in Flt3L cultures as well as in GM-CSF cultures as is expected as the TBM also contains other progenitors, such as lymphoid progenitors. CDPs and MDPs do not show reduced CD135 levels on their surface, in contrast to pre-cDCs do. Nevertheless, both CDPs and MDPs, which were sorted from *Clec9a*$^{cre/cre}$*Rosa*^{DTA} mice, give rise to some DC2 in Flt3L and GM-CSF cultures, however, the yield is significantly lower compared to CDPs and MDPs sorted from control mice. This assumes that some DC progenitors escape the depletion and still produce some cDC2 but also shows that the proliferation in these progenitors is not increased enough to yield equivalent numbers of DC2 as have been observed in the spleen of *Clec9a*$^{cre/cre}$*Rosa*^{DTA} mice. The reason for MDPs and CDPs giving DC progeny at all in the *in vitro* culture could be that in this artificial system the progenitors proliferate very fast. This could be responsible for the

escape, as the cre has been shown to be less efficient in rapidly cycling cells (Jakubzick et al., 2008; Ye et al., 2003; Yona et al., 2013). Finally, escaping myeloid DC progenitors in *Clec9a*$^{cre/cre}$*Rosa*^{DTA} mice does not explain why at least a fraction of the DC2 in *Clec9a*$^{cre/cre}$*Rosa*^{DTA} mice shows D-J rearrangements. An explanation for lymphoid DCs having DJ-rearrangements independent of their progenitor would be that they themselves start to express RAG1 due to differences in the environment in *Clec9a*$^{cre/cre}$*Rosa*^{DTA} mice. The microarray analysis in Salvermoser et al., however, shows no RAG1 gene expression in the lymphoid DC2. Another explanation for D-J rearrangements in DCs is that they derive from RAG1 expressing myeloid progenitors, which have been described by Sathe et al. (Sathe et al., 2013). This RAG-1 expressing myeloid progenitor is still a possible progenitor of the, in this case wrongly termed, “lymphoid DC2”, which requires further investigation.

5.4.2 Monocytes and other myeloid progenitors

Monocytes are known to differentiate into monocyte-derived DCs and they have been shown also increased in *Clec9a*$^{cre/cre}$*Rosa*^{DTA} mice in the context of myeloproliferation, which is a reported phenomenon in mice lacking both cDC1 and cDC2 (Hildner et al., 2008; Ohta et al., 2016). This makes monocytes a potential candidate for the progenitor of lymphoid DC2 in *Clec9a*$^{cre/cre}$*Rosa*^{DTA} mice. DCs have however been identified as CD64^{-} cells with the purpose to exclude monocyte-derived cells. Additionally, transcriptomic analyses were performed to compare bona fide DC2 and lymphoid DC2 in Salvermoser et al., 2018. Here, microarray data from YFP^{+} DC2 from *Clec9a*^{cre}*Rosa*^{YFP} and lymphoid DC2 from *Clec9a*$^{+/cre}$*Rosa*^{DTA} mice were compared (Salvermoser et al., 2018). YFP^{+} *Clec9a*^{cre}*Rosa*^{YFP} mice were chosen as they show *Clec9a* expression history, which proves their CDP origin. This transcriptomic analysis has showed no significant similarities of lymphoid DC2 to published transcriptomes of monocytes (Salvermoser et al., 2018). Furthermore, monocytes belong to the myeloid lineage, which does typically not have a RAG1 expression history and no IgH receptor rearrangement. Therefore, monocytes are unlikely to be the progenitor of lymphoid DC2.

5.4.3 Plasmacytoid dendritic cells

Another explanation for the origin of lymphoid DCs is that pDCs convert their phenotype and function to resemble cDC2. This would explain the DJ-rearrangements that were found in the lymphoid DCs as pDC are known to have DJ-rearrangements because they are known to be (at least in part) derived from lymphoid precursors (Corcoran et al., 2003; Rodrigues et al., 2018; Sathe et al., 2013). The lymphoid origin of pDCs is potentially the reason why pDCs are still present in *Clec9a*$^{cre/cre}$*Rosa*^{DTA} mice although pDCs express DNGR-1 at low levels in the differentiated population in control mice. Additionally, pDCs downregulate the expression of DNGR-1 in *Clec9a*$^{+/cre}$*Rosa*^{DTA} mice compared to control mice. Generally, cells are not thought

to convert to each other but trans-differentiation and trans-determination are known concepts for plasticity of cells (Crompton, Clever, Vizcardo, Rao, & Restifo, 2014) and also pDCs have been shown to be able to convert to DCs when the major defining transcription factor E2-2 is deleted. This has also been recapitulated in a more physiological setting during viral infection in some but not all studies on the topic (Ghosh, Cisse, Bunin, Lewis, & Reizis, 2010; Liou et al., 2008; Manh, Alexandre, Baranek, Crozat, & Dalod, 2013; Zuniga, McGavern, Pruneda-Paz, Teng, & Oldstone, 2004). The development in *Clec9a*$^{cre/cre}$*Rosa*^{DTA} mice is potentially already disturbed due to increased serum Flt3L levels and eventually also other growth factors that have not been tested so that a conversion from one cell to another can potentially happen. Principle component analyses on microarray data comparing bona fide CDP derived cDC2 and lymphoid DC2 however showed that lymphoid DC2 did not cluster closer to published datasets for pDC and therefore does not argue for pDCs as precursors of lymphoid DC2 (Salvermoser et al., 2018). To finally exclude the contribution of pDCs to the development of lymphoid DC2, pDCs could be additionally depleted in *Clec9a*$^{cre/cre}$*Rosa*^{DTA} mice, for example, using antibody-mediated depletion with an α-PDCA-1 antibody.

5.4.4 Common lymphoid progenitors

The current hypothesis for the progenitor of lymphoid DC2 in *Clec9a*$^{cre/cre}$*Rosa*^{DTA} mice is that lymphoid progenitors, such as CLPs give rise to DC2 when the myeloid progenitors are impaired. This is likely because lymphoid progenitors express RAG1 and following that, DJ-rearrangements occur as an early event in the development of the B-cells receptor. This study, therefore, suggests that DC-poiesis can be taken over by lymphoid progenitors when the myeloid progenitors are depleted. CLPs have been shown to develop into DCs *in vitro* as well as in adoptive transfer studies (Izon et al., 2001; Manz, Traver, Miyamoto, Weissman, & Akashi, 2001b; Welner et al., 2009; Wu et al., 2001). The development of DCs from the lymphoid branch also depends on the growth factor Flt3L as Flt3L deficient mice lack all cDCs (Ginhoux et al., 2009; McKenna et al., 2000) and this also explains the development of DCs from TBM in Flt3L cultures. Therefore, CLPs in the *Clec9a*$^{cre/cre}$*Rosa*^{DTA} mice could either be triggered by the disturbed growth factor environment, such as the high levels of Flt3L levels in the serum or by the open DC niche that needs to be filled. A lack of cDCs could again also have an impact on the growth factors as DCs are considered to act as a sink for Flt3L (Birnberg et al., 2008), which goes along the hypothesis that the cDC differentiation is homeostatically regulated by the size of the cDC pool (Hochweller et al., 2009; Kabashima et al., 2005). Additionally, CLPs showed a trend to be increased in *Clec9a*$^{cre/cre}$*Rosa*^{DTA} compared to control mice though more replicates would be required to ensure the results. An increase in the CLP population could argue for a demand of them to fill the DC niche in *Clec9a*$^{cre/cre}$*Rosa*^{DTA} mice but it could also be a secondary effect of increased FLt3L that induces more proliferation in

this population that also expresses the receptor CD135. Interestingly, although the CLP population seems to be increased, the $CD8^+$ T-cells are reduced in *Clec9a*$^{cre/cre}$*Rosa*^{DTA} mice (**Figure 15**). Although (Birnberg et al., 2008) claim that T-cell development is not affected by the DC depletion in *CD11c-DTA* mice, other studies have reported increased frequencies of $CD4^+$ thymocytes and higher numbers of Th1 and Th17 cells in *CD11c-DTA* mice(Ohnmacht et al., 2009) or that IL-2 dependent T-regs are diminished in a similar mouse model *CD11c-DTR* (Stolley & Campbell, 2016). cDC1 depletion and following loss of especially $CD8^+$ T-cell proliferation can explain the differences in the $CD8^+$ T-cell numbers, (Fukaya et al., 2012) however T-cell responses should not occur in a non-infected mouse. To prove CLPs as the true progenitor of lymphoid DCs, adoptive transfer studies would be required. These studies have already been successfully performed by CLP transfers into irradiated mice that demonstrably produced DCs progeny (Izon et al., 2001; Manz, Traver, Miyamoto, Weissman, & Akashi, 2001b; Traver et al., 2000). It is, however, unknown so far in which physiological settings CLPs will give DC progeny.

5.5 THE PHYSIOLOGICAL RELEVANCE OF FUNCTIONAL DIFFERENCES BETWEEN DENDRITIC CELLS WITH DIFFERENT ORIGIN

The redundancy of developmental pathways underlined the importance of DCs as nature has developed a back-up plan for lymphoid emergency DC-poiesis that kicks in when myeloid DC progenitors are impaired. Functional differences between DC2 that derive from myeloid progenitors in control mice and lymphoid progenitors in *Clec9a*$^{cre/cre}$*Rosa*^{DTA} mice would argue for the hypothesis that these cells are produced in different physiological settings that require differentially adapted cell types although they phenotypically overlap and seem to fill the same niches. This study has therefore addressed different functions of DCs from cytokine production and T-cell activation to migration and localization.

5.5.1 CYTOKINE PRODUCTION

After stimulation of DC2 from *Clec9a*$^{cre/cre}$*Rosa*^{DTA} and control mice *in vitro* with LPS or CpG, only slight differences could be observed. More specifically, the percentage of TNFα expressing but not IL-12 expressing DC2 that was reduced by about 0.5% in DC2 from *Clec9a*$^{cre/cre}$*Rosa*^{DTA} mice compared to control cDC2 when stimulated with LPS but not CpG. This very specific difference in cytokine production could indicate a functional impairment of lymphoid DC2 in the defence against infections with gram-negative bacteria, for example. This could further impair the capacity of lymphoid DC2 to activate T-cells or further induce innate immune functions. Following up on the functional differences in cytokine production and furthermore also T-cell stimulation of DC2 from *Clec9a*$^{cre/cre}$*Rosa*^{DTA} and control mice will be important to understand the dual origin of the cells.

5.5.2 MIGRATION

Migration of DCs is very important for the transport of antigen and therefore activation of T-cells and positioning of the DCs within the lymphoid tissues. First observations, that migratory DC2 are about 4-fold reduced in the skin draining inguinal and auricular LN but not in the mesenteric LN of *Clec9a*$^{cre/cre}$*Rosa*^{DTA} in comparison to control mice suggested a reduced migration of lymphoid DC2 specifically from the skin. DCs in the skin have been identified without excluding CD64^{+} cells from the analysis as the identity of CD64^{+} cells in steady-state LNs is unclear, nevertheless in *Clec9a*$^{cre/cre}$*Rosa*^{DTA} mice, a CD64^{+}CD11b^{+} population is increased. The origin of this CD64^{+} population is unclear but due to the marker expression, a monocytic origin is likely and also matches the myeloproliferative disease in *Clec9a*$^{cre/cre}$*Rosa*^{DTA} mice. Of note, a fraction of this population seems to contaminate the DC gates, which implies that the decrease in migratory DC2 in *Clec9a*$^{cre/cre}$*Rosa*^{DTA} mice is even stronger if this unknown population was excluded from the analysis. This has not been done for this experiment as published gating strategies do not include CD64 in the gating strategy on LNs and the identity of the CD64^{+} population is unclear. Additional data for reduced migration of lymphoid DC2 is that they migrate about 5 times less out of the ear towards the CCR7 ligand CCL19 in a crawl-out assay (**Figure 34**). The conclusion that the cells actually migrate less can only truly be stated on the fact that the DC2 numbers in the ears of *Clec9a*$^{cre/cre}$*Rosa*^{DTA} and control mice are equal like they have been found to be equal in the spleen but in fact they were found to be reduced by about 50% in *Clec9a*$^{cre/cre}$*Rosa*^{DTA} mice (**Figure 36**). The fact that the discrepancy in the total DC2 counts in the ear (50%) are lower than the discrepancies in cells migrating out of the ear in the crawl out assay (20%) and also in migratory DCs in the skin draining LN (25%) still suggests that lymphoid DC2 have a reduced migratory capacity but omits further conclusions.

In the spleen, DC migration is necessary for the correct localisation in steady-state and the re-localization after antigen encounter and inflammation (Idoyaga et al., 2009; Reis e Sousa et al., 1997). Under steady-state conditions, splenic lymphoid DC2 showed less migration in a transwell assay. Typically, however, migration of DC is measured after activation with the gram-negative endotoxin LPS, which makes sense in a way that DCs upregulate CCR7 and other activation markers after stimulation and migrate upon a certain stimulus. Activation of the cells was monitored by staining of activation markers on the DC surfaces and was found comparable between DC2 from *Clec9a*$^{cre/cre}$*Rosa*^{DTA} and control mice. It has been previously shown that *ex-vivo* DCs become activated by simple isolation techniques and following culture or transfer into mice (Montoya et al., 2002; Schlecht, Mouriès, Poitrasson-Rivière, Leclerc, & Dadaglio, 2006). Therefore, it was expected that the control cells that were cultured with medium alone also showed an increase in activation markers CD40 and CD86 (**Figure 39).**

Interestingly, after activation in culture with or without LPS, the DCs migrated about 10 times more though the transwells towards both medium and CCR7 ligands, but the differences between DC2 from *Clec9a*$^{cre/cre}$*Rosa*^{DTA} and control mice were abrogated, as well as no differences could be observed in microscopic analyses of 3D migration in a collagen matrix (**Figure 38**; **Figure 40**). It is surprising that steady-state splenic lymphoid DC2 migrate less than steady-state control DC2 but upon activation, both cell types migrate similar, but this could be explained by the intensity of the stimulus. When DCs mature for example by recognizing LPS with the toll like receptor 4 (TLR4), they activate many downstream pathways to induce the expression of co-stimulatory molecules, the production of pro inflammatory cytokines. It is possible that the cells are at the limit of their activation and the program that follows the activation changes the ability of the cell so much that any previous difference in function is masked by the adopted program. It is nevertheless possible that by varying external parameters, such as different or shorter activation period, which is more physiological, differences in migration capacity between DC2 from *Clec9a*$^{cre/cre}$*Rosa*^{DTA} and control mice can be observed also after activation. Furthermore, in transwell experiments that were performed after activation of the cells, also the undirected migration towards medium was with 20% very high. This implies that chemokinesis is increased in activated DC2, which could potentially mask possible differences in chemotaxis of DC2 from *Clec9a*$^{cre/cre}$*Rosa*^{DTA} and control mice. Interestingly also, less LPS activated lymphoid DC2 migrated towards medium only suggesting them to be defective in chemokinesis. In retrospect, however, the differences observed in migration of steady-state splenic lymphoid DC2 can also be explained by differences in the rate of dying cells as more necrotic lymphoid DC2 from *Clec9a*$^{cre/cre}$*Rosa*^{DTA} mice were found after culture in medium compared to CDP-derived DC2 from control mice (**Figure 41**).

The mechanism why migration might be impaired in steady-state lymphoid DCs still has to be addressed, so far it can only be excluded that differences in CCR7 expression on lymphoid and bona fide DC2 in the migratory DC2 in the LNs were responsible and CCR7 levels, as well as some activation markers on activated splenic DC2, showed no differences as well. It would, however, be more interesting to compare CCR7 levels on steady-state or activated DC2 from peripheral tissue, such as the skin because DC2 that have migrated to the draining LN have succeeded the migration. Furthermore, although CCR7 signalling differs in response to either CCL19 or CCL21 no differences were observed in the migration towards both stimuli when tested in steady-state migration of splenocytes through transwell pores. This suggests that both signalling pathways could presumably be affected in lymphoid DC2.

For the biology of the redundant development of DC2 this implies that lymphoid DC2 might show differences in migration in steady-state and potentially other certain circumstance but

not in infection with gram negative bacteria (LPS). DC migration in steady state is happening in very low levels compared to inflammation, nevertheless it is prerequisite for induction of tolerance to peripheral antigens (Audiger, Rahman, Yun, Tarbell, & Lesage, 2017; Förster et al., 2008; Vitali et al., 2012). In this context, an advantage of CDP derived DC2 to migrate better in steady-state makes sense, as, in steady-state, DC2 derive from CDPs and lymphoid DCs develop only in the absence of myeloid DC progenitors and potentially in inflammatory conditions where migration is supposed to happen upon activation anyways.

5.5.3 CELL DEATH

The observations that have led to the conclusion that steady-state lymphoid DC2 migrate less towards CCR7 ligands all depended on counting of cells after migration. The finding that lymphoid DC2, in fact, show higher necrosis than bona fide cDC2 when cultured for 2h with either medium of CCR7 ligands, however, levers out this argumentation and points toward a different phenotypic divergence. Higher or faster induction of necrosis in lymphoid DC2 compared to CDP derived DC2 implies that the cells are more susceptible to stress situation, such as the isolation or enrichment process for unknown reasons. In fact, the analysed activation markers showed no difference but were also measured at a later timepoint. The difference in necrosis, however, is around 30% but the difference in migration of steady-state lymphoid DC2 is around 50% and therefore the difference in necrosis does not account for all the differences observed in the migration assay. To judge if steady-state lymphoid DC2 have an impaired capacity to migrate, the migration can be observed in live-cell imaging as has been performed for the activated splenic DC2 because here not only the counts of migrated cells can be analysed but also differences in velocity, directionality, and shape of the cells can be observed.

5.5.4 LOCALIZATION

Migration of DCs has an impact on their localization within lymphoid organs. The Clec4a4 staining pattern in one of the two analysed iLN section of *Clec9a*$^{cre/cre}$*Rosa*^{DTA} is more dispersed throughout the LN and shows smaller clusters in comparison to the few Clec4a4 clusters that localize to the interfollicular zones in the control iLN section. This points towards a failure of the lymphoid DC2 to migrate to the correct localization in the B-cell T-cell interphase and therefore argues for a migration defect of lymphoid DC2, however, in the second replicate the distribution of Clec4a4^{+} cells seems to be as expected. Nevertheless, the failure of lymphoid DC2 to localize to the T-cell zone in the lymph nodes could have a major influence on the inflammatory response, such as T-cell activation in *Clec9a*$^{cre/cre}$*Rosa*^{DTA} mice. Unexpectedly, the organization in *Clec9a*$^{cre/cre}$*Rosa*^{DTA} iLN of in the analysed section seems abnormal due to a more condensed T-cell zone and a large centre part that is not stained with

CD3 but with MHCII and densely packed with $CD11c^+$ cells, which could be an abnormally enlarged medullary sinus and medullary cord region. The medullary sinus and medullary cord is known to contain medullary sinus/ medullary cord macrophages, respectively, which can in part explain the CD11c staining found in the enlarged centre region in the *Clec9a*$^{cre/cre}$*Rosa*^{DTA} iLN, however, these macrophages are typically classified as $CD11c^{low}$ cells (Gray & Cyster, 2012). The deviant LN organization indicates a generally aberrant LN organization in *Clec9a*$^{cre/cre}$*Rosa*^{DTA} mice that can be a secondary effect of the dysregulation of growth factors like Flt3L. Furthermore, **Figure 15** shows that $CD8^+$ T-cells are indeed diminished in the spleen of *Clec9a*$^{cre/cre}$*Rosa*^{DTA} mice indicating that the development of T-cells is dysregulated in *Clec9a*$^{cre/cre}$*Rosa*^{DTA} mice and can therefore also be the reason for the altered assembly of T-cell zones in the LN of *Clec9a*$^{cre/cre}$*Rosa*^{DTA} mice although the quantification of B-and T-cells has not been analysed in the LNs in this study. **Figure 42** however only shows two analysed LN sections and it is possible that, for both LN sections, the depth of the sections is not equal in the *Clec9a*$^{cre/cre}$*Rosa*^{DTA} and LN section, which certainly has an effect on the organization. To confirm the aberrant LN organization and localization of lymphoid DC2 further localization analyses on LN or spleen sections need to be performed.

Although no final conclusions can be drawn from the localization of the lymphoid DC2 in the LN before further confirmation, the data suggests that a lymphoid DC2 in the iLN of *Clec9a*$^{cre/cre}$*Rosa*^{DTA} mice do not properly localize to the interfollicular region. This implies that lymphoid DC2 are less capable of presenting antigens to T-cells due to lacking contact and further suggests that lymphoid DC2 are inferior in inducing T-cell responses. This hypothesis has to further be tested using *in vivo* models for T-cell proliferation after antigen exposure.

The distinct functions of lymphoid DC2 and bona fide cDC2 that have been observed in terms of TNFα production after LPS stimulation and potentially migration in steady-state, but also the fact that lymphoid DC2 are more susceptible to cell death support the hypothesis that lymphoid DC2, which replace cDC2 in the in the artificial setting of the *Clec9a*$^{cre/cre}$*Rosa*^{DTA} DC depletion model, are not redundant but they have a distinct physiological role. This distinct role is presumably required in certain inflammatory settings, which trigger the differentiation of DC2 from lymphoid progenitors. Future studies will be required to confirm the putative functional differences between lymphoid derived DC2 and CDP derived DC2 and identify under which physiological settings CDP derived DC2 are replaced by lymphoid DC2. This basic knowledge will help to understand when and why developmentally distinct DCs are recruited and provide a basis to redirect immune responses.

REFERENCES

Aliberti, J., Schulz, O., Pennington, D. J., Tsujimura, H., Reis e Sousa, C., Ozato, K., & Sher, A. (2003). Essential role for ICSBP in the in vivo development of murine CD8alpha + dendritic cells. *Blood*, *101*(1), 305–310. http://doi.org/10.1182/blood-2002-04-1088

Allan, R. S., Waithman, J., Bedoui, S., Jones, C. M., Villadangos, J. A., Zhan, Y., et al. (2006). Migratory dendritic cells transfer antigen to a lymph node-resident dendritic cell population for efficient CTL priming. *Immunity*, *25*(1), 153–162. http://doi.org/10.1016/j.immuni.2006.04.017

Alvarez, D., Vollmann, E. H., & Andrian, von, U. H. (2008). Mechanisms and consequences of dendritic cell migration. *Immunity*, *29*(3), 325–342. http://doi.org/10.1016/j.immuni.2008.08.006

Arora, P., Baena, A., Yu, K. O. A., Saini, N. K., Kharkwal, S. S., Goldberg, M. F., et al. (2014). A single subset of dendritic cells controls the cytokine bias of natural killer T cell responses to diverse glycolipid antigens. *Immunity*, *40*(1), 105–116. http://doi.org/10.1016/j.immuni.2013.12.004

Audiger, C., Rahman, M. J., Yun, T. J., Tarbell, K. V., & Lesage, S. (2017). The Importance of Dendritic Cells in Maintaining Immune Tolerance. *Journal of Immunology*, *198*(6), 2223–2231. http://doi.org/10.4049/jimmunol.1601629

Auffray, C., Fogg, D. K., Narni-Mancinelli, E., Senechal, B., Trouillet, C., Saederup, N., et al. (2009). CX3CR1+ CD115+ CD135+ common macrophage/DC precursors and the role of CX3CR1 in their response to inflammation. *The Journal of Experimental Medicine*, *206*(3), 595–606. http://doi.org/10.1084/jem.20081385

Bachelerie, F., Ben-Baruch, A., Burkhardt, A.M., Combadiere,C., Farber, J.M., Graham, G.J., et al. (2014). International Union of Basic and Clinical Pharmacology. LXXXIX. Update on the Extended Family of Chemokine Receptors and Introducing a New Nomenclature for Atypical Chemokine Receptors. *Pharmacological Reviews, 66*(1), 1-79. http://dx.doi.org/10.1124/pr.113.007724

Banchereau, J., & Steinman, R. M. (1998). Dendritic cells and the control of immunity. *Nature*, *392*(6673), 245–252. http://doi.org/10.1038/32588

Bar-On, L., Birnberg, T., Lewis, K. L., Edelson, B. T., Bruder, D., Hildner, K., et al. (2010). CX3CR1+ CD8alpha+ dendritic cells are a steady-state population related to plasmacytoid dendritic cells. *Proceedings of the National Academy of Sciences of the United States of America*, *107*(33), 14745–14750. http://doi.org/10.1073/pnas.1001562107

Bardi, G., Lipp, M., Baggiolini, M., & Loetscher, P. (2001). The T cell chemokine receptor CCR7 is internalized on stimulation with ELC, but not with SLC. *European Journal of Immunology*, *31*(11), 3291–3297. https://doi.org/10.1002/1521-4141(200111)31:11<3291::AID-IMMU3291>3.0.CO;2-Z

Bennett, C. L., & Clausen, B. E. (2007). DC ablation in mice: promises, pitfalls, and challenges. *Trends in Immunology*, *28*(12), 525–531. http://doi.org/10.1016/j.it.2007.08.011

Birnberg, T., Bar-On, L., Sapoznikov, A., Caton, M. L., Cervantes-Barragán, L., Makia, D., et al. (2008). Lack of Conventional Dendritic Cells Is Compatible with Normal Development and T Cell Homeostasis, but Causes Myeloid Proliferative Syndrome. *Immunity*, *29*(6), 986–997. http://doi.org/10.1016/j.immuni.2008.10.012

Björck, P., & Kincade, P. W. (1998). Cutting Edge: CD19+ Pro-B Cells Can Give Rise to Dendritic Cells In Vitro. *The Journal of Immunology*, 1–6.

Bogunovic, M., Ginhoux, F., Helft, J., Shang, L., Hashimoto, D., Greter, M., et al. (2009). Origin of the lamina propria dendritic cell network. *Immunity*, *31*(3), 513–525. http://doi.org/10.1016/j.immuni.2009.08.010

Borghesi, L., Hsu, L.-Y., Miller, J. P., Anderson, M., Herzenberg, L., Herzenberg, L., et al. (2004). B Lineage–specific Regulation of V(D)J Recombinase Activity Is Established in Common Lymphoid Progenitors. *The Journal of Experimental Medicine*, *199*(4), 491–502. http://doi.org/10.1084/jem.20031800

Braun, A., Worbs, T., Moschovakis, G. L., Halle, S., Hoffmann, K., Bölter, J., et al. (2011). Afferent lymph-derived T cells and DCs use different chemokine receptor CCR7-dependent routes for entry into the lymph node and intranodal migration. *Nature Immunology*, *12*(9), 879–887. http://doi.org/10.1038/ni.2085

Byers, M. A., Calloway, P. A., Shannon, L., Cunningham, H. D., Smith, S., Li, F., et al. (2008). Arrestin 3 mediates endocytosis of CCR7 following ligation of CCL19 but not CCL21. *Journal of Immunology*, *181*(7), 4723–4732. http://doi.org/10.4049/jimmunol.181.7.4723

Calabro, S., Liu, D., Gallman, A., Nascimento, M. S. L., Yu, Z., Zhang, T.-T., et al. (2016). Differential Intrasplenic Migration of Dendritic Cell Subsets Tailors Adaptive Immunity. *Cell Reports*, *16*(9), 2472–2485. http://doi.org/10.1016/j.celrep.2016.07.076

Caminschi, I., Lahoud, M. H., & Shortman, K. (2009). Enhancing immune responses by targeting antigen to DC. *European Journal of Immunology*, *39*(4), 931–938. http://doi.org/10.1002/eji.200839035

Carlsen, H. S., Haraldsen, G., Brandtzaeg, P., & Bækkevold, E. S. (2005). Disparate lymphoid chemokine expression in mice and men: no evidence of CCL21 synthesis by human high endothelial venules. *Blood*, *106*(2), 444–446. http://doi.org/10.1182/blood-2004-11-4353

Caton, M. L., Smith-Raska, M. R., & Reizis, B. (2007). Notch-RBP-J signaling controls the homeostasis of CD8- dendritic cells in the spleen. *Journal of Experimental Medicine*, *204*(7), 1653–1664. http://doi.org/10.1084/jem.20062648

Cella, M., Jarrossay, D., Facchetti, F., Alebardi, O., Nakajima, H., Lanzavecchia, A., & Colonna, M. (1999). Plasmacytoid monocytes migrate to inflamed lymph nodes and produce large amounts of type I interferon. *Nature Medicine*, *5*(8), 919–923. http://doi.org/10.1038/11360

Cheong, C., Matos, I., Choi, J.-H., Dandamudi, D. B., Shrestha, E., Longhi, M. P., et al. (2010). Microbial stimulation fully differentiates monocytes to DC-SIGN/CD209(+) dendritic cells for immune T cell areas. *Cell*, *143*(3), 416–429. http://doi.org/10.1016/j.cell.2010.09.039

Chopin, M., Lun, A. T., Zhan, Y., Schreuder, J., Coughlan, H., D'Amico, A., et al. (2018). Transcription Factor PU.1 Promotes Conventional Dendritic Cell Identity and Function via Induction of Transcriptional Regulator DC-SCRIPT. *Immunity*. http://doi.org/10.1016/j.immuni.2018.11.010

Cook, S. J., Lee, Q., Wong, A. C., Spann, B. C., Vincent, J. N., Wong, J. J., et al. (2018). Differential chemokine receptor expression and usage by pre-cDC1 and pre-cDC2. *Immunology and Cell Biology*, *7*, 663. http://doi.org/10.1111/imcb.12186

Corcoran, L., Ferrero, I., Vremec, D., Lucas, K., Waithman, J., O'Keeffe, M., et al. (2003). The lymphoid past of mouse plasmacytoid cells and thymic dendritic cells. *The Journal of Immunology*, *170*(10), 4926–4932.

Cosway, E. J., Ohigashi, I., Schauble, K., Parnell, S. M., Jenkinson, W. E., Luther, S., et al. (2018). Formation of the Intrathymic Dendritic Cell Pool Requires CCL21-Mediated Recruitment of CCR7 +Progenitors to the Thymus. *The Journal of Immunology*, *201*(2), 516-523. http://doi.org/10.4049/jimmunol.1800348

Crompton, J. G., Clever, D., Vizcardo, R., Rao, M., & Restifo, N. P. (2014). Reprogramming antitumor immunity. *Trends in Immunology*, *35*(4), 178–185. http://doi.org/10.1016/j.it.2014.02.003

D'Agostino, P. M., Gottfried-Blackmore, A., Anandasabapathy, N., & Bulloch, K. (2012). Brain dendritic cells: biology and pathology. *Acta Neuropathologica*, *124*(5), 599–614. http://doi.org/10.1007/s00401-012-1018-0

De Smedt, T., Pajak, B., Muraille, E., Lespagnard, L., Heinen, E., De Baetselier, P., et al. (1996). Regulation of dendritic cell numbers and maturation by lipopolysaccharide in vivo. *Journal of Experimental Medicine*, *184*(4), 1413–1424. http://doi.org/10.1084/jem.184.4.1413

Deckers, J., Hammad, H., & Hoste, E. (2018). Langerhans Cells: Sensing the Environment in Health and Disease. *Frontiers in Immunology*, *9*, 93. http://doi.org/10.3389/fimmu.2018.00093

Dudziak, D., Kamphorst, A., Heidkamp, G., Buchholz, V., & Nussenzweig, M. (2007). Differential Antigen Processing by Dendritic Cell Subsets in Vivo, 1–6. http://doi.org/10.1126/science.1132514

Durai, V., & Murphy, K. M. (2016). Functions of Murine Dendritic Cells. *Immunity*, *45*(4), 719–736. http://doi.org/10.1016/j.immuni.2016.10.010

Durai, V., Bagadia, P., Briseño, C. G., Theisen, D. J., Iwata, A., Davidson, J. T., et al. (2018). Altered compensatory cytokine signaling underlies the discrepancy between Flt3-/- and Flt3l-/- mice. *The Journal of Experimental Medicine*, *215*(5),1417-1435. http://doi.org/10.1084/jem.20171784

Eisenbarth, S. C. (2019). Dendritic cell subsets in T cell programming: location dictates function. *Nature Publishing Group*, *19*(2), 89–103. http://doi.org/10.1038/s41577-018-0088-1

Ersland, K., Wüthrich, M., & Klein, B. S. (2010). Dynamic interplay among monocyte-derived, dermal, and resident lymph node dendritic cells during the generation of vaccine immunity to fungi. *Cell Host & Microbe*, *7*(6), 474–487. http://doi.org/10.1016/j.chom.2010.05.010

Finger Stadler, A., Patel, M., Pacholczyk, R., Cutler, C. W., & Arce, R. M. (2017). Long-term sustainable dendritic cell-specific depletion murine model for periodontitis research. *Journal of Immunological Methods*, *449*, 7–14. http://doi.org/10.1016/j.jim.2017.06.007

Fogg, D. K., Sibon, C., Miled, C., Jung, S., Aucouturier, P., Littman, D. R., et al. (2006). A clonogenic bone marrow progenitor specific for macrophages and dendritic cells. *Science*, *311*(5757), 83–87. http://doi.org/10.1126/science.1117729

Förster, R., Davalos-Misslitz, A. C., & Rot, A. (2008). CCR7 and its ligands: balancing immunity and tolerance. *Nature Publishing Group*, *8*(5), 362–371. http://doi.org/10.1038/nri2297

Förster, R., Schubel, A., Breitfeld, D., Kremmer, E., Renner-Müller, I., Wolf, E., & Lipp, M. (1999). CCR7 coordinates the primary immune response by establishing functional microenvironments in secondary lymphoid organs. *Cell*, *99*(1), 23–33.

Fry, T. J., Sinha, M., Milliron, M., Chu, Y.-W., Kapoor, V., Gress, R. E., et al. (2004). Flt3 ligand enhances thymic-dependent and thymic-independent immune reconstitution. *Blood*, *104*(9), 2794–2800. http://doi.org/10.1182/blood-2003-11-3789

Fukaya, T., Murakami, R., Takagi, H., Sato, K., Sato, Y., Otsuka, H., et al. (2012). Conditional ablation of CD205+ conventional dendritic cells impacts the regulation of T-cell immunity and homeostasis in vivo. *Proceedings of the National Academy of Sciences of the United States of America*, *109*(28), 11288–11293. http://doi.org/10.1073/pnas.1202208109

Gallo, P. M., & Gallucci, S. (2013). The dendritic cell response to classic, emerging, and homeostatic danger signals. Implications for autoimmunity. *Frontiers in Immunology*, *4*, 138. http://doi.org/10.3389/fimmu.2013.00138

Gerner, M. Y., Kastenmüller, W., Ifrim, I., Kabat, J., & Germain, R. N. (2012). Histo-cytometry: a method for highly multiplex quantitative tissue imaging analysis applied to dendritic cell subset microanatomy in lymph nodes. *Immunity*, *37*(2), 364–376. http://doi.org/10.1016/j.immuni.2012.07.011

Gerner, M. Y., Torabi-Parizi, P., & Germain, R. N. (2015). Strategically localized dendritic cells promote rapid T cell responses to lymph-borne particulate antigens. *Immunity*, *42*(1), 172–185. http://doi.org/10.1016/j.immuni.2014.12.024

Ghosh, H. S., Cisse, B., Bunin, A., Lewis, K. L., & Reizis, B. (2010). Continuous expression of the transcription factor e2-2 maintains the cell fate of mature plasmacytoid dendritic cells. *Immunity*, *33*(6), 905–916. http://doi.org/10.1016/j.immuni.2010.11.023

Ginhoux, F., Guilliams, M., & Naik, S. H. (2016). Editorial: Dendritic Cell and Macrophage Nomenclature and Classification. *Frontiers in Immunology*, *7*, 168. http://doi.org/10.3389/fimmu.2016.00168

Ginhoux, F., Liu, K., Helft, J., Bogunovic, M., Greter, M., Hashimoto, D., et al. (2009). The origin and development of nonlymphoid tissue CD103+ DCs. *The Journal of Experimental Medicine*, *206*(13), 3115–3130. http://doi.org/10.1084/jem.20091756

Grajales-Reyes, G. E., Iwata, A., Albring, J., Wu, X., Tussiwand, R., KC, W., et al. (2015). Batf3 maintains autoactivation of Irf8 for commitment of a CD8α(+) conventional DC clonogenic progenitor. *Nature Immunology*, *16*(7), 708–717. http://doi.org/10.1038/ni.3197

Gray, E. E., & Cyster, J. G. (2012). Lymph Node Macrophages. *Journal of Innate Immunity*, *4*(5-6), 424–436. http://doi.org/10.1159/000337007

Guerriero, A., Langmuir, P. B., Spain, L. M., & Scott, E. W. (2000). PU.1 is required for myeloid-derived but not lymphoid-derived dendritic cells. *Blood*, *95*(3), 879–885.

Guilliams, M., Ginhoux, F., Jakubzick, C., Naik, S. H., Onai, N., Schraml, B. U., et al. (2014). Dendritic cells, monocytes and macrophages: a unified nomenclature based on ontogeny. *Nature Reviews Immunology*, *14*(8), 571–578. http://doi.org/10.1038/nri3712

Gurevich, I., Feferman, T., Milo, I., Tal, O., Golani, O., Drexler, I., & Shakhar, G. (2017). Active dissemination of cellular antigens by DCs facilitates CD8+ T-cell priming in lymph nodes. *European Journal of Immunology*, *47*(10), 1802–1818. http://doi.org/10.1002/eji.201747042

Hashimoto, D., Miller, J., & Merad, M. (2011). Dendritic cell and macrophage heterogeneity in vivo. *Immunity*, *35*(3), 323–335. http://doi.org/10.1016/j.immuni.2011.09.007

Hauser, M. A., Kindinger, I., Laufer, J. M., Späte, A.-K., Bucher, D., Vanes, S. L., et al. (2016). Distinct CCR7 glycosylation pattern shapes receptor signaling and endocytosis to modulate chemotactic responses. *Journal of Leukocyte Biology*, *99*(6), 993–1007. http://doi.org/10.1189/jlb.2VMA0915-432RR

Helft, J., Anjos-Afonso, F., van der Veen, A. G., Chakravarty, P., Bonnet, D., & Sousa, C. R. E. (2017). Dendritic Cell Lineage Potential in Human Early Hematopoietic Progenitors. *CellReports*, *20*(3), 529–537. http://doi.org/10.1016/j.celrep.2017.06.075

Helft, J., Böttcher, J., Chakravarty, P., Zelenay, S., Huotari, J., Schraml, B. U., et al. (2015). GM-CSF Mouse Bone Marrow Cultures Comprise a Heterogeneous Population of CD11c+MHCII+ Macrophages and Dendritic Cells, 1–16. http://doi.org/10.1016/j.immuni.2015.05.018

Henri, S., Guilliams, M., Poulin, L. F., Tamoutounour, S., Ardouin, L., Dalod, M., & Malissen, B. (2010a). Disentangling the complexity of the skin dendritic cell network. *Immunology and Cell Biology*, *88*(4), 366–375. http://doi.org/10.1038/icb.2010.34

Henri, S., Poulin, L. F., Tamoutounour, S., Ardouin, L., Guilliams, M., de Bovis, B., et al. (2010b). CD207+ CD103+ dermal dendritic cells cross-present keratinocyte-derived antigens irrespective of the presence of Langerhans cells. *The Journal of Experimental Medicine*, *207*(1), 189–206. http://doi.org/10.1084/jem.20091964

Henri, S., Vremec, D., Kamath, A., Waithman, J., Williams, S., Benoist, C., et al. (2001). The dendritic cell populations of mouse lymph nodes. *The Journal of Immunology*, *167*(2), 741–748.

Hildner, K., Edelson, B. T., Purtha, W. E., Diamond, M., Matsushita, H., Kohyama, M., et al. (2008). Batf3 Deficiency Reveals a Critical Role for CD8α+ Dendritic Cells in Cytotoxic T Cell Immunity. *Science*, *322*(5904), 1097–1100. http://doi.org/10.1126/science.1164206

Hjortø, G. M., Larsen, O., Steen, A., Daugvilaite, V., Berg, C., Fares, S., et al. (2016). Differential CCR7 Targeting in Dendritic Cells by Three Naturally Occurring CC-Chemokines. *Frontiers in Immunology*, *7*, 568. http://doi.org/10.3389/fimmu.2016.00568

Hochweller, K., Miloud, T., Striegler, J., Naik, S., Hämmerling, G. J., & Garbi, N. (2009). Homeostasis of dendritic cells in lymphoid organs is controlled by regulation of their precursors via a feedback loop. *Blood*, *114*(20), 4411–4421. http://doi.org/10.1182/blood-2008-11-188045

Hochweller, K., Striegler, J., Hämmerling, G. J., & Garbi, N. (2008). A novel CD11c.DTR transgenic mouse for depletion of dendritic cells reveals their requirement for homeostatic proliferation of natural killer cells. *European Journal of Immunology*, *38*(10), 2776–2783. http://doi.org/10.1002/eji.200838659

Hoffmann, F., Ender, F., Schmudde, I., Lewkowich, I. P., Köhl, J., König, P., & Laumonnier, Y. (2016). Origin, Localization, and Immunoregulatory Properties of Pulmonary Phagocytes in Allergic Asthma. *Frontiers in Immunology*, *7*(1333–1342), 107. http://doi.org/10.3389/fimmu.2016.00107

Hromas, R., Kim, C. H., Klemsz, M., Krathwohl, M., Fife, K., Cooper, S., et al. (1997). Isolation and characterization of Exodus-2, a novel C-C chemokine with a unique 37-amino acid carboxyl-terminal extension. *The Journal of Immunology*, *159*(6), 2554–2558.

Iberg, C. A., Jones, A., & Hawiger, D. (2017). Dendritic Cells As Inducers of Peripheral Tolerance. *Trends in Immunology*, *38*(11), 793–804. http://doi.org/10.1016/j.it.2017.07.007

Idoyaga, J., Suda, N., Suda, K., Park, C. G., & Steinman, R. M. (2009). Antibody to Langerin/CD207 localizes large numbers of CD8alpha+ dendritic cells to the marginal zone of mouse spleen. *Proceedings of the National Academy of Sciences of the United States of America*, *106*(5), 1524–1529. http://doi.org/10.1073/pnas.0812247106

Inaba, K., Inaba, M., Romani, N., Aya, H., Deguchi, M., Ikehara, S., et al. (1992). Generation of large numbers of dendritic cells from mouse bone marrow cultures supplemented with granulocyte/macrophage colony-stimulating factor. *Journal of Experimental Medicine*, *176*(6), 1693–1702. http://doi.org/10.1084/jem.176.6.1693

Izon, D., Rudd, K., DeMuth, W., Pear, W. S., Clendenin, C., Lindsley, R. C., & Allman, D. (2001). A Common Pathway for Dendritic Cell and Early B Cell Development. *The Journal of Immunology*, *167*(3), 1387–1392. http://doi.org/10.4049/jimmunol.167.3.1387

Jakubzick, C., Bogunovic, M., Bonito, A. J., Kuan, E. L., Merad, M., & Randolph, G. J. (2008). Lymph-migrating, tissue-derived dendritic cells are minor constituents within steady-state lymph nodes. *The Journal of Experimental Medicine*, *205*(12), 2839–2850. http://doi.org/10.1084/jem.20081430

Jiao, J., Dragomir, A.-C., Kocabayoglu, P., Rahman, A. H., Chow, A., Hashimoto, D., et al. (2014). Central Role of Conventional Dendritic Cells in Regulation of Bone Marrow Release and Survival of Neutrophils, 1–10. http://doi.org/10.4049/jimmunol.1300237/-/DCSupplemental

Jung, S., Unutmaz, D., Wong, P., Sano, G.-I., De los Santos, K., Sparwasser, T., et al. (2002). In vivo depletion of CD11c+ dendritic cells abrogates priming of CD8+ T cells by exogenous cell-associated antigens. *Immunity*, *17*(2), 211–220.

Kabashima, K., Banks, T. A., Ansel, K. M., Lu, T. T., Ware, C. F., & Cyster, J. G. (2005). Intrinsic lymphotoxin-beta receptor requirement for homeostasis of lymphoid tissue dendritic cells. *Immunity*, *22*(4), 439–450. http://doi.org/10.1016/j.immuni.2005.02.007

Kamath, A. T., Henri, S., Battye, F., Tough, D. F., & Shortman, K. (2002). Developmental kinetics and lifespan of dendritic cells in mouse lymphoid organs. *Blood*, *100*(5), 1734–1741.

Karsunky, H., Merad, M., Cozzio, A., Weissman, I. L., & Manz, M. G. (2003). Flt3 ligand regulates dendritic cell development from Flt3+ lymphoid and myeloid-committed progenitors to Flt3+ dendritic cells in vivo. *Journal of Experimental Medicine*, *198*(2), 305–313. http://doi.org/10.1084/jem.20030323

Kashiwada, M., Pham, N.-L. L., Pewe, L. L., Harty, J. T., & Rothman, P. B. (2011). NFIL3/E4BP4 is a key transcription factor for CD8α$^+$ dendritic cell development. *Blood*, *117*(23), 6193–6197. http://doi.org/10.1182/blood-2010-07-295873

Katou, F., Ohtani, H., Nakayama, T., Nagura, H., Yoshie, O., & Motegi, K. (2003). Differential expression of CCL19 by DC-Lamp+ mature dendritic cells in human lymph node versus chronically inflamed skin. *The Journal of Pathology*, *199*(1), 98–106. http://doi.org/10.1002/path.1255

Kinnebrew, M. A., Buffie, C. G., Diehl, G. E., Zenewicz, L. A., Leiner, I., Hohl, T. M., et al. (2012). Interleukin 23 production by intestinal CD103(+)CD11b(+) dendritic cells in response to bacterial flagellin enhances mucosal innate immune defense. *Immunity*, *36*(2), 276–287. http://doi.org/10.1016/j.immuni.2011.12.011

Kissenpfennig, A., Henri, S., Dubois, B., Laplace-Builhé, C., Perrin, P., Romani, N., et al. (2005). Dynamics and Function of Langerhans Cells In Vivo. *Immunity*, *22*(5), 643–654. http://doi.org/10.1016/j.immuni.2005.04.004

Kitano, M., Yamazaki, C., Takumi, A., Ikeno, T., Hemmi, H., Takahashi, N., et al. (2016). Imaging of the cross-presenting dendritic cell subsets in the skin-draining lymph node. *Proceedings of the National Academy of Sciences of the United States of America*, *113*(4), 1044–1049. http://doi.org/10.1073/pnas.1513607113

Kohout, T. A., Nicholas, S. L., Perry, S. J., Reinhart, G., Junger, S., & Struthers, R. S. (2004). Differential desensitization, receptor phosphorylation, beta-arrestin recruitment, and ERK1/2 activation by the two endogenous ligands for the CC chemokine receptor 7. *The Journal of Biological Chemistry*, *279*(22), 23214–23222. http://doi.org/10.1074/jbc.M402125200

Kraal, G., Twisk, A., Tan, B., & Scheper, R. (1986). A surface molecule on guinea pig lymphocytes involved in adhesion and homing. *European Journal of Immunology*, *16*(12), 1515–1519. http://doi.org/10.1002/eji.1830161208

Langlet, C., Tamoutounour, S., Henri, S., Luche, H., Ardouin, L., Grégoire, C., et al. (2012). CD64 expression distinguishes monocyte-derived and conventional dendritic cells and reveals their distinct role during intramuscular immunization. *Journal of Immunology (Baltimore, Md. : 1950)*, *188*(4), 1751–1760. http://doi.org/10.4049/jimmunol.1102744

Lee, H. K., Zamora, M., Linehan, M. M., Iijima, N., Gonzalez, D., Haberman, A., & Iwasaki, A. (2009). Differential roles of migratory and resident DCs in T cell priming after mucosal or skin HSV-1 infection. *The Journal of Experimental Medicine*, *206*(2), 359–370. http://doi.org/10.1084/jem.20080601

Lewis, K. L., Caton, M. L., Bogunovic, M., Greter, M., Grajkowska, L. T., Ng, D., et al. (2011). Notch2 receptor signaling controls functional differentiation of dendritic cells in the spleen and intestine. *Immunity*, *35*(5), 780–791. http://doi.org/10.1016/j.immuni.2011.08.013

Li, J., Park, J., Foss, D., & Goldschneider, I. (2009). Thymus-homing peripheral dendritic cells constitute two of the three major subsets of dendritic cells in the steady-state thymus. *The Journal of Experimental Medicine*, *206*(3), 607–622. http://doi.org/10.1084/jem.20082232

Link, A., Vogt, T. K., Favre, S., Britschgi, M. R., Acha-Orbea, H., Hinz, B., et al. (2007). Fibroblastic reticular cells in lymph nodes regulate the homeostasis of naive T cells. *Nature Immunology*, *8*(11), 1255–1265. http://doi.org/10.1038/ni1513

Liou, L.-Y., Blasius, A. L., Welch, M. J., Colonna, M., Oldstone, M. B. A., & Zuniga, E. I. (2008). In vivo conversion of BM plasmacytoid DC into CD11b+ conventional DC during virus infection. *European Journal of Immunology*, *38*(12), 3388–3394. http://doi.org/10.1002/eji.200838282

Liu, K., Victora, G. D., Schwickert, T. A., Guermonprez, P., Meredith, M. M., Yao, K., et al. (2009). In vivo analysis of dendritic cell development and homeostasis. *Science (New York, N.Y.)*, *324*(5925), 392–397. http://doi.org/10.1126/science.1170540

Lorenz, N., Loef, E. J., Kelch, I. D., Verdon, D. J., Black, M. M., Middleditch, M. J., et al. (2016). Plasmin and regulators of plasmin activity control the migratory capacity and adhesion of human T cells and dendritic cells by regulating cleavage of the chemokine CCL21. *Immunology and Cell Biology*, *94*(10), 955–963. http://doi.org/10.1038/icb.2016.56

Love, M., Sandberg, J. L., Ziarek, J. J., Gerarden, K. P., Rode, R. R., Jensen, D. R., et al. (2012). Solution structure of CCL21 and identification of a putative CCR7 binding site. *Biochemistry*, *51*(3), 733–735. http://doi.org/10.1021/bi201601k

Lu, E., Dang, E. V., McDonald, J. G., & Cyster, J. G. (2017). Distinct oxysterol requirements for positioning naïve and activated dendritic cells in the spleen. *Science Immunology*, *2*(10), eaal5237. http://doi.org/10.1126/sciimmunol.aal5237

Luther, S. A., Tang, H. L., Hyman, P. L., Farr, A. G., & Cyster, J. G. (2000). Coexpression of the chemokines ELC and SLC by T zone stromal cells and deletion of the ELC gene in the plt/plt mouse. *Proceedings of the National Academy of Sciences*, *97*(23), 12694–12699. http://doi.org/10.1073/pnas.97.23.12694

Ma, Q., Jones, D., & Springer, T. A. (1999). The chemokine receptor CXCR4 is required for the retention of B lineage and granulocytic precursors within the bone marrow microenvironment. *Immunity*, *10*(4), 463–471.

Malissen, B., Tamoutounour, S., & Henri, S. (2014). The origins and functions of dendritic cells and macrophages in the skin. *Nature Publishing Group*, *14*(6), 417–428. http://doi.org/10.1038/nri3683

Manh, T.-P. V., Alexandre, Y., Baranek, T., Crozat, K., & Dalod, M. (2013). Plasmacytoid, conventional, and monocyte-derived dendritic cells undergo a profound and convergent genetic reprogramming during their maturation. *European Journal of Immunology*, *43*(7), 1706–1715. http://doi.org/10.1002/eji.201243106

Manz, M. G., Traver, D., Akashi, K., Merad, M., Miyamoto, T., Engleman, E. G., & Weissman, I. L. (2001a). Dendritic cell development from common myeloid progenitors. *Annals of the New York Academy of Sciences*, *938*(1), 167–74. http://doi.org/10.1111/j.1749-6632.2001.tb03586.x

Manz, M. G., Traver, D., Miyamoto, T., Weissman, I. L., & Akashi, K. (2001b). Dendritic cell potentials of early lymphoid and myeloid progenitors. *Blood*, *97*(11), 3333–3341. http://doi.org/10.1182/blood.V97.11.3333

Maraskovsky, E., Teepe, M., Morrissey, P. J., Braddy, S., Miller, R. E., Lynch, D. H., & Peschon, J. J. (1996). Impaired survival and proliferation in IL-7 receptor-deficient peripheral T cells. *The Journal of Immunology*, *157*(12), 5315–5323.

Mazo, I. B., Massberg, S., & Andrian, von, U. H. (2011). Hematopoietic stem and progenitor cell trafficking. *Trends in Immunology*, *32*(10), 493–503. http://doi.org/10.1016/j.it.2011.06.011

McKenna, H. J., Stocking, K. L., Miller, R. E., Brasel, K., De Smedt, T., Maraskovsky, E., et al. (2000). Mice lacking flt3 ligand have deficient hematopoiesis affecting hematopoietic progenitor cells, dendritic cells, and natural killer cells. *Blood*, *95*(11), 3489–3497.

Mebius, R. E., & Kraal, G. (2005). Structure and function of the spleen. *Nature Reviews Immunology*, *5*(8), 606–616. http://doi.org/10.1038/nri1669

Merad, M., Sathe, P., Helft, J., Miller, J., & Mortha, A. (2013). The Dendritic Cell Lineage: Ontogeny and Function of Dendritic Cells and Their Subsets in the Steady State and the Inflamed Setting. *Annual Review of Immunology*, *31*(1), 563–604. http://doi.org/10.1146/annurev-immunol-020711-074950

Meredith, M. M., Liu, K., Darrasse-Jeze, G., Kamphorst, A. O., Schreiber, H. A., Guermonprez, P., et al. (2012). Expression of the zinc finger transcription factor zDC (Zbtb46, Btbd4) defines the classical dendritic cell lineage. *The Journal of Experimental Medicine*, *209*(6), 1153–1165. http://doi.org/10.1084/jem.20112675

Mildner, A., & Jung, S. (2014). Development and function of dendritic cell subsets. *Immunity*, *40*(5), 642–656. http://doi.org/10.1016/j.immuni.2014.04.016

Montoya, M., Schiavoni, G., Mattei, F., Gresser, I., Belardelli, F., Borrow, P., & Tough, D. F. (2002). Type I interferons produced by dendritic cells promote their phenotypic and functional activation. *Blood*, *99*(9), 3263–3271.

Muzaki, A. R. B. M., Tetlak, P., Sheng, J., Loh, S. C., Setiagani, Y. A., Poidinger, M., et al. (2016). Intestinal CD103(+)CD11b(-) dendritic cells restrain colitis via IFN-γ-induced anti-inflammatory response in epithelial cells. *Mucosal Immunology*, *9*(2), 336–351. http://doi.org/10.1038/mi.2015.64

Naik, S. H., Perié, L., Swart, E., Gerlach, C., van Rooij, N., de Boer, R. J., & Schumacher, T. N. (2013). Diverse and heritable lineage imprinting of early haematopoietic progenitors. *Nature*, *496*(7444), 229–232. http://doi.org/10.1038/nature12013

Naik, S. H., Proietto, A. I., Wilson, N. S., Dakic, A., Schnorrer, P., Fuchsberger, M., et al. (2005). Cutting Edge: Generation of Splenic CD8+ and CD8- Dendritic Cell Equivalents in Fms-Like Tyrosine Kinase 3 Ligand Bone Marrow Cultures. *The Journal of Immunology*, *174*(11), 6592–6597. http://doi.org/10.4049/jimmunol.174.11.6592

Naik, S. H., Sathe, P., Park, H.-Y., Metcalf, D., Proietto, A. I., Dakic, A., et al. (2007). Development of plasmacytoid and conventional dendritic cell subtypes from single precursor cells derived in vitro and in vivo. *Nature Immunology*, *8*(11), 1217–1226. http://doi.org/10.1038/ni1522

Nakano, H., Lyons-Cohen, M. R., Whitehead, G. S., Nakano, K., & Cook, D. N. (2017). Distinct functions of CXCR4, CCR2, and CX3CR1 direct dendritic cell precursors from the bone marrow to the lung. *Journal of Leukocyte Biology*, *101*(5), 1143-1153. http://doi.org/10.1189/jlb.1A0616-285R

Ngo, V. N., Tang, H. L., & Cyster, J. G. (1998). Epstein-Barr virus-induced molecule 1 ligand chemokine is expressed by dendritic cells in lymphoid tissues and strongly attracts naive T cells and activated B cells. *Journal of Experimental Medicine*, *188*(1), 181–191. http://doi.org/10.1084/jem.188.1.181

Nimmo, R. A., May, G. E., & Enver, T. (2015). Primed and ready: understanding lineage commitment through single cell analysis. *Trends in Cell Biology*, *25*(8), 459–467. http://doi.org/10.1016/j.tcb.2015.04.004

Noor, S., & Wilson, E. H. (2012). Role of C-C chemokine receptor type 7 and its ligands during neuroinflammation. *Journal of Neuroinflammation*, *9*(1), 77. http://doi.org/10.1186/1742-2094-9-77

Nussenzweig, M. C., Steinman, R. M., Unkeless, J. C., Witmer, M. D., Gutchinov, B., & Cohn, Z. A. (1981). Studies of the cell surface of mouse dendritic cells and other leukocytes. *Journal of Experimental Medicine*, *154*(1), 168–187. http://doi.org/10.1084/jem.154.1.168

Ohl, L., Mohaupt, M., Czeloth, N., Hintzen, G., Kiafard, Z., Zwirner, J., et al. (2004). CCR7 governs skin dendritic cell migration under inflammatory and steady-state conditions. *Immunity*, *21*(2), 279–288. http://doi.org/10.1016/j.immuni.2004.06.014

Ohnmacht, C., Pullner, A., King, S. B. S., Drexler, I., Meier, S., Brocker, T., & Voehringer, D. (2009). Constitutive ablation of dendritic cells breaks self-tolerance of CD4 T cells and results in spontaneous fatal autoimmunity. *The Journal of Experimental Medicine*, *206*(3), 549–559. http://doi.org/10.1084/jem.20082394

Ohta, T., Sugiyama, M., Hemmi, H., Yamazaki, C., Okura, S., Sasaki, I., et al. (2016). Crucial roles of XCR1-expressing dendritic cells and the XCR1- XCL1 chemokine axis in intestinal immune homeostasis. *Scientific Reports, 6*, 23505. http://doi.org/10.1038/srep23505

Onai, N., Obata-Onai, A., Schmid, M. A., Ohteki, T., Jarrossay, D., & Manz, M. G. (2007). Identification of clonogenic common Flt3+M-CSFR+ plasmacytoid and conventional dendritic cell progenitors in mouse bone marrow. *Nature Immunology*, *8*(11), 1207–1216. http://doi.org/10.1038/ni1518

Otero, C., Groettrup, M., & Legler, D. F. (2006). Opposite fate of endocytosed CCR7 and its ligands: recycling versus degradation. *The Journal of Immunology*, *177*(4), 2314–2323. http://doi.org/10.4049/jimmunol.177.4.2314

Ott, T. R., Lio, F. M., Olshefski, D., Liu, X.-J., Ling, N., & Struthers, R. S. (2006). The N-terminal domain of CCL21 reconstitutes high affinity binding, G protein activation, and chemotactic activity, to the C-terminal domain of CCL19. *Biochemical and Biophysical Research Communications*, *348*(3), 1089–1093. http://doi.org/10.1016/j.bbrc.2006.07.165

Pakalniškytė, D., & Schraml, B. U. (2017). Tissue-Specific Diversity and Functions of Conventional Dendritic Cells. *Advances in Immunology*, *134*, 89–135. http://doi.org/10.1016/bs.ai.2017.01.003

Persson, E. K., Uronen-Hansson, H., Semmrich, M., Rivollier, A., Hägerbrand, K., Marsal, J., et al. (2013). IRF4 transcription-factor-dependent CD103(+)CD11b(+) dendritic cells drive mucosal T helper 17 cell differentiation. *Immunity*, *38*(5), 958–969. http://doi.org/10.1016/j.immuni.2013.03.009

Perussia, B., Fanning, V., & Trinchieri, G. (1985). A leukocyte subset bearing HLA-DR antigens is responsible for in vitro alpha interferon production in response to viruses. *Natural Immunity and Cell Growth Regulation*, *4*(3), 120–137.

Pooley, J. L., Heath, W. R., & Shortman, K. (2001). Cutting edge: intravenous soluble antigen is presented to CD4 T cells by CD8- dendritic cells, but cross-presented to CD8 T cells by CD8+ dendritic cells. *The Journal of Immunology*, *166*(9), 5327–5330. http://doi.org/10.4049/jimmunol.166.9.5327

Poulin, L. F., Reyal, Y., Uronen-Hansson, H., Schraml, B. U., Sancho, D., Murphy, K. M., et al. (2012). DNGR-1 is a specific and universal marker of mouse and human Batf3-dependent dendritic cells in lymphoid and nonlymphoid tissues. *Blood*, *119*(25), 6052–6062. http://doi.org/10.1182/blood-2012-01-406967

Probst, H. C., Tschannen, K., Odermatt, B., Schwendener, R., Zinkernagel, R. M., & Van Den Broek, M. (2005). Histological analysis of CD11c-DTR/GFP mice after in vivo depletion of dendritic cells. *Clinical and Experimental Immunology*, *141*(3), 398–404. http://doi.org/10.1111/j.1365-2249.2005.02868.x

Pulendran, B., Lingappa, J., Kennedy, M. K., Smith, J., Teepe, M., Rudensky, A., et al. (1997). Developmental pathways of dendritic cells in vivo: distinct function, phenotype, and localization of dendritic cell subsets in FLT3 ligand-treated mice. *The Journal of Immunology*, *159*(5), 2222–2231.

Qi, H., Egen, J. G., Huang, A. Y. C., & Germain, R. N. (2006). Extrafollicular activation of lymph node B cells by antigen-bearing dendritic cells. *Science*, *312*(5780), 1672–1676. http://doi.org/10.1126/science.1125703

Randolph, G. J., Inaba, K., Robbiani, D. F., Steinman, R. M., & Muller, W. A. (1999). Differentiation of phagocytic monocytes into lymph node dendritic cells in vivo. *Immunity*, *11*(6), 753–761.

Rapp, M., Wintergerst, M. W. M., Kunz, W. G., Vetter, V. K., Knott, M. M. L., Lisowski, D., et al. (2019). CCL22 controls immunity by promoting regulatory T cell communication with dendritic cells in lymph nodes. *The Journal of Experimental Medicine*, *216*(5), 1170-1181.http://doi.org/10.1084/jem.20170277

Reis e Sousa, C., Hieny, S., Scharton-Kersten, T., Jankovic, D., Charest, H., Germain, R. N., & Sher, A. (1997). In vivo microbial stimulation induces rapid CD40 ligand-independent production of interleukin 12 by dendritic cells and their redistribution to T cell areas. *Journal of Experimental Medicine*, *186*(11), 1819–1829.

Rescigno, M., Rotta, G., Valzasina, B., & Ricciardi-Castagnoli, P. (2001). Dendritic cells shuttle microbes across gut epithelial monolayers. *Immunobiology*, *204*(5), 572–581. http://doi.org/10.1078/0171-2985-00094

Reuter, A., Panozza, S. E., Macri, C., Dumont, C., Li, J., Liu, H., et al. (2015). Criteria for dendritic cell receptor selection for efficient antibody-targeted vaccination. *Journal of Immunology*, *194*(6), 2696–2705. http://doi.org/10.4049/jimmunol.1402535

Ricart, B. G., Yang, M. T., Hunter, C. A., Chen, C. S., & Hammer, D. A. (2011). Measuring traction forces of motile dendritic cells on micropost arrays. *Biophysical Journal*, *101*(11), 2620–2628. http://doi.org/10.1016/j.bpj.2011.09.022

Rodrigues, P. F., Alberti-Servera, L., Eremin, A., Grajales-Reyes, G. E., Ivanek, R., & Tussiwand, R. (2018). Distinct progenitor lineages contribute to the heterogeneity of plasmacytoid dendritic cells. *Nature Immunology*, *19*(7), 711–722. http://doi.org/10.1038/s41590-018-0136-9

Romani, N., Gruner, S., Brang, D., Kämpgen, E., Lenz, A., Trockenbacher, B., et al. (1994). Proliferating dendritic cell progenitors in human blood. *Journal of Experimental Medicine*, *180*(1), 83–93. http://doi.org/10.1084/jem.180.1.83

Rombouts, M., Cools, N., Grootaert, M. O. J., de Bakker, F., Van Brussel, I., Wouters, A., et al. (2017). Long-Term Depletion of Conventional Dendritic Cells Cannot Be Maintained in an Atherosclerotic Zbtb46-DTR Mouse Model. *PLoS ONE*, *12*(1), e0169608. http://doi.org/10.1371/journal.pone.0169608

Sallusto, F., & Lanzavecchia, A. (1994). Efficient presentation of soluble antigen by cultured human dendritic cells is maintained by granulocyte/macrophage colony-stimulating factor plus interleukin 4 and downregulated by tumor necrosis factor alpha. *Journal of Experimental Medicine*, *179*(4), 1109–1118. http://doi.org/10.1084/jem.179.4.1109

Salvermoser, J., van Blijswijk, J., Papaioannou, N. E., Rambichler, S., Pasztoi, M., Pakalniškytė, D., et al. (2018). Clec9a-Mediated Ablation of Conventional Dendritic Cells Suggests a Lymphoid Path to Generating Dendritic Cells In Vivo. *Frontiers in Immunology*, *9*, 563–15. http://doi.org/10.3389/fimmu.2018.00699

Sancho, D., Joffre, O. P., Keller, A. M., Rogers, N. C., Martínez, D., Hernanz-Falcón, P., et al. (2009). Identification of a dendritic cell receptor that couples sensing of necrosis to immunity. *Nature*, *458*(7240), 899–903. http://doi.org/10.1038/nature07750

Sathe, P., Vremec, D., Wu, L., Corcoran, L., & Shortman, K. (2013). Convergent differentiation: myeloid and lymphoid pathways to murine plasmacytoid dendritic cells. *Blood*, *121*(1), 11–19. http://doi.org/10.1182/blood-2012-02-413336

Satpathy, A. T., Briseño, C. G., Lee, J. S., Ng, D., Manieri, N. A., KC, W., et al. (2013). Notch2-dependent classical dendritic cells orchestrate intestinal immunity to attaching-and-effacing bacterial pathogens. *Nature Immunology*, *14*(9), 937–948. http://doi.org/10.1038/ni.2679

Satpathy, A. T., KC, W., Albring, J. C., Edelson, B. T., Kretzer, N. M., Bhattacharya, D., et al. (2012). Zbtb46expression distinguishes classical dendritic cells and their committed progenitors from other immune lineages. *The Journal of Experimental Medicine*, *209*(6), 1135–1152. http://doi.org/10.1084/jem.20120030

Saunders, D., Lucas, K., Ismaili, J., Wu, L., Maraskovsky, E., Dunn, A., & Shortman, K. (1996). Dendritic cell development in culture from thymic precursor cells in the absence of granulocyte/macrophage colony-stimulating factor. *Journal of Experimental Medicine*, *184*(6), 2185–2196. http://doi.org/10.1084/jem.184.6.2185

Schiavoni, G., Mattei, F., Sestili, P., Borghi, P., Venditti, M., Morse, H. C., et al. (2002). ICSBP is essential for the development of mouse type I interferon-producing cells and for the generation and activation of CD8alpha(+) dendritic cells. *Journal of Experimental Medicine*, *196*(11), 1415–1425. http://doi.org/10.1084/jem.20021263

Schlecht, G., Mouriès, J., Poitrasson-Rivière, M., Leclerc, C., & Dadaglio, G. (2006). Purification of splenic dendritic cells induces maturation and capacity to stimulate Th1 response in vivo. *International Immunology*, *18*(3), 445–452. http://doi.org/10.1093/intimm/dxh384

Schlenner, S. M., Madan, V., Busch, K., Tietz, A., Läufle, C., Costa, C., et al. (2010). Fate Mapping Reveals Separate Origins of T Cells and Myeloid Lineages in the Thymus. *Immunity*, *32*(3), 426–436. http://doi.org/10.1016/j.immuni.2010.03.005

Schlissel, M. S., Corcoran, L. M., & Baltimore, D. (1991). Virus-transformed pre-B cells show ordered activation but not inactivation of immunoglobulin gene rearrangement and transcription. *The Journal of Experimental Medicine*, *173*(3), 711–720.

Schlitzer, A., & Ginhoux, F. (2014). Organization of the mouse and human DC network. *Current Opinion in Immunology*, *26*, 90–99. http://doi.org/10.1016/j.coi.2013.11.002

Schlitzer, A., McGovern, N., Teo, P., Zelante, T., Atarashi, K., Low, D., et al. (2013). IRF4 Transcription Factor-Dependent CD11b+ Dendritic Cells in Human and Mouse Control Mucosal IL-17 Cytokine Responses. *Immunity*, *38*(5), 970–983. http://doi.org/10.1016/j.immuni.2013.04.011

Schlitzer, A., Sivakamasundari, V., Chen, J., Sumatoh, H. R. B., Schreuder, J., Lum, J., et al. (2015). Identification of cDC1- and cDC2-committed DC progenitors reveals early lineage priming at the common DC progenitor stage in the bone marrow. *Nature Immunology*, *16*(7), 718–728. http://doi.org/10.1038/ni.3200

Schraml, B. U., & Reis e Sousa, C. (2015). Defining dendritic cells. *Current Opinion in Immunology*, *32*, 13–20. http://doi.org/10.1016/j.coi.2014.11.001

Schraml, B. U., van Blijswijk, J., Zelenay, S., Whitney, P. G., Filby, A., Acton, S. E., et al. (2013). Genetic Tracing via DNGR-1 Expression History Defines Dendritic Cells as a Hematopoietic Lineage, *154*(4), 843–858. http://doi.org/10.1016/j.cell.2013.07.014

Schumann, K., Lämmermann, T., Bruckner, M., Legler, D. F., Polleux, J., Spatz, J. P., et al. (2010). Immobilized chemokine fields and soluble chemokine gradients cooperatively shape migration patterns of dendritic cells. *Immunity*, *32*(5), 703–713. http://doi.org/10.1016/j.immuni.2010.04.017

Schutte, B., Nuydens, R., Geerts, H., & Ramaekers, F. (1998). Annexin V binding assay as a tool to measure apoptosis in differentiated neuronal cells. *Journal of Neuroscience Methods*, *86*(1), 63–69.

Scott, C. L., Tfp, Z. M., Beckham, K. S. H., Douce, G., & Mowat, A. M. (2014). Signal regulatory protein alpha (SIRPα) regulates the homeostasis of CD103(+) CD11b(+) DCs in the intestinal lamina propria. *European Journal of Immunology*, *44*(12), 3658–3668. http://doi.org/10.1002/eji.201444859

Sichien, D., Scott, C. L., Martens, L., Vanderkerken, M., Van Gassen, S., Plantinga, M., et al. (2016). IRF8 Transcription Factor Controls Survival and Function of Terminally Differentiated Conventional and Plasmacytoid Dendritic Cells, Respectively. *Immunity*, *45*(3), 626–640. http://doi.org/10.1016/j.immuni.2016.08.013

Siegal, F. P., Kadowaki, N., Shodell, M., Fitzgerald-Bocarsly, P. A., Shah, K., Ho, S., et al. (1999). The nature of the principal type 1 interferon-producing cells in human blood. *Science*, *284*(5421), 1835–1837. http://doi.org/10.1126/science.284.5421.1835

Sixt, M., & Lämmermann, T. (2011). In vitro analysis of chemotactic leukocyte migration in 3D environments. *Methods in Molecular Biology*, *769*, 149–165. http://doi.org/10.1007/978-1-61779-207-6_11

Sokol, C. L., Camire, R. B., Jones, M. C., & Luster, A. D. (2018). The Chemokine Receptor CCR8 Promotes the Migration of Dendritic Cells into the Lymph Node Parenchyma to Initiate the Allergic Immune Response. *Immunity*, *49*(3), 449–463.e6. http://doi.org/10.1016/j.immuni.2018.07.012

Steinman, R. M., & Cohn, Z. A. (1973). Identification of a novel cell type in peripheral lymphoid organs of mice. I. Morphology, quantitation, tissue distribution. *Journal of Experimental Medicine*, *137*(5), 1142–1162.

Steinman, R. M., & Witmer, M. D. (1978). Lymphoid dendritic cells are potent stimulators of the primary mixed leukocyte reaction in mice. *Proceedings of the National Academy of Sciences*, *75*(10), 5132–5136.

Steinman, R. M., Kaplan, G., Witmer, M. D., & Cohn, Z. A. (1979). Identification of a novel cell type in peripheral lymphoid organs of mice. V. Purification of spleen dendritic cells, new surface markers, and maintenance in vitro. *Journal of Experimental Medicine*, *149*(1), 1–16.

Stolley, J. M., & Campbell, D. J. (2016). A 33D1+ Dendritic Cell/Autoreactive CD4+ T Cell Circuit Maintains IL-2-Dependent Regulatory T Cells in the Spleen. *Journal of Immunology*, *197*(7), 2635–2645. http://doi.org/10.4049/jimmunol.1600974

Stutte, S., Quast, T., Gerbitzki, N., Savinko, T., Novak, N., Reifenberger, J., et al. (2010). Requirement of CCL17 for CCR7- and CXCR4-dependent migration of cutaneous dendritic cells.

Proceedings of the National Academy of Sciences of the United States of America, *107*(19), 8736–8741. http://doi.org/10.1073/pnas.0906126107

Sung, S.-S. J., Fu, S. M., Rose, C. E., Gaskin, F., Ju, S.-T., & Beaty, S. R. (2006). A major lung CD103 (alphaE)-beta7 integrin-positive epithelial dendritic cell population expressing Langerin and tight junction proteins. *The Journal of Immunology*, *176*(4), 2161–2172. http://doi.org/10.4049/jimmunol.176.4.2161

Suzuki, S., Honma, K., Matsuyama, T., Suzuki, K., Toriyama, K., Akitoyo, I., et al. (2004a). Critical roles of interferon regulatory factor 4 in CD11bhighCD8alpha- dendritic cell development. *Proceedings of the National Academy of Sciences*, *101*(24), 8981–8986. http://doi.org/10.1073/pnas.0402139101

Suzuki, Y., Wakita, D., Chamoto, K., Narita, Y., Tsuji, T., Takeshima, T., et al. (2004b). Liposome-encapsulated CpG oligodeoxynucleotides as a potent adjuvant for inducing type 1 innate immunity. *Cancer Research*, *64*(23), 8754–8760. http://doi.org/10.1158/0008-5472.CAN-04-1691

Tamoutounour, S., Guilliams, M., Montanana Sanchis, F., Liu, H., Terhorst, D., Malosse, C., et al. (2013). Origins and functional specialization of macrophages and of conventional and monocyte-derived dendritic cells in mouse skin. *Immunity*, *39*(5), 925–938. http://doi.org/10.1016/j.immuni.2013.10.004

Tittel, A. P., Heuser, C., Ohliger, C., Llanto, C., Yona, S., Hämmerling, G. J., et al. (2012). Functionally relevant neutrophilia in CD11c diphtheria toxin receptor transgenic mice. *Nature Methods*, *9*(4), 385–390. http://doi.org/10.1038/nmeth.1905

Traver, D., Akashi, K., Manz, M., Merad, M., Miyamoto, T., Engleman, E. G., & Weissman, I. L. (2000). Development of CD8alpha-positive dendritic cells from a common myeloid progenitor. *Science*, *290*(5499), 2152–2154.

van Blijswijk, J., Schraml, B. U., & Reis e Sousa, C. (2013). Advantages and limitations of mouse models to deplete dendritic cells. *European Journal of Immunology*, *43*(1), 22–26. http://doi.org/10.1002/eji.201243022

van Blijswijk, J., Schraml, B. U., Rogers, N. C., Whitney, P. G., Zelenay, S., Acton, S. E., & Reis e Sousa, C. (2014). Altered Lymph Node Composition in Diphtheria Toxin Receptor–Based Mouse Models To Ablate Dendritic Cells. *The Journal of Immunology*, *194*(1), 307–315. http://doi.org/10.4049/jimmunol.1401999

Vitali, C., Mingozzi, F., Broggi, A., Barresi, S., Zolezzi, F., Bayry, J., et al. (2012). Migratory, and not lymphoid-resident, dendritic cells maintain peripheral self-tolerance and prevent autoimmunity via induction of iTreg cells. *Blood*, *120*(6), 1237–1245. http://doi.org/10.1182/blood-2011-09-379776

Vu Manh, T.-P., Bertho, N., Hosmalin, A., Schwartz-Cornil, I., & Dalod, M. (2015). Investigating Evolutionary Conservation of Dendritic Cell Subset Identity and Functions. *Frontiers in Immunology*, *6*(3), 260. http://doi.org/10.3389/fimmu.2015.00260

Waithman, J., Zanker, D., Xiao, K., Oveissi, S., Wylie, B., Ng, R., et al. (2013). Resident CD8(+) and migratory CD103(+) dendritic cells control CD8 T cell immunity during acute influenza infection. *PLoS ONE*, *8*(6), e66136. http://doi.org/10.1371/journal.pone.0066136

Weber, M., Hauschild, R., Schwarz, J., Moussion, C., de Vries, I., Legler, D. F., et al. (2013). Interstitial dendritic cell guidance by haptotactic chemokine gradients. *Science*, *339*(6117), 328–332. http://doi.org/10.1126/science.1228456

Welner, R. S., Esplin, B. L., Garrett, K. P., Pelayo, R., Luche, H., Fehling, H. J., & Kincade, P. W. (2009). Asynchronous RAG-1 Expression during B Lymphopoiesis. *The Journal of Immunology*, *183*(12), 7768–7777. http://doi.org/10.4049/jimmunol.0902333

Welner, R. S., Pelayo, R., Nagai, Y., Garrett, K. P., Wuest, T. R., Carr, D. J., et al. (2008). Lymphoid precursors are directed to produce dendritic cells as a result of TLR9 ligation during herpes infection. *Blood*, *112*(9), 3753–3761. http://doi.org/10.1182/blood-2008-04-151506

Whitney, P. G., Bär, E., Osorio, F., Rogers, N. C., Schraml, B. U., Deddouche, S., et al. (2014). Syk signaling in dendritic cells orchestrates innate resistance to systemic fungal infection. *PLOS Pathogens*, *10*(7), e1004276. http://doi.org/10.1371/journal.ppat.1004276

Williams, N. L., Morris, J. L., Rush, C. M., & Ketheesan, N. (2014). Migration of dendritic cells facilitates systemic dissemination of Burkholderia pseudomallei. *Infection and Immunity*, *82*(10), 4233–4240. http://doi.org/10.1128/IAI.01880-14

Worbs, T., Mempel, T. R., Bölter, J., Andrian, von, U. H., & Förster, R. (2007). CCR7 ligands stimulate the intranodal motility of T lymphocytes in vivo. *Journal of Experimental Medicine*, *204*(3), 489–495. http://doi.org/10.1084/jem.20061706

Wu, L., & Shortman, K. (2005). Heterogeneity of thymic dendritic cells. *Seminars in Immunology*, *17*(4), 304–312. http://doi.org/10.1016/j.smim.2005.05.001

Wu, L., D'Amico, A., Hochrein, H., O'Keeffe, M., Shortman, K., & Lucas, K. (2001). Development of thymic and splenic dendritic cell populations from different hemopoietic precursors. *Blood*, *98*(12), 3376–3382. http://doi.org/10.1182/blood.V98.12.3376

Wu, L., D'Amico, A., Winkel, K. D., Suter, M., Lo, D., & Shortman, K. (1998). RelB is essential for the development of myeloid-related CD8alpha- dendritic cells but not of lymphoid-related CD8alpha+ dendritic cells. *Immunity*, *9*(6), 839–847.

Yamazaki, C., Sugiyama, M., Ohta, T., Hemmi, H., Hamada, E., Sasaki, I., et al. (2013). Critical roles of a dendritic cell subset expressing a chemokine receptor, XCR1. *Journal of Immunology (Baltimore, Md. : 1950)*, *190*(12), 6071–6082. http://doi.org/10.4049/jimmunol.1202798

Yanagihara, S., Komura, E., Nagafune, J., Watarai, H., & Yamaguchi, Y. (1998). EBI1/CCR7 is a new member of dendritic cell chemokine receptor that is up-regulated upon maturation. *The Journal of Immunology*, *161*(6), 3096–3102.

Yáñez, A., Coetzee, S. G., Olsson, A., Muench, D. E., Berman, B. P., Hazelett, D. J., et al. (2017). Granulocyte-Monocyte Progenitors and Monocyte- Dendritic Cell Progenitors Independently Produce Functionally Distinct Monocytes. *Immunity*, *47*(5), 890–902.e4. http://doi.org/10.1016/j.immuni.2017.10.021

Ye, M., Iwasaki, H., Laiosa, C. V., Stadtfeld, M., Xie, H., Heck, S., et al. (2003). Hematopoietic stem cells expressing the myeloid lysozyme gene retain long-term, multilineage repopulation potential. *Immunity*, *19*(5), 689–699.

Yi, T., & Cyster, J. G. (2013). EBI2-mediated bridging channel positioning supports splenic dendritic cell homeostasis and particulate antigen capture. *eLife*, *2*, e00757. http://doi.org/10.7554/eLife.00757

Yona, S., Kim, K.-W., Wolf, Y., Mildner, A., Varol, D., Breker, M., et al. (2013). Fate mapping reveals origins and dynamics of monocytes and tissue macrophages under homeostasis. *Immunity*, *38*(1), 79–91. http://doi.org/10.1016/j.immuni.2012.12.001

Zidar, D. A., Violin, J. D., Whalen, E. J., & Lefkowitz, R. J. (2009). Selective engagement of G protein coupled receptor kinases (GRKs) encodes distinct functions of biased ligands. *Proceedings of the National Academy of Sciences of the United States of America*, *106*(24), 9649–9654. http://doi.org/10.1073/pnas.0904361106

Zou, Y. R., Kottmann, A. H., Kuroda, M., Taniuchi, I., & Littman, D. R. (1998). Function of the chemokine receptor CXCR4 in haematopoiesis and in cerebellar development. *Nature*, *393*(6685), 595–599. http://doi.org/10.1038/31269

Zuniga, E. I., McGavern, D. B., Pruneda-Paz, J. L., Teng, C., & Oldstone, M. B. A. (2004). Bone marrow plasmacytoid dendritic cells can differentiate into myeloid dendritic cells upon virus infection. *Nature Immunology*, *5*(12), 1227–1234. http://doi.org/10.1038/ni1136

APPENDIX

PUBLICATIONS ARISING FROM THIS WORK:

Major parts of the present work have been published in the journal *Frontiers in Immunology*:

Salvermoser, J., van Blijswijk, J., Papaioannou, N. E., Rambichler, S., Pasztoi, M., Pakalniškytė, D., et al. (2018). Clec9a-Mediated Ablation of Conventional Dendritic Cells Suggests a Lymphoid Path to Generating Dendritic Cells In Vivo. *Frontiers in Immunology*, *9*, 563–15. http://doi.org/10.3389/fimmu.2018.00699

ACKNOWLEDGEMENTS

I would like to thank my supervisor Prof. Dr. Barbara Schraml for her excellent guidance and supervision throughout the project.

Furthermore, I want to thank my thesis advisory committee Prof. Dr. Anne Krug, Prof. Dr. Christoph Scheiermann and Prof. Dr. Jörg Renkawitz for their constructive suggestions on my project.

Thank you to all group members, Vanessa Küntzel, Ramona Mettler, Dalia Pakalniškytė, Nikolaos Papaioannou, Jelena Popović, Stephan Rambichler, Natallia Salei, Maria Pasztoi, Claudia Schmalhofer for their help and advice.

I also would like to acknowledge the SFB 914 and associated IRTG914 for financial support and excellent seminars and courses. In particular, I would like to thank Dr. Verena Kochan, for coordinating the program.

LMU LUDWIG-MAXIMILIANS-UNIVERSITÄT MÜNCHEN

Dean's Office
Medical Faculty

MMRS

Affidavit

Salvermoser, Johanna

Surname, first name

Street

Zip code, town

Country

I hereby declare, that the submitted thesis entitled

Dendritic cell progenitor trafficking and identification and functional analyses of dendritic cells with distinct developmental origin

is my own work. I have only used the sources indicated and have not made unauthorised use of services of a third party. Where the work of others has been quoted or reproduced, the source is always given.

I further declare that the submitted thesis or parts thereof have not been presented as part of an examination degree to any other university.

Ulm, 11.05.2020

Place, date

Johanna Salvermoser

Signature doctoral candidate

LMU LUDWIG-MAXIMILIANS-UNIVERSITÄT MÜNCHEN

Dean's Office
Medical Faculty

MMRS

Confirmation of congruency between printed and electronic version of the doctoral thesis

Salvermoser, Johanna

Surname, first name

Street

Zip code, town

Country

I hereby declare that the electronic version of the submitted thesis, entitled

Dendritic cell progenitor trafficking and identification and functional analyses of dendritic cells with distinct developmental origin

is congruent with the printed version both in content and format.

Ulm, 11.05.2020

Place, date

Johanna Salvermoser

Signature doctoral candidate